

AD A094162

✓
AFAPL-TR-78-6

Part VI

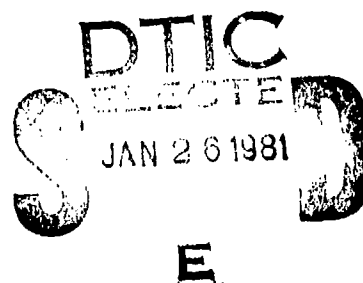
LEVEL III

ROTOR-BEARING DYNAMICS
TECHNOLOGY DESIGN GUIDE

Part VI Status of Gas Bearing Technology Applicable
to Aero Propulsion Machinery

SHAKER RESEARCH
BALLSTON LAKE, NEW YORK 12019

OCTOBER 1980



TECHNICAL REPORT AFAPL-TR-78-6, Part VI
Interim Report for Period January 1980 - May 1980

DDC FILE COPY

Approved for public release; distribution unlimited.

AERO PROPULSION LABORATORY
AIR FORCE WRIGHT AERONAUTICAL LABORATORIES
AIR FORCE SYSTEMS COMMAND
WRIGHT-PATTERSON AIR FORCE BASE, OH 45433


23 016

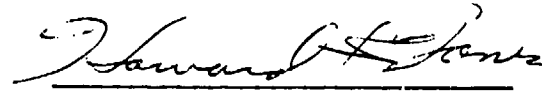
NOTICE

When Government drawings, specifications, or other data are used for any purpose other than in connection with a definitely related Government procurement operation, the United States Government thereby incurs no responsibility nor any obligation whatsoever; and the fact that the government may have formulated, furnished, or in any way supplied the said drawings, specifications, or other data, is not to be regarded by implication or otherwise as in any manner licensing the holder or any other person or corporation, or conveying any rights or permission to manufacture use, or sell any patented invention that may in any way be related thereto.


This report has been reviewed by the Office of Public Affairs (ASD/PA) and is releasable to the National Technical Information Service (NTIS). At NTIS, it will be available to the general public, including foreign nations.

This technical report has been reviewed and is approved for publication.


JOHN B. SCHRAND
Project Engineer


HOWARD F. JONES
Chief, Lubrication Branch

FOR THE COMMANDER


ROBERT D. SHERRILL
Chief, Fuels and Lubrication Division

"If your address has changed, if you wish to be removed from our mailing list, or if the addressee is no longer employed by your organization, please notify AFWAL/POSL, WPAFB, OH 45433 to help us maintain a current mailing list."

Copies of this report should not be returned unless return is required by security considerations, contractual obligations, or notice on a specific document.

19171 - 1 PT-6

SECURITY CLASSIFICATION OF THIS PAGE (When Data Entered)

REPORT DOCUMENTATION PAGE		READ INSTRUCTIONS BEFORE COMPLETING FORM
1. REPORT NUMBER	2. GOVT ACCESSION NO.	3. RECIPIENT'S CATALOG NUMBER
AFAPL/78-6, Part VI	11 14167	
4. TITLE (and Subtitle)	5. TYPE OF REPORT & PERIOD COVERED	
ROTOR-BEARING DYNAMICS TECHNOLOGY DESIGN GUIDE, Part VI, Status of Gas Bearing Technology Applicable to Aero Propulsion Machinery	Interim RPT. January 1980 - May 1980	
6. AUTHOR(s)	6. PERFORMING ORG. REPORT NUMBER	8. CONTRACT OR GRANT NUMBER(s)
Coda H. T./Pan	80-TR-57	F33615-76-C-2038
9. PERFORMING ORGANIZATION NAME AND ADDRESS		10. PROGRAM ELEMENT, PROJECT, TASK AREA & WORK UNIT NUMBERS
Shaker Research Corporation Northway 10 Executive Park Ballston Lake, NY 12019		3048/06/85
11. CONTROLLING OFFICE NAME AND ADDRESS		12. REPORT DATE
Aero Propulsion Laboratory/AFWAL/POSL) AF Wright Aeronautical Laboratories, AFSC Wright-Patterson AFB, Ohio 45433		October 1980
14. MONITORING AGENCY NAME & ADDRESS (if different from Controlling Office)		13. NUMBER OF PAGES
		94
		15. SECURITY CLASS. (of this report)
		Unclassified
		15a. DECLASSIFICATION/DOWNGRADING SCHEDULE
16. DISTRIBUTION STATEMENT (of this Report)		
Approved for public release; distribution unlimited		
17. DISTRIBUTION STATEMENT (of the abstract entered in Block 20, if different from Report)		
18. SUPPLEMENTARY NOTES		
19. KEY WORDS (Continue on reverse side if necessary and identify by block number)		
Air bearings, gas bearings, air lubrication, gas lubrication, rotor dynamics, gas turbines, turbomachinery, foil bearings, compliant bearings		
20. ABSTRACT (Continue on reverse side if necessary and identify by block number)		
This report reviews gas lubrication technology as applicable to the support of aero propulsion equipment. It contains a historical sketch of the evolution of the field, a review of relevant fundamentals, a discussion of the whirl stability phenomena, the design of thrust bearings for turbomachines, a brief report on the current state of materials development, and a general review of gas lubricated compliant bearings.		

DD FORM 1 JAN 73 1473 EDITION OF 1 NOV 65 IS OBSOLETE

SECURITY CLASSIFICATION OF THIS PAGE (When Data Entered)

391231

JCB

FOREWORD

This report was prepared by Shaker Research Corporation under USAF Contract No. AF33615-76-C-2038. The contract was initiated under Project 3048, "Fuels, Lubrication, and Fire Protection," Task 304806, "Aerospace Lubrication," Work Unit 30480685, "Rotor-Bearing Dynamics Design."

The work reported herein was performed during the period January 1980 to May 1980, under the direction of John B. Schrand (AFWAL/POSL) and Dr. James F. Dill (AFWAL/POSL), Project Engineers. The report was released by the authors in June 1980.

Accession For	
NTIS GRA&I	<input checked="checked" type="checkbox"/>
DTIC TAB	<input type="checkbox"/>
Unannounced	<input type="checkbox"/>
Justification	
By	
Distribution/	
Accession Codes	
Dissemination/or	
Distribution	
A	

TABLE OF CONTENTS

Section		Page
I	INTRODUCTION _____	1
II	HISTORICAL PERSPECTIVE _____	3
III	REVIEW OF FUNDAMENTALS _____	9
	3.1 Plain Journal Bearing _____	9
	3.2 One Dimensional Sliders _____	14
	3.3 Side Leakages of Finite Sliders _____	28
	3.4 Practical Implications of a High Compressibility Number _____	33
IV	WHIRL INSTABILITY _____	35
	4.1 Limitations of Small Perturbation Analysis _____	35
	4.2 Kinematics of Journal Bearing Motion _____	36
	4.3 Dynamic Perturbation Impedance of a Journal Bearing _____	39
	4.4 Characteristic Stiffness and Damping of a Journal Bearing _____	41
	4.5 Stability Criteria from the Isotropic Impedance Matrix _____	45
	4.6 Whirl Free Journal Bearing Configurations _____	46
V	GAS LUBRICATED THRUST BEARINGS _____	57
	5.1 External Pressurization _____	57
	5.2 Surface Features for Self Acting Thrust Bearings _____	59
	5.3 Dimensional Control _____	67
	5.4 Stability of Thrust Bearings _____	71
VI	STATUS OF AIR BEARING MATERIALS TECHNOLOGY APPLICABLE TO AERO PROPULSION SYSTEMS _____	72
VII	PROSPECTS OF COMPLIANT GAS BEARINGS _____	75

Section		Page
7.1	The Evolution_____	75
7.2	Panaromic View of Foil Bearing Technology_____	76
7.3	Challenges in Aero Propulsion Applications___	83
REFERENCES	_____	86

LIST OF ILLUSTRATIONS

Figure		Page
1	Cross Section of Eccentric Journal_____	10
2(a)	Axial Distribution of Pressure Peak in Plain Journal Bearing at Small Eccentricity_____	12
2(b)	Axial Distribution of Local Attitude Angle in Plain Journal Bearing at Small Eccentricity_____	13
3(a)	Small Eccentricity Tangential Force Plain Journal Bearing_____	15
3(b)	Small Eccentricity Radial Force Plain Journal Bearing_____	16
4	Gap Profile of a Flat Slider_____	17
5	Peak Pressure of High Speed Flat Slider_____	21
6	Pressure Distributions in Tapered Slider_____	22
7	Asymptotic Load vs Gap Ratio of Flat Slider_____	24
8(a)	Optimized Gas Lubricated Slider - Geometrical Parameters_____	26
8(b)	Optimized Slider - Performance Parameters_____	27
9	End Leakage Functions of Flat Slider_____	32
10	Side Leakage Effects of High Speed, Flat Slider_____	34
11	Load Displacement Velocity_____	37
12	Parameters of an Elliptical Orbit_____	40
13	Conceptual Design of a Pivoted Pad Journal Air Bearing for a 3.5 lb/sec Flow Rate Gas Turbine_____	47
14	Load Chart, 120° Partial Arc L/D = 1 [63]_____	49
15	Spring-Mounted Compliant-Pivot Journal Bearing [68]_____	50
16	Stabilizing Surface Features of Journal Bearing_____	52

LIST OF ILLUSTRATIONS

(Continued)

Figure		Page
17	Characteristics of 3 Lobe, Preloaded Journal Bearing [61] _____	54
18	Foil Type Journal Bearings _____	56
19	Schematic of Externally Pressurized Annular Thrust Bearing _____	58
20	Pressure Loss Characteristics of Inherently Compensated Restrictor _____	60
21	Film Inlet Pressure Perturbation Coefficient of Externally Pressurized Annular Thrust Bearing _____	61
22	Surface Features of Self-Acting Thrust Bearings _____	63
23	Optimized Load Capacity of Fixed Thrust Bearings _____	65
24	Thrust Bearing Support Flexure [21] _____	69
25	Tension Intershaft Foil Bearing Assembly _____	78
26	Schematic of One-Dimensional Leaf Thrust Bearing _____	79
27	Schematic Drawing of Coil Type Journal Foil-Bearing With Integral Leaf Spring [107] _____	81
28	Compliantly Supported Spiral Groove Thrust Bearings [108] _____	82

LIST OF SYMBOLS

Symbol	Definition
b	Length of a slider
b_{α}	Damping coefficient of the α th mode
b_{xx} , etc.	xx element of damping matrix, etc.
C	Radial clearance; reference gap; a constant in the solution for an optimized compressible slider
e	Eccentricity
d	Feedhole (inherent restrictor) diameter
D	Diameter of journal, $2R$
F_R	Radial component of journal bearing reaction force
F_T	Tangential component of journal bearing reaction force
$\{\delta F\}$	Perturbation force, a column vector
h	Film thickness
h_e	Exit film thickness of a slider
h_{β}	Film thickness at the step of an optimized, compressible slider
h_o	Equilibrium film thickness
h^*	A constant parameter in the solution of an infinitely long, flat slider
\bar{h}	Dimensionless film thickness, h/C
δh	Perturbed film thickness
Δh	Excess of inlet film thickness above the exit film thickness of an infinitely long slider
Δh_{β}	Step depth of an optimized compressible slider
H	$\frac{h}{h_e + \Delta h}$
j	$\sqrt{-1}$
k_{α}	Stiffness coefficient of the α th mode

k_{xx} , etc.	xx element of stiffness matrix, etc.
K	Pressure loss coefficient of inherent restriction
ℓ	Width of slider
L	Length of journal
\dot{m}	Mass flow rate through feed hole
n	Number of feedholes
N_R	Restrictor flow Reynolds number
p	Film pressure
p_a	Ambient pressure
p_{in}	Film inlet pressure
p_o	Equilibrium film pressure
p_s	Supply pressure
δp	Perturbed film pressure
δr_1	Major radius of elliptical orbit
δr_2	Minor radius of an elliptical orbit
R	Radius of journal, $D/2$; universal gas constant
R_i	Inner radius of annular thrust bearing
R_o	Outer radius of annular thrust bearing
t_1	Time at major radius of elliptical orbit
T_c	Moment about the leading edge of a flat slider excluding side leakage effects
T_D	Moment deficiency due to side leakage effects
$\delta u, \delta v$	Forward and backward circular whirl components of a perturbed orbit
V	Sliding speed
$\{\delta w\}$	Perturbation displacement
$\{\delta w_\alpha\}$	Eigenvector of the α th mode
W_c	Load of a flat slider excluding side leakage effects
W_D	Load deficiency due to side leakages
W_∞	Limit of bearing load capacity for $\Lambda \rightarrow \infty$

\bar{W}	Dimensionless load of a slider, $\frac{W}{p_a \ell b}$
$\delta x, \delta y$	Instantaneous displacement components of journal center
$\delta x_o, \delta y_o$	Equilibrium displacement components of journal center; values of $(\delta x', \delta y')$ at reference time
$\delta x_\alpha, \delta y_\alpha$	Elements of $\{\delta w_\alpha\}$
$\delta x', \delta y'$	Perturbed displacement components of journal center
$\dot{\delta x}, \dot{\delta y}$	Perturbation velocity components of journal center
x	Distance from leading edge; Cartesian coordinate in the direction of load
y	Cartesian coordinate in the radial plane in quadrature with the direction of load
z	Axial coordinate
$Z_{xx}, \text{etc.}$	xx element of $[Z]$, $k_{xx} + j\omega b_{xx}$, etc.
$Z_{//}$	Diagonal element of an isotropic $[Z]$, $1/2 (Z_{xx} + Z_{yy})$
Z_{\perp}	Off diagonal element of an isotropic $[Z]$, $1/2 (Z_{xy} - Z_{yx})$
$[Z]$	Perturbation impedance matrix of journal bearing
$(\dot{})$	Time derivative

α	Mode number index; width fraction of groove
β	Width fraction of step of an optimized slider; helix angle of groove measured from circumference
β_1	$\frac{\lambda}{2} + \sqrt{\left(\frac{\lambda}{2}\right)^2 - \lambda h^*}$; inclination of major axis of an elliptical orbit to the load direction
β_2	$\frac{\lambda}{2} - \sqrt{\left(\frac{\lambda}{2}\right)^2 - \lambda h^*}$
γ	Radial fraction of grooved surface of an annular, spiral groove, thrust bearing
δ^*	Penetration depth of side leakage effects
Δ	Depth/gap ratio of groove
ϵ	Eccentricity ratio, e/C
ζ	$\sqrt{\frac{\Delta h}{h_e + \Delta h}} \quad \eta$
η	Stretched coordinate for side leakage analysis of a compressible slider, Eq. (33)
θ	Angular coordinate measured from minimum gap
λ	$\frac{6\mu V\ell}{p_a h_e \Delta h}$
Λ	Compressibility number: $\frac{6\mu\omega R^2}{p_a C^2}$ for journal bearing, $\frac{6\mu V\ell}{p_a h_e^2}$ for slider
Λ_i	$\frac{6\mu V\ell}{p_a (h_e + \Delta h)^2}$

$\Lambda(t)$	$\frac{6\mu(\omega \pm 2\nu)R^2}{p_a C^2}$
μ	Viscosity coefficient
ν	Circular frequency of oscillation
ξ	x/ℓ
ϕ	Attitude angle
ϕ_x	Phase angle of $\delta x'$
ψ	$\frac{ph}{p_a h_e}$
Ψ	$\frac{ph}{p_a (h_e + \Delta h)}$
ω	Angular speed of rotation

SECTION I

INTRODUCTION

Interest in the use of air bearings to support the rotor of an aircraft type gas turbine power plant is based on the expectations that

- use of air bearings improves the prospect of raising the turbine inlet temperature to achieve savings in fuel economy;
- air bearings are inherently more suitable for high speed operation and therefore can enhance the power density of the power plant;
- potential system reliability may be improved because of overall mechanical simplicity of the air bearing system;
- vulnerability of the power plant is reduced by the elimination of oil lines and lube system hardware; and
- cost realism appears to be achievable with potential of cost improvement in several air bearing concepts.

While the technology status of gas lubrication has significantly matured in the recent two decades, many profitable applications of air or gas bearings have become well established. However, the momentum in the technological growth of gas lubrication has shown signs of waning in recent years. There are three reasons for this trend.

- (1) Essential technological foundations are well in place. Meaningful engineering applications can run their course without need for special attention.
- (2) The element of indispensibility of using gas bearings is significantly reduced with the reorientation and downscoping of America's space program in recent years.
- (3) Successful applications of gas bearings are most of the time

associated with very benign environments. This image tends to inhibit serious consideration in more demanding circumstances.

In the specific area of air bearings for high temperature machinery, however, the interest has continued. While many problems remain in the practical use of air bearings in a high temperature environment, there have been important advances which raise hope for its ultimate realization. The emergence of air lubricated compliant bearings deserves special note in that it leaves open the possibility for the thin load carrying air film to be maintained despite inherent thermal transients and gradients in high temperature machinery. The state of development is moving rapidly. Similar but competitive approaches are being actively pursued. Opportunities for major innovations are still open. It is not realistic to attempt a definitive coverage of the subject at this time. Therefore, as a part of the Rotor-Bearing Dynamics Technology Design Guide update, this document is prepared with the spirit of sober assessment. A historical review of events in the evolution of gas lubrication is included as general background, with emphasis of identifying successful gas bearing applications. Selected topics of fundamentals which address vital aspects of aero propulsion applications are reviewed in some details. Some technological approaches which may not be in current favor are discussed, if they are concerned with issues which are still relevant, hoping their knowledge may inspire more fruitful efforts in the future. Major recent and current developments are recounted to the best of the writer's ability. A deliberate attempt, however, is made to suppress enthusiasm or criticism in favor of objectivity.

SECTION II

HISTORICAL PERSPECTIVE

First knowledge of gas lubrication as a physical phenomenon was attributed to the French scientist-engineer Gustav Adolph Hirn [1]. He measured the friction between a bronze half bearing and a polished cylindrical drum using as lubricants fats, and twelve natural oils, in addition to water and air. Because his findings were contrary to Coulomb's law of friction, formal publication of his results was delayed for seven years. Half a century later, in the United States, Albert Kingsbury demonstrated the operation of an air-lubricated, self-acting journal bearing prior to his subsequent exposure to Reynolds' theory of lubrication. Kingsbury's model bearing carried a unit load of over 1 psi. He also recorded the pressure profile around the bearing. Some 20 years later, W. J. Harrison, while a lecturer at the University of Liverpool, successfully performed a numerical computation of the isothermal, gas lubrication equation as applied to an eccentric journal bearing. Harrison compared compressible and incompressible solutions of the pressure profile with the experimental data published by Kingsbury, and confirmed the effect of compressibility. Harrison's feat was convincing testimony of the power of perseverance combined with ingenuity. To complete a single set of calculations, he had to record 12,000 digits of number by hand.

These momentous events took place within a century following the period of industrial revolution in Western history. They are truly pioneering landmarks in the scientific development of the theory of lubrication. They contained the elements of multi-disciplinary and international contributions which have been characteristic of the modern developments of tribology.*

*The word tribology was promulgated by the British government in 1966. It is derived from the Greek tribos (rubbing) and is defined as "the science and practice of interacting surfaces in relative motion and of the practices related thereto."

Gas lubrication had also attracted an incidental attention from the great Arnold Sommerfeld, who is recognized as the father of modern theoretical physics, being the mentor of such notables as Berthe, Debye, Echart, Heisenberg, Herzfeld, Lande, London, von Laue, Pauli, and Pauling. Sommerfeld's association with gas lubrication was rather passive. During the brief sojourn at the Technological Academy of Aachen, where his famous solution of the Reynolds equation for the journal bearing was completed, he took notice that gas lubrication interferes with the study of dry friction between solids. The same view was independently expressed by Charron [2].

Early interests in the industrial use of gas lubricated bearings were associated with textile spindles [3,4,5] and grinding spindles [6]. It is quite evident that the inherent advantage of gas bearings for high speed applications was already recognized.

While scientific interests in friction and lubrication began with primarily the physical and the mechanistic points of view, early advances in the art of bearing engineering were mainly associated with wheel axles of carriages and railroad activities. Increased human exploitations in the use of mineral oils soon dictated the course of development in all phases of tribology. The term lubricant, most of the time, suggests a mineral oil. The significance of chemistry in the field of lubrication and wear was soon established through the pioneering efforts of William Bate Hardy (a biologist!). The classical dissertations of Hardy and Doubleday [7,8,9] clarified once and for all the role of the surface layers. A mineral oil lubricant allows oriented long molecules to be attached to each bearing surface. The solid surfaces are separated by the layers of oriented molecules so that sliding friction is low, and the attendant danger of surface damage is minimal. This factor is so important in the endurance of machine elements in real applications that because of its absence in gas bearings, very little serious attempt was put forth to promote large scale use of gas bearings for many years. Thus, the invention of various types of engines, the wide spread use of automobiles,

and the human's success in becoming airborne were all associated with oil lubricated processes. Many advances in rolling element and fluid film bearings have been possible because adequate boundary lubrication can be taken for granted. Improvements in the technique of boundary lubrication have paced the progress of industrial tribology. In fact, it took none other than the inadequacies of oil lubrication in special environments to revitalize interests in gas bearings.

Shortly after the conclusion of World War II, growth of nuclear technology rekindled industrial interest in gas lubrication. Nuclear engineers soon realized that conventional machinery with oil lubricated bearings are not suitable for various nuclear processes. A radioactive environment causes rapid deterioration of the lubricating oil. In addition, a minute trace of oil vapor can seriously impede the desired reaction process. Early gas bearing machines for the nuclear industry were equipped with externally pressurized gas bearings. There were two reasons for this practice. Wearing of the bearing surfaces is unavoidable during starts and stops. By employing external pressurization, sliding contact of bearing surfaces is avoided altogether. Thus bearing designers bypassed the materials problems in the early years. A second reason for preferring externally pressurized bearings is related to the possibility of a high speed journal bearing to become dynamically unstable. Although this problem also exists for oil or other liquid lubricated journal bearings, it is more serious for gas bearings because gas bearing rotating machines tend to run at higher speeds.

The penalty of power consumption required by externally pressurized gas bearings spurred an intensive development of the self-acting gas bearing technology in the ensuing years. By that time the race to the moon between the two leading world powers had begun. Gas bearings appeared very attractive to space program planners. Because auxiliary equipment for lube treatment would not be needed, weight reduction for the overall system could be considerable. Furthermore, gas lubrication was a natural concept associated

with high power-density dynamic machines then envisioned for space applications. The environment of weightlessness underscored the importance of avoiding dynamic instability of high speed journal bearings. Up to that time, the provision of a static load, which is naturally present in the earth environment, was the main engineering approach to achieve journal bearing stability.

The impetus of the space race added to the already considerable expectations of gas lubrication from defense and atomic energy programs. Important advances were made in bearing materials as well as on theoretical issues. Numerical computation evolved as a powerful engineering tool for gas bearing design activities. A variety of hard coatings, bonded to a more or less conventional structural substrate proved to be very promising candidates as gas bearing materials [10]. Typically, like materials are used on both surfaces of the bearing. Theoretical means to assess the stability issue, with or without the direct use of a computer program, have in essence been firmly established [11,12,13]. A number of journal bearing configurations, possessing inherent features to assure high speed stability, have become known. They include tilting pads [14], lobed bushings [15], shrouded step pads [16], helical grooving [17], and foil type journal bearings [18,19,20].

In turbomachinery applications, the thrust bearing design can be very problematic. Impellers tend to have thrust loads which vary with operating conditions. Such thrust load levels attain very large magnitudes in high power-density turbomachines. In order to meet the required load capacity, the thrust bearing may have to be extremely large [21]. Accordingly, the bearing friction power can become a limiting factor in the realizable efficiency of the machine. The large bearing friction power also impedes the achievable load capacity directly by causing thermal distortions of the bearing surface [22]. Thus, there is a high premium associated with thrust bearing configurations of the most favorable load/friction ratio. An additional complication is the possibility for a thrust bearing to become unstable [23,24,25]. This phenomenon is more prominent at a reduced ambient environment.

The frenzy of the space race aided the technology growth of gas lubrication in many other ways. Use of air lubricated devices began to appear in precision machine shops. Use of high speed spindles for the grinding head was given the credit for achieving both dimensional accuracy and super fine surface finishes. Air gaging became a common inspection practice. Linearly-traversing and rotary tables added to the list of sophisticated metrology equipment made possible by air bearings [26]. The advances in precision fabrication in turn facilitated the realization of some gas bearing applications. The most prominent example included gas lubricated inertial sensors of both rotating and non-rotating varieties. A high quality gyroscope may have a gas lubricated spin bearing with a nominal radial clearance in the neighborhood of 1 micron. This type of gyroscope is still the standard for accuracy in navigation systems. It has filled a common need shared by marine, aircraft, and space flight navigation systems [27].

The first major large scale use of air bearings is the air turbine dental drill [28]. Rotating at about 500,000 rpm, such a tool requires very low contact force to remove hard materials. Consequently tooth repair can be performed with minimal sensation felt by the patient. Stability of the drill spindle is achieved by rubber mounting the bearing bushing. Undoubtedly, the introduction of such a tool into the practice of dentistry added to the requirement of nimble hand skill in the profession.

Another important application of air bearings is the foil mill tension gage [29]. Externally pressurized air bearings support a series of tandemly arranged rollers which are in contact with the fast moving foil wrapped around a small arc angle of the rollers. Tension in the foil is thus directly proportional to the radial load experienced by the individual rollers. Differential pressure sensing of pressure in the bearing film at the midplane along the bisector of the wrap angle thus provides the signal to actuate necessary control functions to maintain uniformity of tension.

Gas lubrication has also played a non-trivial role in the phenomenal growth of computer technology in recent years. Mass magnetic memory devices such as the tape drive [30] and the disc or drum [31,32,33] depend on air lubrication for reliable operation. In both cases, the memory surface slides past the read-write flying head with an air gap no more than one half of a micron. The common experience of trouble free operation of such devices is a most impressive testimony of the dependability of air lubrication. Application of air lubrication to the spindle of high speed magnetic storage drums appears to be the logical next step [34].

Technology advances related to the tape drive have spurred the prospect of utilizing foil bearings for the support of high speed rotors [35]. Flexibility of the foil enhances relative conformity and thus maintains a relatively uniform film pressure for load support. The foil bearing also appears to be more capable of surviving accidental high speed contacts [36,37,38]. Air cycle machines supported on air lubricated foil bearings have been in commercial use since 1972 [39]. Favorable field experience for this application has stimulated efforts to demonstrate the feasibility of other large scale applications of air lubricated foil bearings [40,41,42].

It is presumptuous to suggest any parity between the recent developments in gas lubrication with the historic events described in Professor Dowson's anthology. It is nevertheless possible to recount the more significant happenings with some retrospective wisdom. An honest attempt to look back at these events with objectivity and aloofness is believed to be beneficial to all workers in this field. The cautious and prudent may be reassured that good judgment combined with patience and perseverance had surmounted very difficult problems. The innovative and ambitious should be alerted to meaningful guiding principles so that their energy and enthusiasm may be directed along paths which are compatible with laws of nature.

SECTION III

REVIEW OF FUNDAMENTALS

The operation of gas bearings for turbomachines is governed by the isothermal theory of gas lubrication [43,44,45]. For the present purpose, the self-acting type bearings are of interest. Modern design methods of gas bearings generally involve some form of numerical computation of the governing equations [46,47]. Separate attention must be given to the specific bearing configuration. In the present chapter, model problems which reveal generally valid trends are discussed.

3.1 Plain Journal Bearing (See Figure 1)

The solution of the film pressure of the plain, gas-lubricated, journal bearing under a small steady eccentricity is

$$p = p_a \left[1 + \epsilon \operatorname{Re} \left\{ \frac{j e^{j\theta} \Lambda}{1+j\Lambda} \left[1 - \frac{\cosh \sqrt{1+j\Lambda} (z/R)}{\cosh \sqrt{1+j\Lambda} (L/D)} \right] \right\} \right] \quad (1)$$

This result contains two parameters; namely the geometric parameter L/D and the compressibility number $\Lambda = 6\mu\omega(R/C)^2/p_a$. The latter is peculiar to gas bearings. The small Λ approximation corresponds to the case of an incompressible fluid film:

$$\lim_{\Lambda \rightarrow 0} \frac{(p - p_a)}{\epsilon p_a} = -\Lambda \left[1 - \frac{\cosh (z/R)}{\cosh (L/D)} \right] \sin \theta \quad (2)$$

Three important characteristics may be observed.

1. Pressure rise above ambient is linearly proportional to Λ , or the product $\mu\omega$.
2. Peak of pressure is 90 degrees upstream of the minimum gap location.
3. Axial pressure is quite flat for a large (L/D) except near

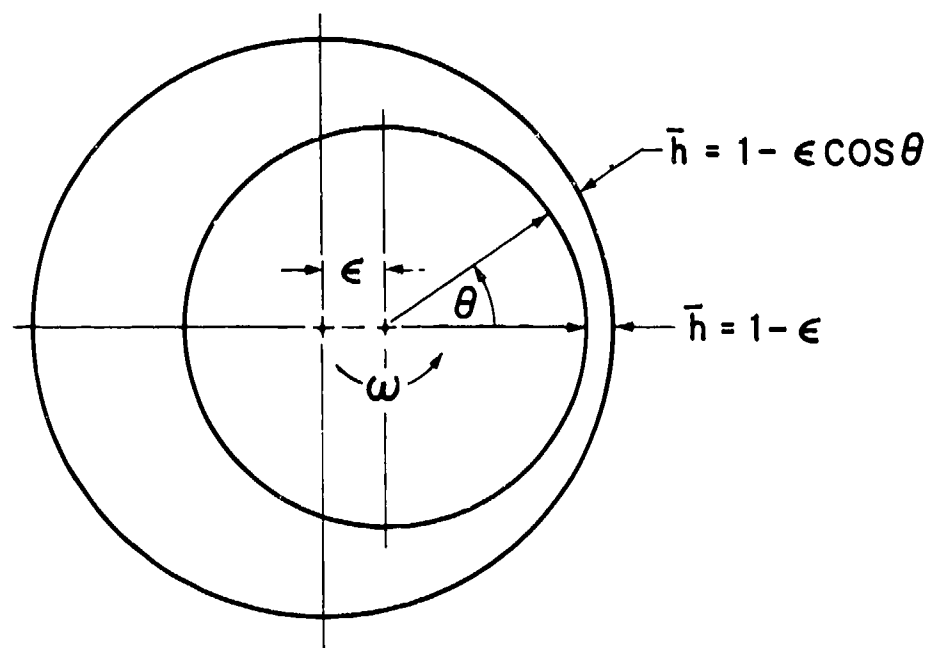


Figure 1 Cross Section of Eccentric Journal

the bearing ends, and is nearly parabolic for a small L/D .

In the other extreme, if Λ is very large,

$$\lim_{\Lambda \rightarrow \infty} \frac{p - p_a}{\epsilon p_a} = \text{Re} \left\{ \left[1 - \frac{\cosh \sqrt{j\Lambda} (z/R)}{\cosh \sqrt{j\Lambda} (L/L)} \right] e^{j0} \right\} \quad (3)$$

The contrasting features are

1. Pressure rise above ambient is proportional to the ambient pressure but independent of the product $\mu\omega$.
2. Peak pressure at the midplane is in line with the minimum gap location.
3. The apparent L/D is $\sqrt{\Lambda} (L/D)$. In addition, there is an undulating behavior in its axial distribution.

To illustrate these ideas, the peak pressure, scaled by the factor $\Lambda/\sqrt{1+\Lambda^2}$, and its angular location (local attitude) are plotted against the axial location for various combinations of (L/D) and Λ in Figure 2.

In terms of physical parameters, Λ depends principally on the ambient pressure level, gas viscosity, shaft speed, and the radial clearance ratio C/R . Representative values of Λ are shown below:

RPM	Viscosity (Reyns) 2.7×10^{-9}				5.4×10^{-9}		
	Ambient (psia)	5.0	14.7	50.0	5.0	14.7	50.0
10,000	$C/R = 10^{-3}$	3.3929	1.1541	0.3393	6.7858	2.3082	0.6786
	5×10^{-4}	13.5717	4.6162	1.3572	27.1434	9.2324	2.7144
	2×10^{-4}	84.8230	28.8514	8.4823	169.6460	57.7028	16.9646
	1×10^{-4}	339.2920	115.4054	33.9292	678.5840	230.8108	67.8584
50,000	10^{-3}	16.9646	5.7703	1.6965	33.9292	11.5405	3.3930
	5×10^{-4}	67.8584	23.0811	6.7858	135.7168	46.1622	13.5716
	2×10^{-4}	424.1150	144.2568	42.4115	848.2300	288.5136	84.8223
	1×10^{-4}	1696.4600	577.0272	169.6460	3392.9201	1154.0544	339.2920

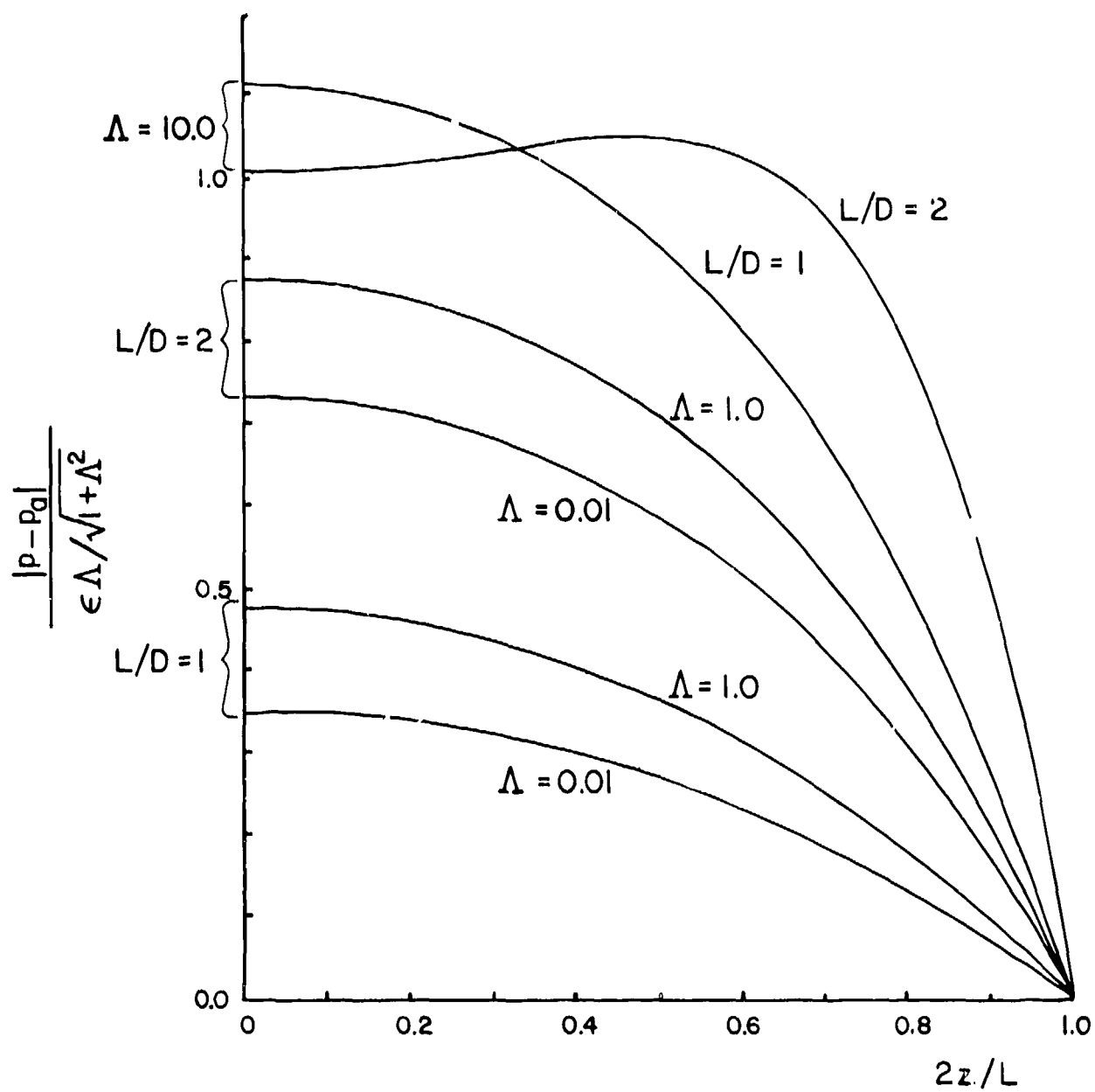


Figure 2(a) Axial Distribution of Pressure Peak in Plain Journal Bearing at Small Eccentricity

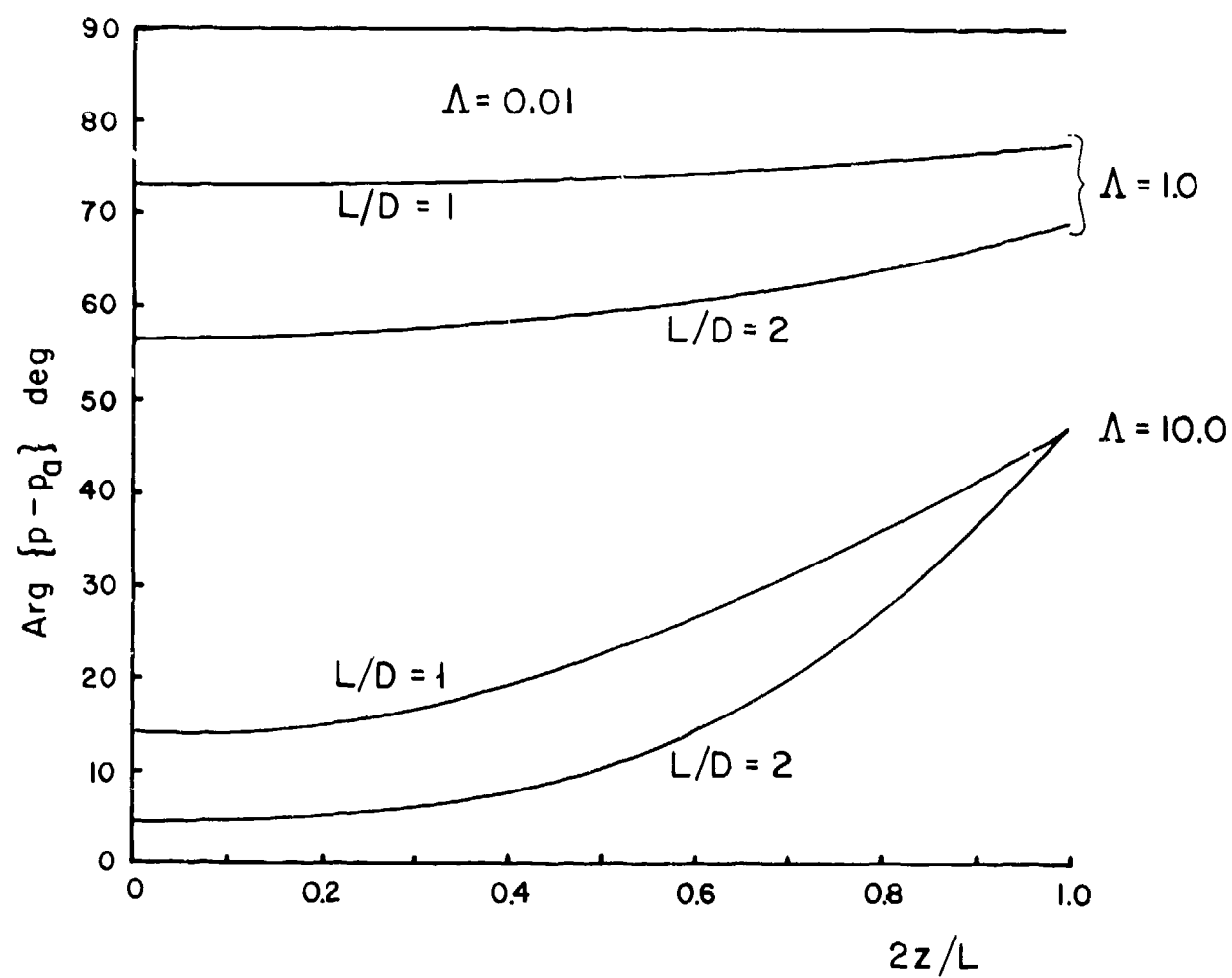


Figure 2(b) Axial Distribution of Local Attitude Angle in Plain Journal Bearing at Small Eccentricity

The strongest effect is associated with (C/R) . The value 2×10^{-4} is a reasonable estimate for the overload condition. An even smaller value may apply for the liftoff condition. It is quite evident that a moderate to a very large value of Λ is of interest.

The bearing reaction is directly proportional to the radial displacement in the small eccentricity approximation. It is in general inclined to the displacement vector and is thus defined by its radial and tangential components as shown in Figure 3. It may be observed that relative insensitivity of the bearing reaction to Λ occurs beyond $\Lambda = 3.6$ for $L/D = 1$, where the tangential component peaks.

3.2 One Dimensional Sliders

The flat slider is an important configuration to understand. Its film pressure is amenable to analytical examination and can thus render considerable insight regarding the basic character of gas bearings. The film pressure distributions in a tilting pad and in the leaf type foil bearings are similar to that in the flat slider. The high compressibility number condition of a slider is essentially that of the flying head of a disc memory device, although the recent design trend tends to favor a short strip configuration so that the end leakages may not be negligible. The optimized slider is a model for the liftoff problem. At the liftoff incipience, the effective film thickness is roughly twice the surface roughness; and thus, depending on the surface finish, would be in the order of $1 \mu\text{m}$ or less for gas bearings. The liftoff speed is a function of the prevailing load. If liftoff is to take place at a certain speed, the corresponding compressibility number is accordingly fixed. The maximum load must be limited by the load capacity of the optimized slider. In principle, in order to realize such a liftoff capability, the bearing gap should somehow be shaped according to that of the optimized slider.

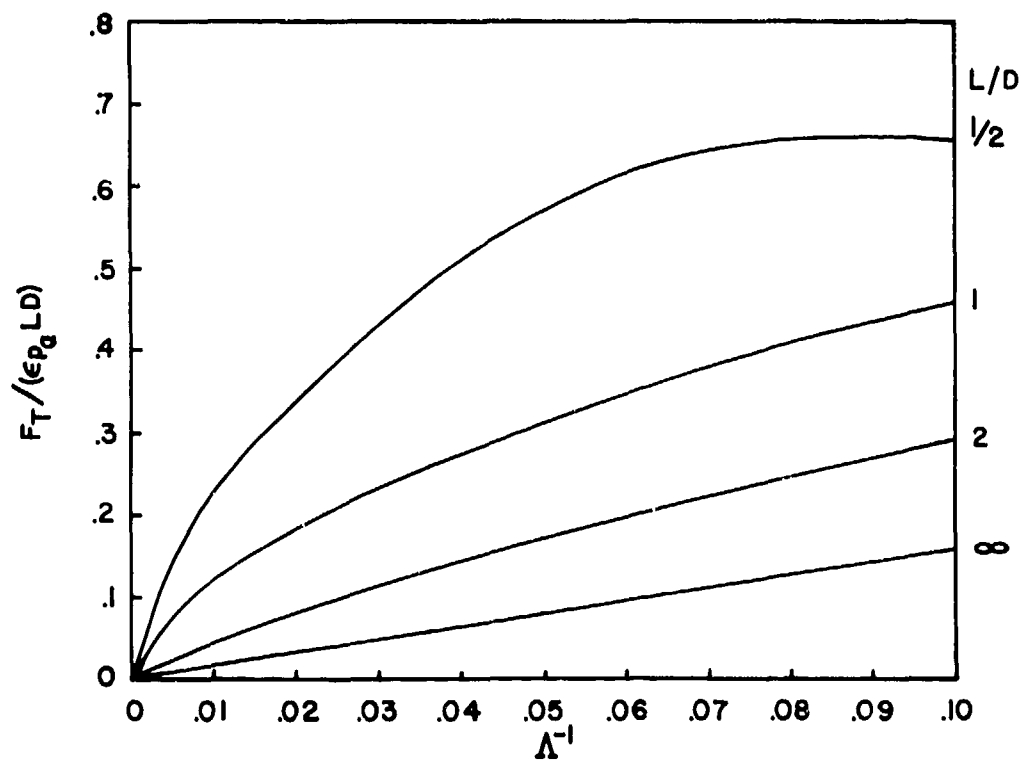
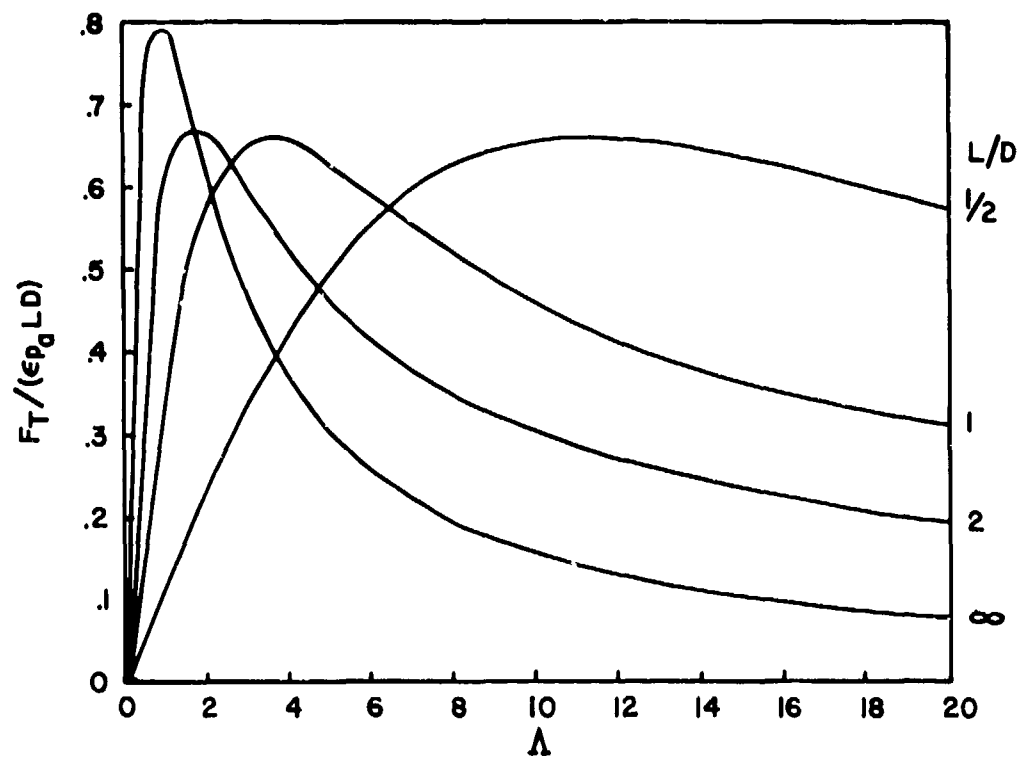


Figure 3(a) Small Eccentricity Tangential Force
Plain Journal Bearing

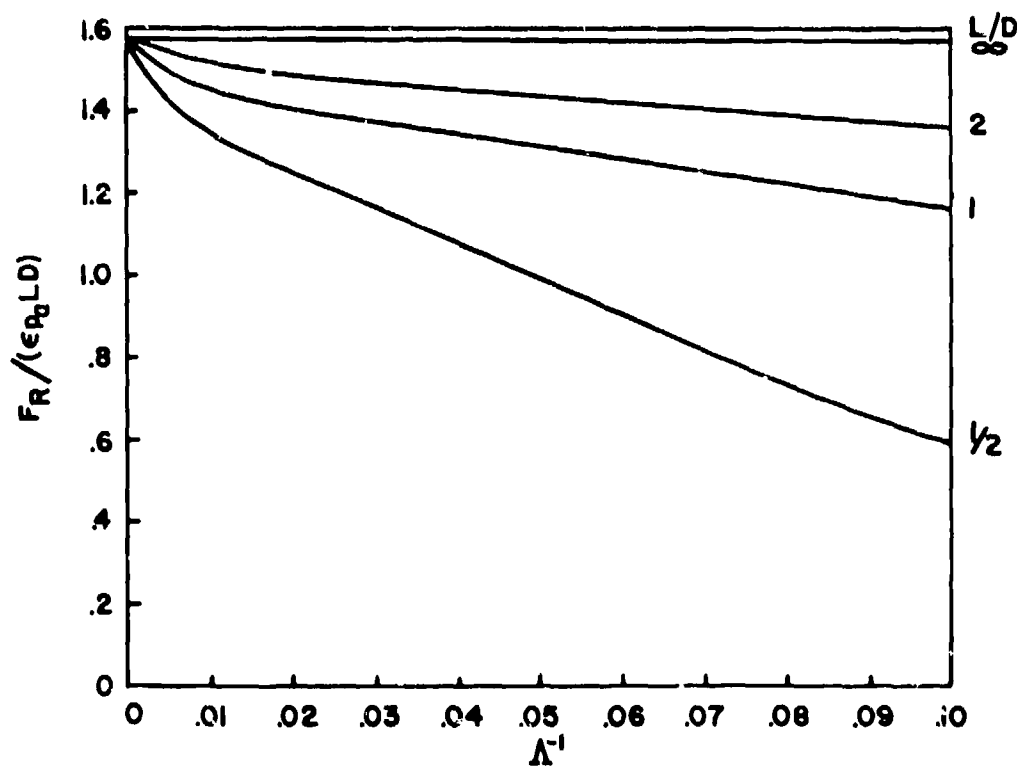
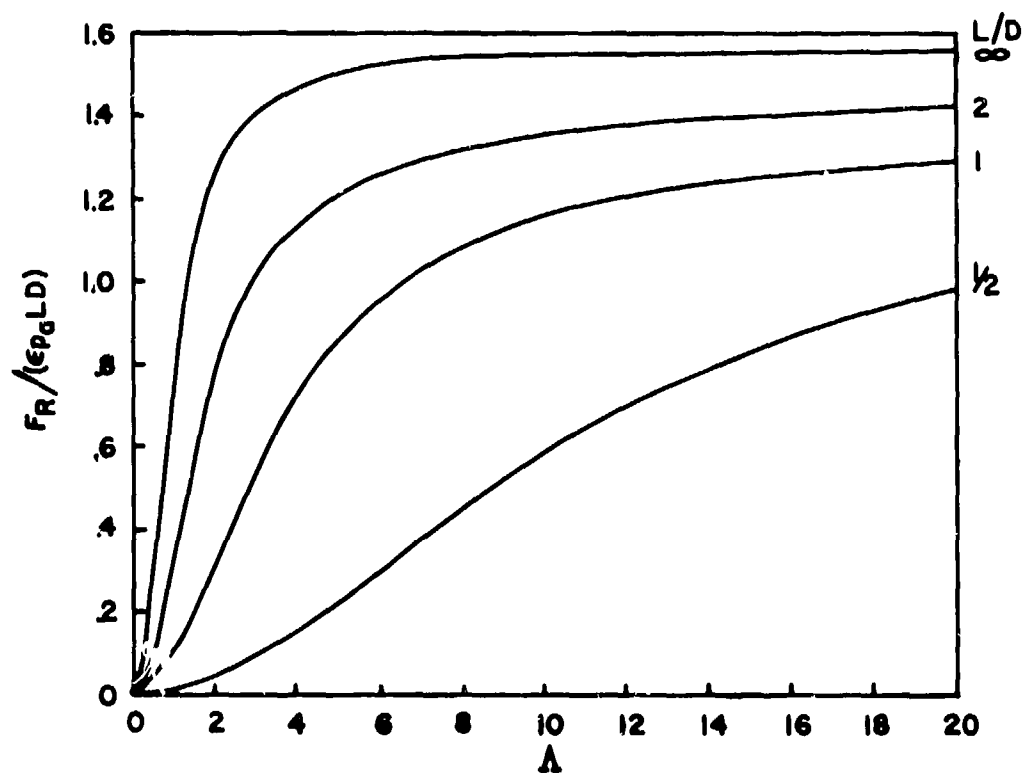


Figure 3(b) Small Eccentricity Radial Force Plain Journal Bearing

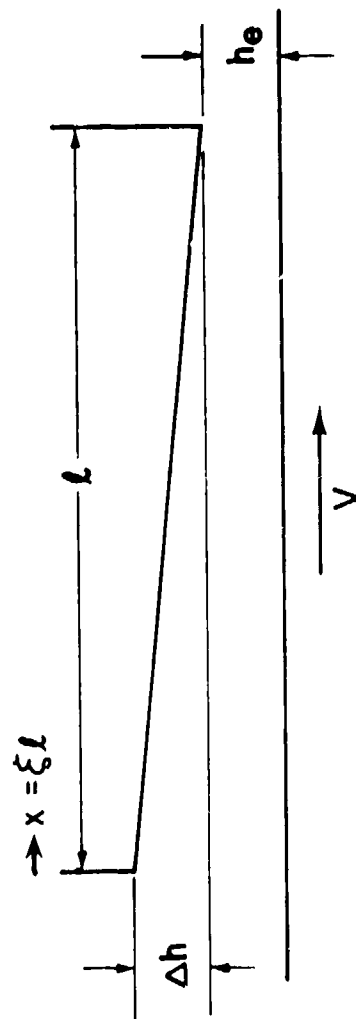


Figure 4 Gap Profile of a Flat Slider

The theoretical result for the infinitely long, gas-lubricated, flat slider (Figure 4) was included in Harrison's classical treatise [45,48]. The solution of the film pressure can be expressed in terms of the variable

$$\psi = \frac{ph}{p_a h_e} \quad (4)$$

which is to satisfy the relationship

$$\frac{(\psi - \beta_1)(\psi - \beta_2)}{(1 - \beta_1)(1 - \beta_2)} \left[\begin{pmatrix} 1 - \beta_2 \\ 1 - \beta_1 \end{pmatrix} \begin{pmatrix} \psi - \beta_1 \\ \psi - \beta_2 \end{pmatrix} \right]^{\lambda / (\beta_1 - \beta_2)} = \left(\frac{h}{h_e} \right)^2 \quad (5)$$

where,

$$\lambda = \frac{6\mu V \ell}{p_a h_e \Delta h}$$

$$(\beta_1, \beta_2) = \frac{\lambda}{2} \pm \sqrt{\left(\frac{\lambda}{2}\right)^2 - \lambda h^*} \quad (6)$$

Equation (5) is of a form that the exit condition is always satisfied. The inlet condition:

$$\psi = p_a (h_e + \Delta h); h = h_e + \Delta h \quad (7)$$

represents a constraint which fixes the value of h^* . h^* is the value of ψ at the pressure peak.

The condition of a large λ is of special interest in turbomachine application because it governs the overload capability and the lift off speed. Since

$$\lim_{\lambda \rightarrow \infty} \begin{cases} \frac{\psi - \beta_1}{1 - \beta_1} = 1 + o\left(\frac{1}{\lambda}\right) \\ \frac{\lambda}{\beta_1 - \beta_2} = 1 + \frac{2h^*}{\lambda} + o\left(\frac{1}{\lambda^2}\right) \\ \beta_2 = h^* + o\left(\frac{1}{\lambda}\right) \end{cases}$$

Equation (5) becomes

$$\lim_{\lambda \rightarrow \infty} \left(\frac{\beta_2 - \psi}{\beta_2 - 1} \right)^{-\beta_2/\lambda} = \frac{h}{h_e} \quad (8)$$

In order to satisfy the inlet boundary condition as given by Equation (7),

$$\lim_{\lambda \rightarrow \infty} \left[\frac{\beta_2 - (h_e + \Delta h)/h_e}{\beta_2 - 1} \right]^{-\beta_2/\lambda} = \frac{h_e + \Delta h}{h_e}$$

which yields

$$\beta_2 = \left(1 + \frac{\Delta h}{h_e}\right) + \frac{\Delta h}{h_e} \left(1 + \frac{\Delta h}{h_e}\right)^{-\lambda h_e / (h_e + \Delta h)} \quad (9)$$

$$h^* = \left(1 + \frac{\Delta h}{h_e}\right) - \frac{1}{\lambda} \left(1 + \frac{\Delta h}{h_e}\right)^2 \quad (10)$$

The gap where pressure peaks is found by substituting h^* for ψ and making use of Equations (9) and (10) in Equation (8):

$$\left(\frac{h}{h_e}\right)_{\text{pressure peak}} = \left[\frac{(1 + \Delta h/h_e)^2}{\lambda \Delta h/h_e} \right]^{-\frac{1}{\lambda} (1 + \Delta h/h_e)} \quad (11)$$

Accordingly the peak pressure is

$$\left(\frac{p}{p_a}\right)_{\text{peak}} = \left(1 + \frac{\Delta h}{h_e}\right) \left[\frac{(1 + \Delta h/h_e)^2}{\lambda \Delta h/h_e} \right]^{\frac{1}{\lambda} (1 + \Delta h/h_e)} + o\left\{\frac{1}{\lambda}\right\} \quad (12)$$

The peak pressure rise above ambient is seen to be bounded by $(\Delta h/h_e) p_a$ due to compressibility. Figure 5 shows the dependence of the peak pressure on $\Delta h/h_e$ and λ .

The dependence of the entire pressure on λ for a fixed geometry is illustrated in Figure 6. The asymptotic pressure profile is seen to be the upper bound envelope, which is

$$p_\infty = p_a \left[\frac{h_e + \Delta h}{h_e + (\ell - x) \Delta h / \ell} \right] \quad (13)$$

The asymptotic load (per unit length)

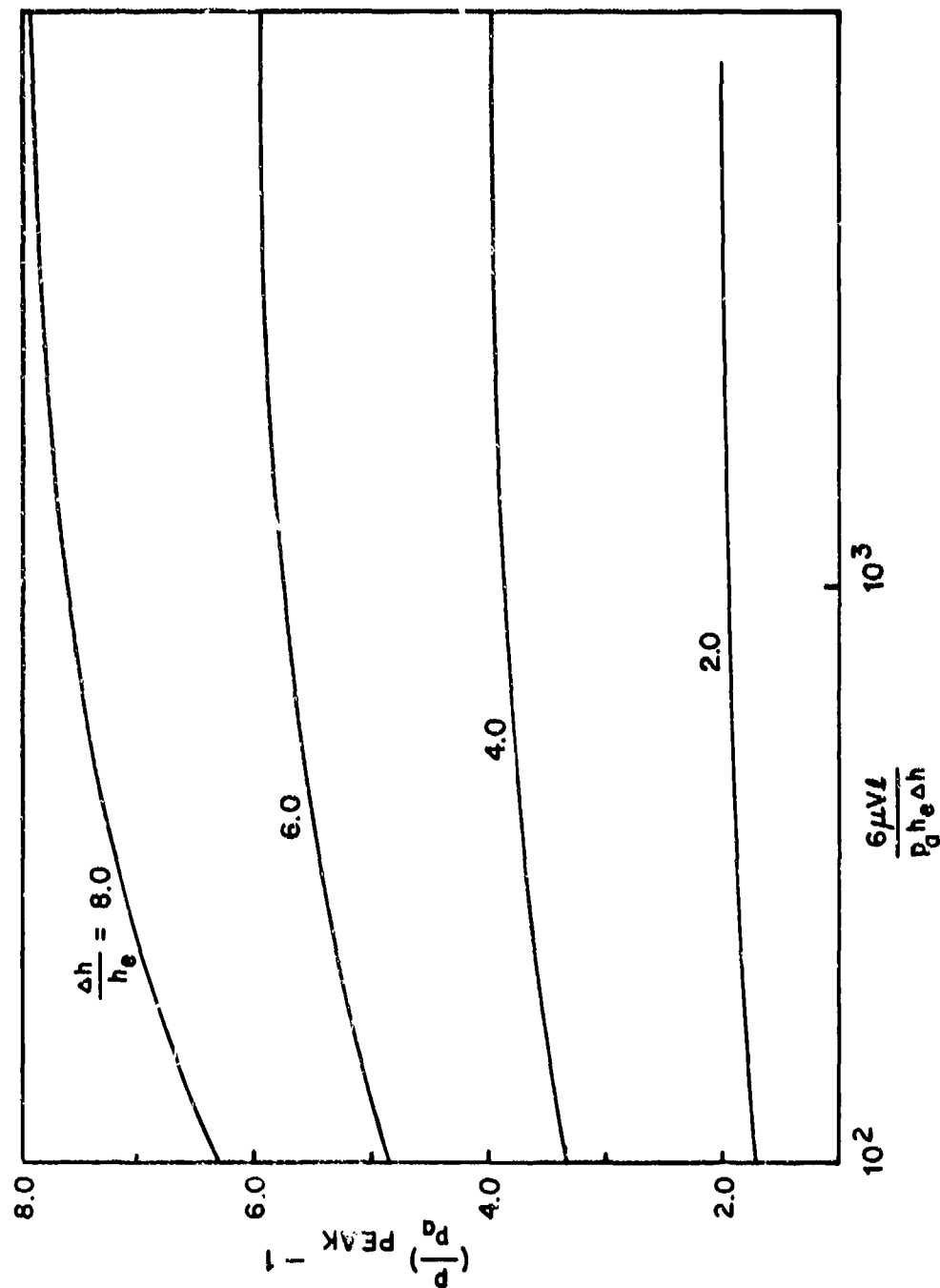


Figure 5 Peak Pressure of High Speed Flat Slider

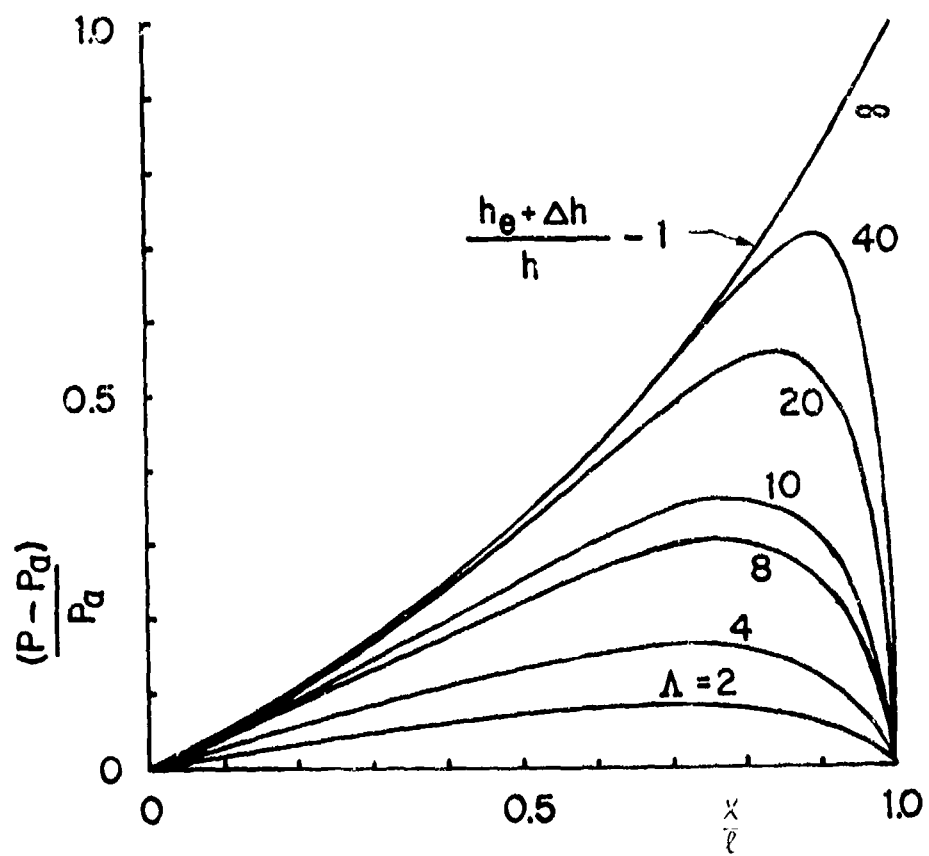


Figure 6 Pressure Distributions in Tapered Slider
 $\Delta h/h_e = 1$

$$\begin{aligned}
W_{\infty} &= \int_0^{\ell} (p_{\infty} - p_a) b dx \\
&= p_a \ell b \left\{ \left(\frac{h_e + \Delta h}{\Delta h} \right) \ln \left[(h_e + \Delta h) / h_e \right] - 1 \right\}
\end{aligned} \tag{14}$$

is the upper bound load capacity of the gas-lubricated, flat slider, and is determined by $\Delta h/h_e$ in the dimensionless form as shown in Figure 7.

The optimum compressible slider problem was considered by Maday [49] and re-examined by McAllister, et al [50]. The global optimum slider, that is the slider which carries the largest possible load with the given minimum gap and compressibility number, was found to have the gap profile of a tapered step as illustrated in Figure 8. The compressibility number of the optimum gas slider is defined in terms of the exit gap:

$$\Lambda = \frac{6\mu V \ell}{p_a h_e^2} \tag{15}$$

The gap profile is characterized by three parameters; namely the inlet gap excess $\Delta h/h_e$, the location of the step β , and the step $\Delta h_{\beta}/h_e$. The peak pressure p_{β} is located at the step. The celebrated Rayleigh solution of 1918 [51] is the special case for $\Lambda \rightarrow 0$. The gap is

$$\begin{aligned}
H &= \frac{3}{2} C \left[1 - \left(\frac{4\Lambda}{27C^2} \right) \left(\frac{x}{\ell} \right) \right] \text{ for } 0 \leq x < \beta \ell \\
H &= 1 \text{ for } \beta \ell < x \leq \ell
\end{aligned} \tag{16}$$

The pressure distribution in the inlet taper is

$$p/p_a = \left[1 - \left(\frac{4\Lambda}{27C^2} \right) \left(\frac{x}{\ell} \right) \right]^{-1} \tag{17}$$

for $0 \leq x < \beta \ell$. That in the exit land satisfies the transcendental equation

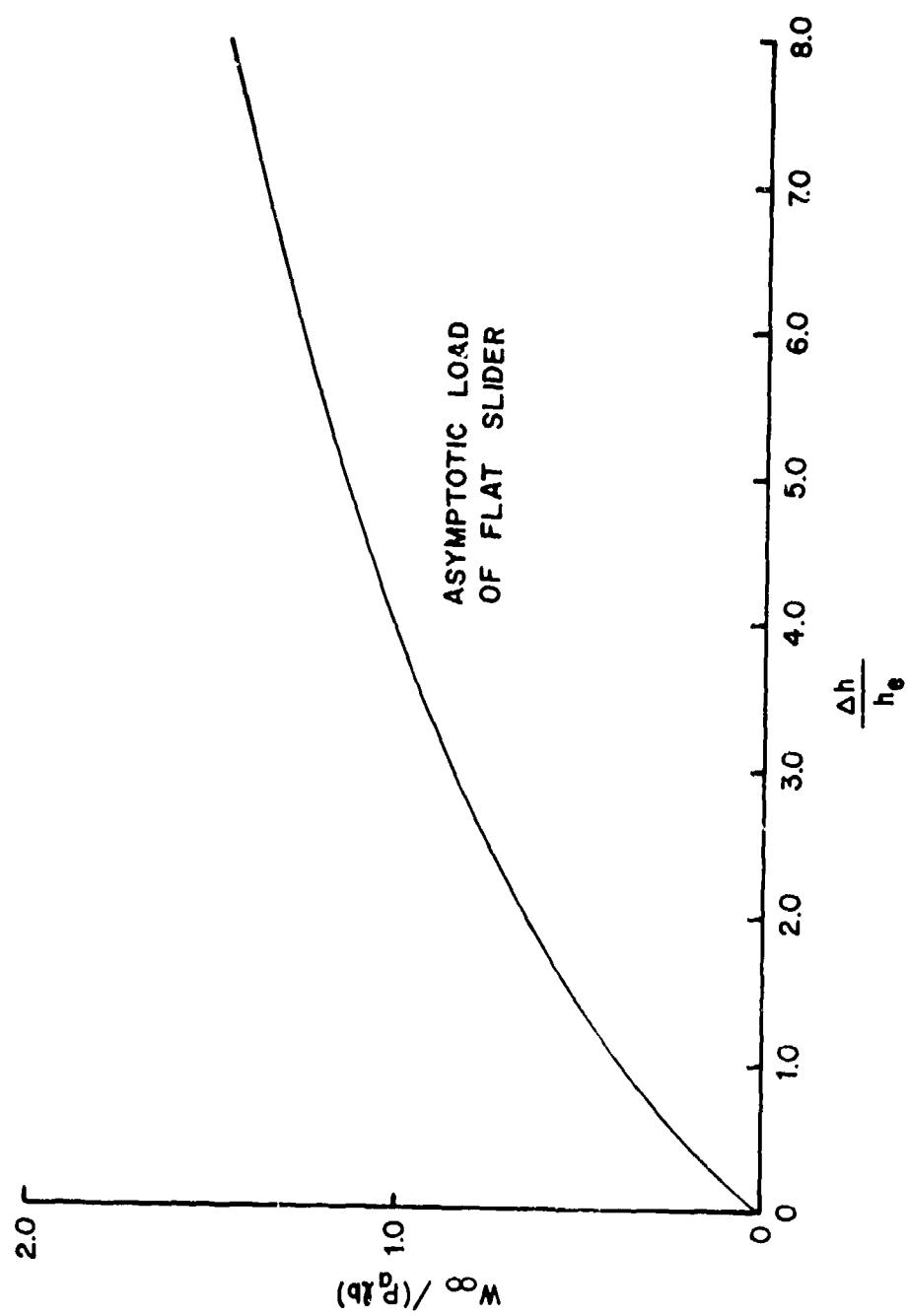


Figure 7 Asymptotic Load vs. Gap Ratio of Flat Slider

$$\left(\frac{p}{p_a} - 1\right) + C \ln \left(\frac{C - p/p_a}{C-1} \right) = \Lambda \left(\frac{x}{\ell} - 1 \right) \quad (18)$$

for $\beta\ell < x \leq \ell$. The film pressure is matched at $x = \beta\ell$ from either side so that there is a constraint requiring the same p_β be obtained from both Equations (16) and (17); i.e.,

$$p_\beta/p_a = \left[1 - \left(\frac{4\Lambda}{27C^2} \right) \beta \right]^{-1} \quad (19)$$

$$\left(\frac{p_\beta}{p_a} - 1 \right) + C \ln \left(\frac{C - p_\beta/p_a}{C-1} \right) = \Lambda(\beta-1) \quad (20)$$

must be simultaneously satisfied. The dimensionless load is

$$\begin{aligned} \bar{W} &= \frac{W}{p_a \ell b} \\ &= \frac{27C^2}{4\Lambda} \left[\ln \left(\frac{p_\beta}{p_a} \right) - C \left(1 - \frac{p_a}{p_\beta} \right) \right] + \frac{1 - (p_\beta/p_a)^2}{2\Lambda} + C - 1 \end{aligned} \quad (21)$$

The stationary condition of Equation (21) with respect to C , treating (p_β/p_a) to be also dependent on C through Equations (19) and (20), yields the optimum design. The geometrical design parameters are shown graphically as a function of Λ in Figure 8(a). Since at each Λ , there corresponds a fixed value of the inlet/exit gap ratio, one can relate the performance parameters, i.e., load and peak pressure to the gap ratio as shown in Figure 8(b). Also shown in the same figure are asymptotic values of these parameters of a flat slider. One may observe that for $\Lambda h/h_e > 2.25$ ($\Lambda > 30$), the optimized slider has a much larger load capacity than the asymptotic flat slider ($\Lambda \rightarrow \infty$). Curiously, though, the peak pressure of the optimized slider is significantly lower than that of the asymptotic flat slider (at the same $\Lambda h/h_e$). Clearly, a broader pressure profile is responsible for the superior load capacity of the optimized slider.

For an asymptotically large Λ , Equations (19) and (20) reveal the following limiting conditions:

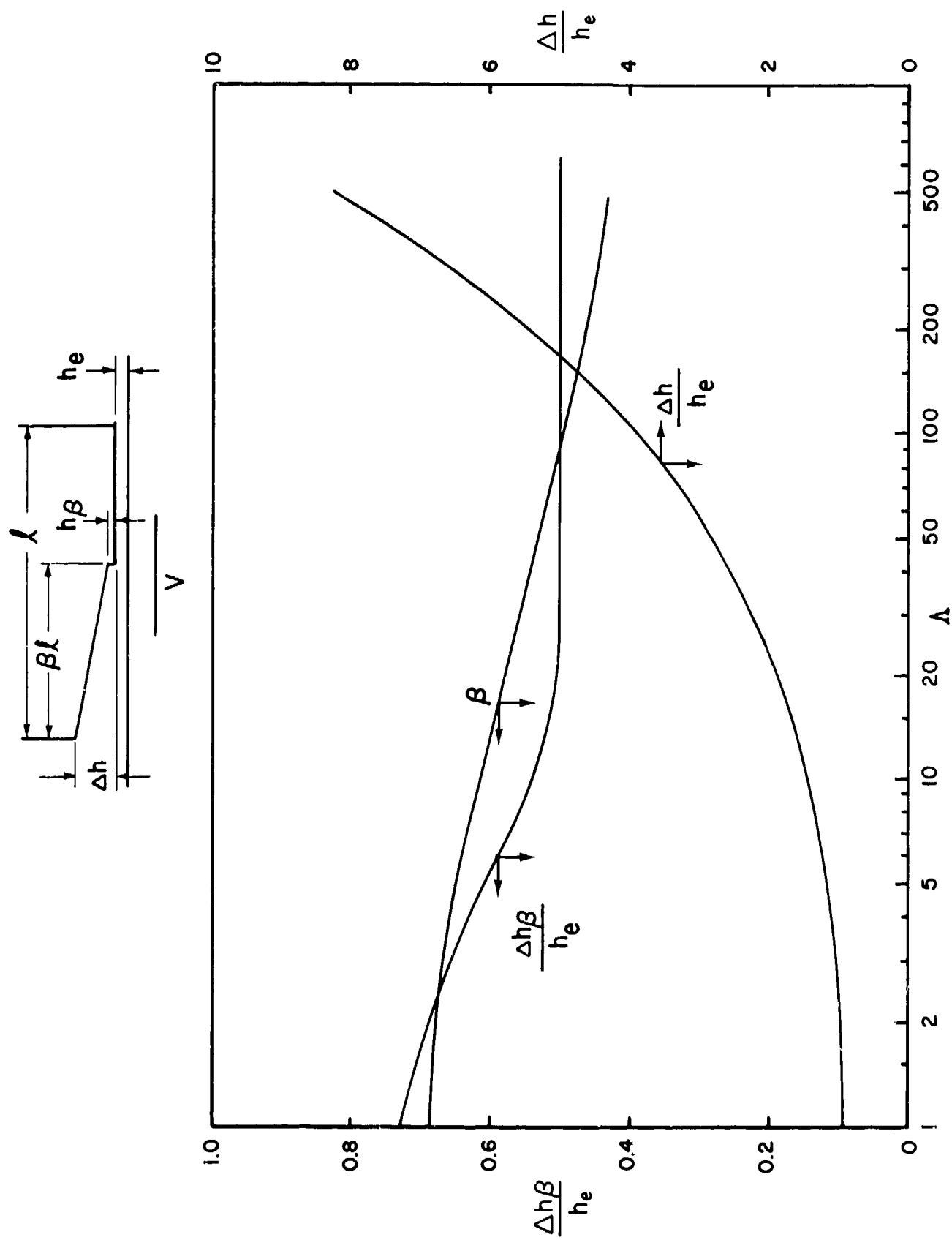


Figure 8(a) Optimized Gas Lubricated Slider - Geometrical Parameters

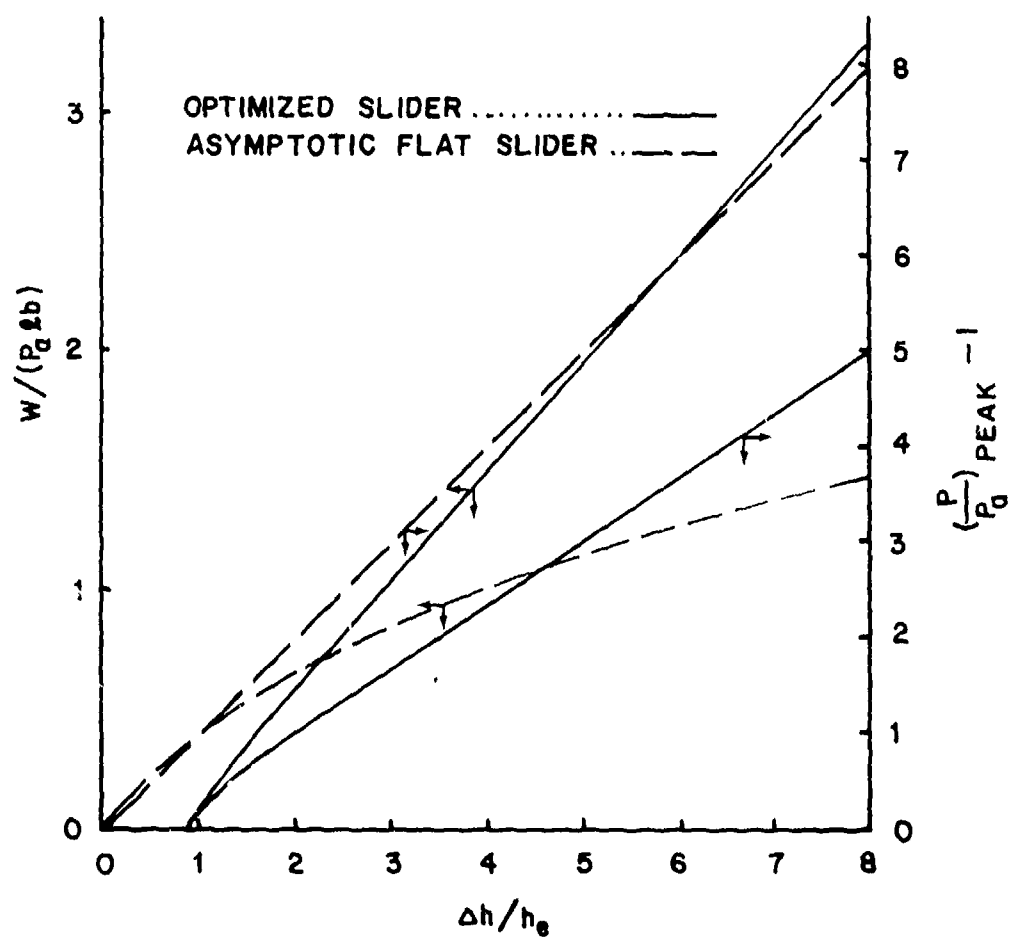


Figure 8(b) Optimized Slider - Performance Parameters

$$\lim_{\Lambda \rightarrow \infty} \begin{cases} \Lambda/C^2 = O\{1\} \\ \frac{C - p_\beta/p_a}{C-1} = \exp \left\{ - \left[(1-\beta) \frac{\Lambda}{C} + 1 - \frac{1}{C} \right] \right\} \end{cases} \quad (22)$$

The corresponding maximal condition of Equation (21) becomes

$$0 = \Lambda - C - \frac{81}{4} C [C - (\frac{2}{3} \ln C + 1)] \quad \text{for } \Lambda \rightarrow \infty \quad (23)$$

The step location is given by

$$\lim_{\Lambda \rightarrow \infty} \beta = \frac{27(C-1)C}{4\Lambda} \quad (24)$$

and the corresponding step depth is

$$\lim_{\Lambda \rightarrow \infty} \Delta h_\beta / h_e = \frac{1}{2} \quad (25)$$

The pressure profile in the exit land is

$$\lim_{\Lambda \rightarrow \infty} p(\beta \ell \leq x < \ell) = C p_a \quad (26)$$

It drops abruptly to the ambient condition only in the immediate vicinity of the exit edge $\ell - x = O\{1/\Lambda\}$. The asymptotic load is

$$\lim_{\Lambda \rightarrow \infty} \bar{W}_\infty = \frac{\beta C \ell \ln C}{(C-1)} + (1-\beta)C - \frac{(C^2-1)}{2\Lambda} - 1 \quad (27)$$

This can be of a very respectable magnitude at large values of Λ .

3.3 Side Leakages of Finite Sliders

The results indicated in the previous section pertain to infinitely long sliders, for which the sliding wedge action causes the film pressure to build up to provide for the load capacity. All bearing elements of the slider type

in real use have side edges which are exposed to the ambient environment. Consequently, any pressure build up in the film is accompanied by side leakages which tend to detract from the load capacity.

The side leakage problem of a high speed flat slider was treated by Elrod and McCabe [52]. For a gap distribution such as that illustrated in Figure 4, the high speed solution as given by Equation (13) is to be reconciled with the exit boundary condition through the exit boundary layer, which is of $O\{1/\Lambda\}$; and with the side boundary conditions, through the side boundary layers, which penetrate from either side edge to a depth of $O\{1/\sqrt{\Lambda}\}$. The exit boundary layer solution is already contained in Harrison's solution, which becomes, in the limit of a very large Λ ,

$$\lim_{\Lambda \rightarrow \infty} \psi(\xi \approx 1) = \left(1 + \frac{\Delta h}{h_e}\right) - \left(\frac{\Delta h}{h_e}\right) \exp \left\{ - \left(\frac{\psi-1}{\beta_2}\right) - \frac{(\beta_1 - \beta_2)}{\beta_2} \left(\frac{\Delta h}{h_e}\right) (1-\xi) \right\}$$

for $1 - \xi = O\{1/\Lambda\}$ (28)

and

$$\lim_{\Lambda \rightarrow \infty} \psi(\xi < 1) = 1 + \frac{\Delta h}{h_e} + O\left\{\frac{1}{\Lambda^2}\right\} \quad (29)$$

From these expressions, the load and moment of the flat slider can be calculated up to $O\{1/\Lambda\}$ for the central region (not affected by side leakage boundary layers):

$$\frac{W_c}{p_a \ell_b} = \left(\frac{h_e + \Delta h}{\Delta h}\right) \ln\left(\frac{h_e + \Delta h}{h_e}\right) - 1 - \frac{\left(1 + \frac{\Delta h}{h_e}\right)^2 - 1}{2\Lambda} \quad (30)$$

$$\frac{T_c}{p_a \ell_b^2} = \left(\frac{h_e + \Delta h}{\Delta h}\right) \left[\left(\frac{h_e + \Delta h}{\Delta h}\right) \ln\left(\frac{h_e + \Delta h}{\Delta h}\right) - 1 \right] - \frac{1}{2} - \frac{\left(1 + \frac{\Delta h}{h_e}\right)^2 - 1}{2\Lambda} \quad (31)$$

Side leakage corrections, which are of $O(1/\sqrt{\Lambda})$, are yet to be added in order to calculate the high speed behavior of finite width sliders. This problem, as solved by Elrod and McCabe deals with the equation

$$H \frac{\eta}{\partial \eta} \left(\Psi \frac{\partial \Psi}{\partial \eta} \right) = \frac{\partial \Psi}{\partial \xi} \quad (32)$$

where,

$$\eta = \left(\frac{b}{2\ell} - \left| \frac{z}{\ell} \right| \right) \frac{\sqrt{\Lambda}}{(1+\Delta h/h_e)} \quad (33)$$

$$H = \frac{h(\xi)}{h_e + \Delta h} = \frac{h_e + \Delta h(1-\xi)}{h_e + \Delta h}; \quad \Psi = \frac{p h}{p_a (h_e + \Delta h)} = \frac{\psi}{1 + \Delta h/h_e} \quad (34)$$

z is the axial coordinate measured from the midplane of the slider. Equation (32) is reduced from the complete partial differential equation by postulating the predominance of the Couette component of the film flow in the direction of sliding. Equation (33) defines a "stretched" coordinate in the edge region such that comparable scaling in the axial and sliding directions is realized for the end leakage analysis. The applicable boundary conditions are

$$\Psi(\xi=0, \eta) = 1; \quad \Psi(\xi, \eta=0) = H(\xi); \quad \Psi(\xi, \eta \rightarrow \infty) = 1 \quad (35)$$

For the flat slider, as illustrated in Figure 4, H and ξ are linearly related to each other. Therefore Equations (32) and (35) can be replaced by

$$- \frac{1}{H} \frac{\partial \Psi}{\partial H} = \frac{\partial}{\partial \xi} \Psi \frac{\partial \Psi}{\partial \xi} \quad (36)$$

where,

$$\xi = \sqrt{\frac{\Delta h}{h_e + \Delta h}} \eta \quad (37)$$

and

$$\Psi(H=1, \epsilon) = 1; \Psi(H, \epsilon=0) = H; \Psi(H, \epsilon, \infty) = 1 \quad (38)$$

Numerical solutions are presented by Elrod and McCabe in terms of three universal functions, which are:

$$\text{Leakage Penetration: } \left(\frac{\delta^*}{\ell}\right) \sqrt{\frac{\Lambda_i \Lambda_1}{h_e + \Lambda h}}$$

$$\text{Load Deficiency: } \frac{W_D \sqrt{\Lambda_1}}{p_a \ell^2}$$

$$\text{Moment Deficiency: } \frac{T_D \sqrt{\Lambda_1}}{p_a \ell^3}$$

Λ_1 is the compressibility number based on the inlet film thickness; i.e., $\Lambda_1 = 6\mu V \ell / [p_a (h_e + \Lambda h)^2]$. These universal functions depend only on the gap ratio of the flat slider as shown graphically in Figure 9. The leakage penetration should be checked to verify the applicability of this type of analysis, which presumes mutual independence of the leakage effects from the two sides. The recommended rule is

$$\delta^* < b/6 \quad (39)$$

Otherwise, the full compressible Reynolds equation should be used in place of Equation (32) to calculate the film pressure. Upon satisfying the above inequality, load and moment of the flat slider of finite width are calculated as

$$\frac{W}{p_a \ell b} = \frac{W_c}{p_a \ell b} - 2 \left(\frac{\ell}{b}\right) \left(\frac{W_D}{p_a \ell b}\right) \quad (40)$$

$$\frac{T}{p_a \ell^2 b} = \frac{T_c}{p_a \ell^2 b} - 2 \left(\frac{\ell}{b}\right) \left(\frac{T_D}{p_a \ell^3}\right) \quad (41)$$

$W_c/(p_a \ell b)$ and $T_c/(p_a \ell^2 b)$ are to be calculated from Equations (30) and (31).

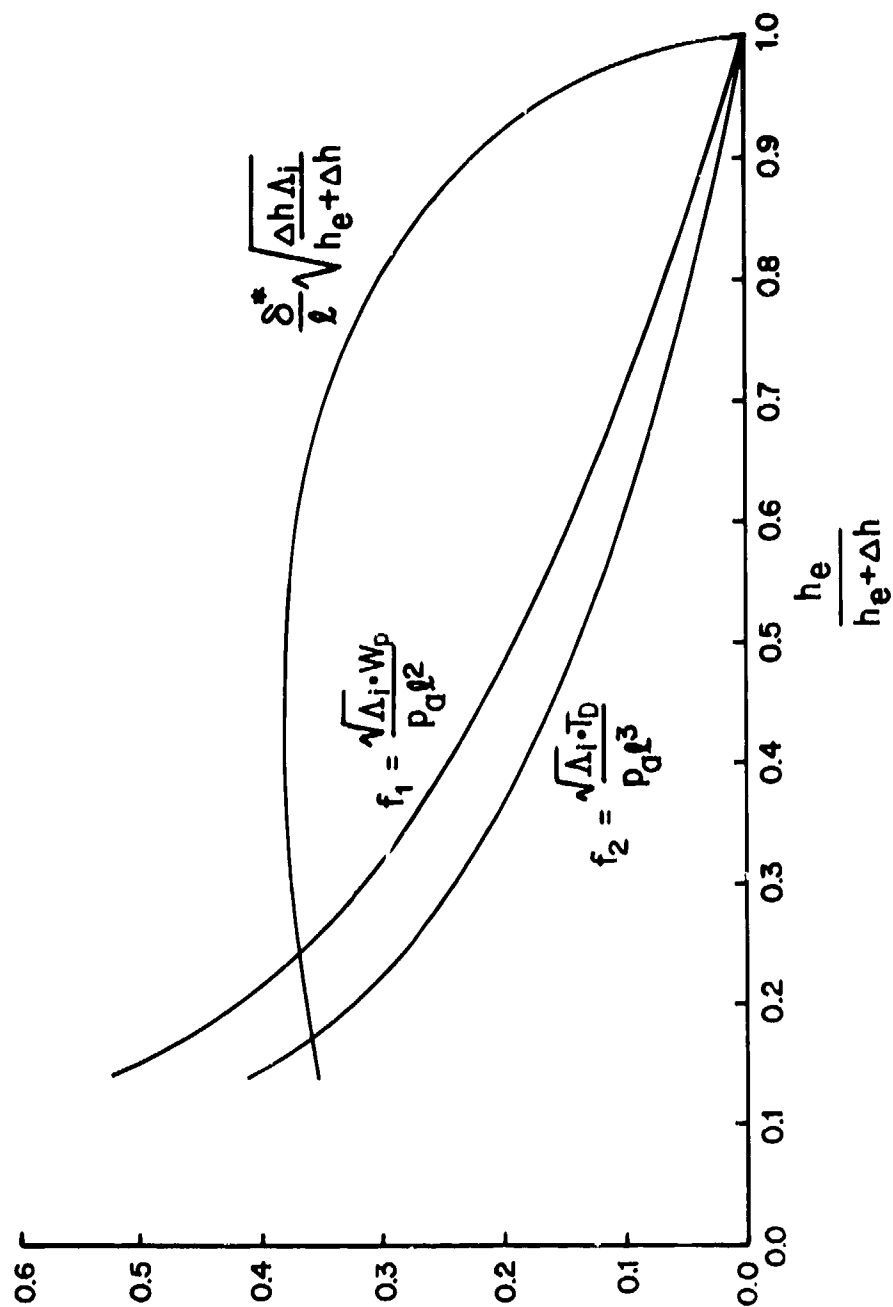


Figure 9 End Leakage Functions of Flat Slider

An illustration in the application of the side leakage analysis is illustrated in Figure 10. The result from Equation (40) is represented by the curve. Numerical finite difference results obtained by a state-of-art algorithm [53] are shown as individual points. The scale of the abscissa is chosen so that the asymptotic behavior for $\Lambda \rightarrow \infty$ would be represented by a straight line passing through the point of unity. This is clearly satisfied by the side leakage analysis. The slight curvature in the curve reflects the contribution from the exit leakage, which is clearly of secondary importance at high speeds. Points obtained by numerical computation do not conform to the asymptotic trend because the exponentially abrupt behavior of the pressure field at the exit edge is not accurately allowed for in the Simpson's quadrature formula which is used to integrate the pressure field over the bearing plan form.

For a slider with other gap profiles, the side leakage analysis can also be carried out [52]. The required computation effort is necessarily more complicated. As a first approximation, the leakage penetration function of the flat slider can be retained as a basis to construct load and moment deficiency effects.

3.4 Practical Implications of a High Compressibility Number

The eccentricity perturbation analysis of the plain journal bearing as well as Harrison's solution of the flat slider reveal that the unit load at a high compressibility number is limited by the ambient pressure. The optimized slider analysis, on the other hand, shows that the maximum realizable load at high compressibility numbers is quite sensitive to the gap profile. Given the same gap excess ($\Delta h/h_e$), the load capacity of an optimized slider at a moderately large compressibility number can be appreciably higher than the asymptotic load of a flat slider. Since the compressibility number is proportional to ω/h^2 , gap profile optimization to achieve the largest possible load at a moderately large compressibility number can simultaneously enhance low speed lift-off and avoid high speed touchdown.

For slider bearings, side leakage effects should be minimal at high compressibility number. Therefore, there is hope that the load level indicated by the optimized slider can be approached in a clever design.

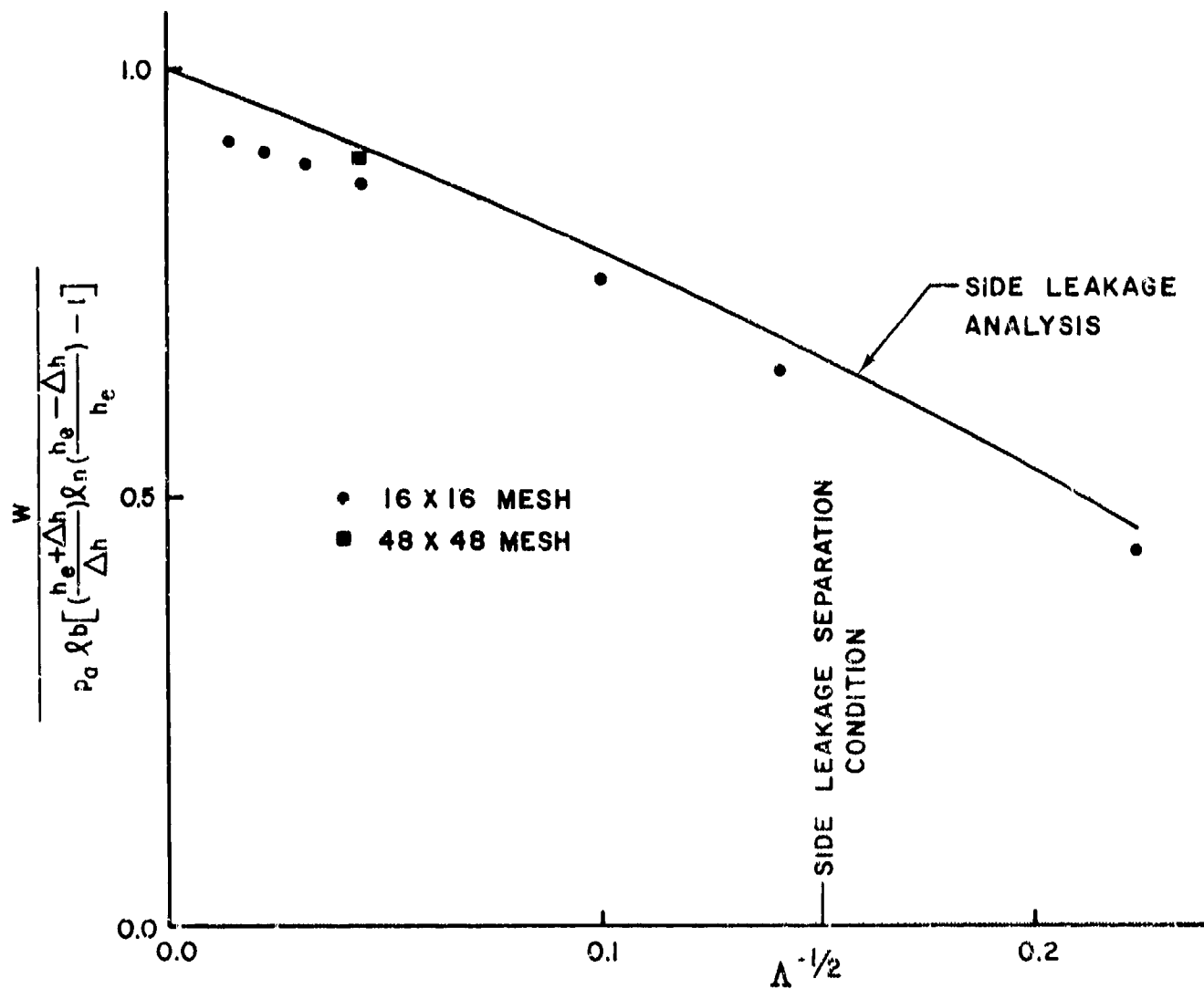


Figure 10 Side Leakage Effects of High Speed, Flat Slider

$$\begin{aligned} l/b &= 1.0 \\ \Delta h/h_e &= 1.0 \\ \Lambda &= 6\mu v l / p_a h_e^2 \end{aligned}$$

SECTION IV

WHIRL INSTABILITY

A complete evaluation of the stability problem requires consideration of the inertia and flexure properties of the rotor together with the dynamic characteristics of the bearing(s). However, an examination of the dynamic characteristics of the journal bearing itself would reveal whether or not necessary conditions for whirl instability may be inherent in the particular journal bearing design. The possibility of whirl instability is not limited to gas lubricated journal bearings only. The same basic phenomenon has been known to be associated with oil lubricated journal bearings for some time [54]. However, because gas lubricated journal bearings tend to operate at a higher peripheral speed than that of oil lubricated journal bearings, and because, in the absence of effective boundary lubrication, the sliding friction of gas bearing materials is typically very high, the consequence of inadvertent high speed touchdown is necessarily much more traumatic for gas lubricated journal bearings. Consequently, much of the latest advances regarding dynamical behavior of journal bearings, including the analysis of whirl stability, were directly linked to gas bearing applications. It should be recognized that much of the discussion to be presented below is not necessarily relevant to the compressibility of the gaseous lubricant. Special features pertaining exclusively to gas lubricated bearings, will therefore be so indicated.

4.1 Limitations of Small Perturbation Analysis

Stability analysis deals with the question of whether or not a small perturbation of an equilibrium state would cause a self-amplifying motion. The assumption of smallness of the perturbation reduces the analysis to that of a linear system. As such there are limitations in the conclusions which can be reached.

- The general motion of a linear system can be determined as the superposition of various linearly independent components. Each

component of the motion is associated with an independent initial condition or a suitable description of the "driving function". For instance, the initial states of displacement and velocity as well as the Fourier responses are the independent components of the perturbed motion.

- Because Fourier functions are mutually orthogonal, the linearized solution is harmonically pure. Each Fourier component of the driving force is associated with a response of the same Fourier order.
- An unstable motion of a perturbation analysis grows without bounds. In reality, a finite amplitude may be contained by large amplitude effects.
- Large amplitude phenomena which cannot be treated by the perturbation analysis include induced harmonic components, auto-parametric excitations, and limit cycle motions.

Because gas bearings cannot tolerate high speed touchdown, they should be designed to avoid large amplitude dynamic motions. Since all finite amplitude motions must grow from small perturbations, the above stated limitations of small perturbation analysis are not serious in gas bearing applications.

4.2 Kinematics of Journal Bearing Motion

The journal, as confined by the bearing gap, has two degrees of freedom in its cross sectional plane. It is a common practice to neglect transverse angular displacements of the journal axis and to describe the journal motion in terms of transverse lineal displacements at its midplane. A right handed Cartesian coordinate system can be assigned with the origin chosen to coincide with the static load direction as indicated in Figure 11. It is a peculiarity of self-acting journal bearings that the bearing reaction force may not be colinear with the journal displacement. In a dynamic situation, the reaction force, the displacement from a static equilibrium location, and the velocity may have different directions at any given instant.

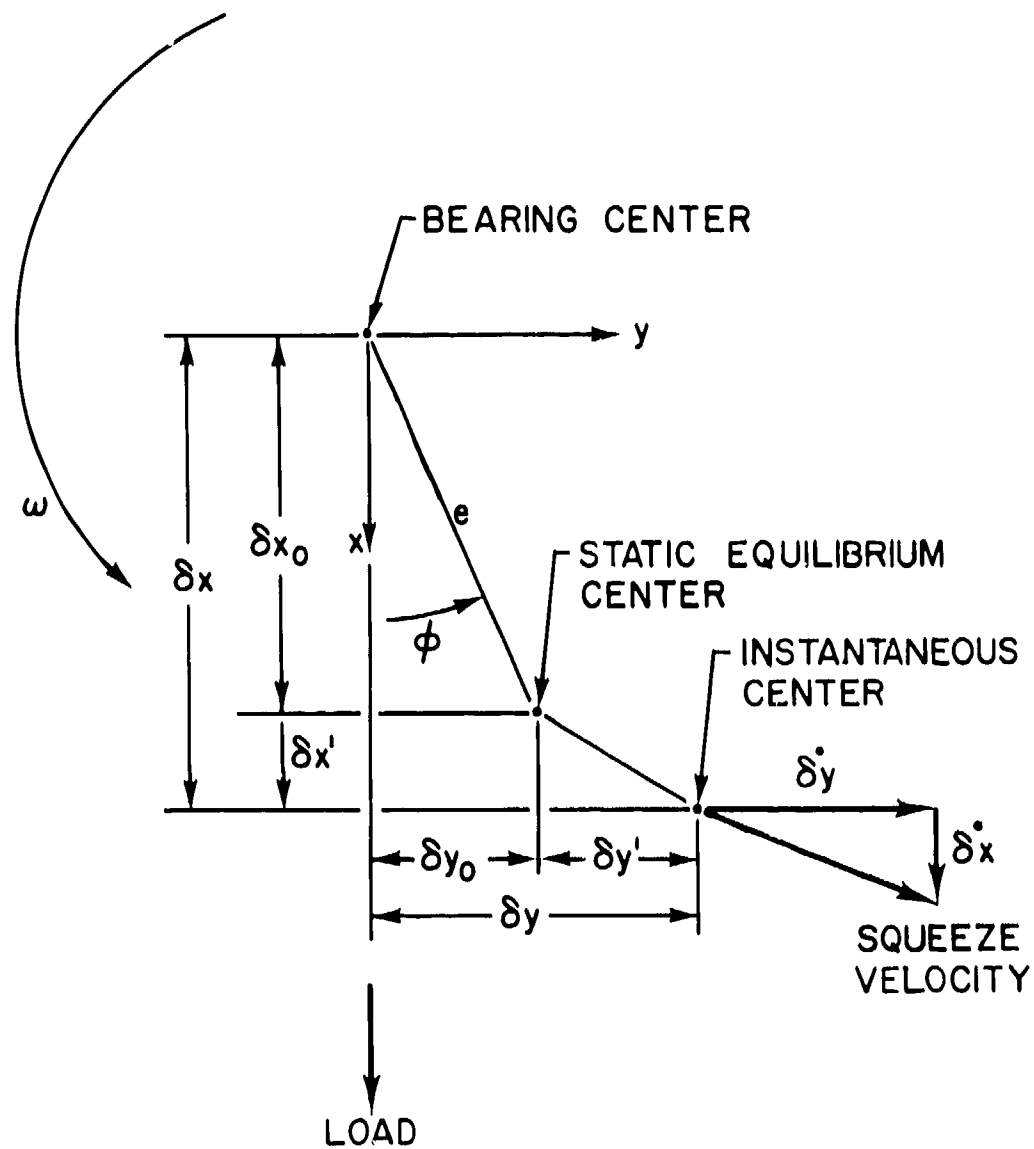


Figure 11 Displacement and Velocity Diagram of Journal Bearing

A simple harmonic motion of an arbitrary circular frequency ν may be assumed for the performance of a perturbation analysis. Use of the complex Argand notation allows considerable symbolic simplification. Thus $|\delta x'| \cos(\nu t + \phi_x)$ $= R_e \{ \delta x' e^{j(\nu t + \phi_x)} \}$ is abbreviated as δx which is complex and $\text{Arg} \{ \delta x' \}$ is understood to be ϕ_x . Furthermore, the time-derivative operation is directly replaced by the multiplication of $j\nu$.

The kinematic behavior of the planar motion can be readily understood through the representation by circular whirl components. One can write

$$\delta x' = \delta u + \delta v; \quad \delta y' = -j\delta u + j\delta v \quad (42)$$

And conversely,

$$\delta u = \frac{1}{2} (\delta x' + j\delta y'); \quad \delta v = \frac{1}{2} (\delta x' - j\delta y') \quad (43)$$

Equation (43) may thus be regarded as the constructional proof of the possibility of the representation of the simple harmonic orbit $(\delta x', \delta y')$ by circular whirl components. The simple harmonic orbit can thus be demonstrated to be an ellipse. The major radius is reached when the two circular whirl components coincide at t_1 ; that is

$$\nu t_1 + \text{Arg}\{\delta v\} = 2\pi - [\nu t_1 + \text{Arg}\{\delta u\}]$$

or,

$$\nu t_1 = \pi - \frac{1}{2} [\text{Arg}\{\delta u\} + \text{Arg}\{\delta v\}] \quad (44)$$

The inclination of the major axis is consequently

$$\beta_1 = \pi + \frac{1}{2} [\text{Arg}\{\delta u\} - \text{Arg}\{\delta v\}] \quad (45)$$

One quadrant later, the two whirl components respectively are at $\beta_1 \pm \pi/2$ and are thus oppositely directed. The orbit point, now represented by the

difference of the whirl radii, is one quadrant counterclockwise of β_1 if $|\delta u| > |\delta v|$ or clockwise of β_1 if $|\delta u| < |\delta v|$. One can therefore regard the principal radii to be

$$\delta r_1 = |\delta u| + |\delta v|; \quad \delta r_2 = |\delta u| - |\delta v| \quad (46)$$

A negative δr_2 indicates a backward whirling elliptical orbit. The temporal reference is given by the position of the journal center at $t = 0$:

$$\delta x_0 = \text{Re} \{u+v\}; \quad \delta y_0 = \text{Im} \{u-v\} \quad (47)$$

Various parameters of the elliptical orbit are illustrated in Figure 12.

4.3 Dynamic Perturbation Impedance of a Journal Bearing

The reaction of a journal bearing corresponding to the harmonic perturbation motion is represented by the impedance equation

$$\{\delta F\} = - [Z] \{\delta w\} \quad (48)$$

$\{\delta F\}$ is a column vector, the elements of which are the Cartesian components of the dynamic bearing reaction. The elements of $\{\delta w\}$ are the Cartesian components of the dynamic perturbation motion. The elements of the 2x2 matrix $[Z]$ are complex; i.e.,

$$Z_{xx} = k_{xx} + j\omega b_{xx} \quad \text{etc.} \quad (49)$$

They are found by integrating the perturbed film pressure over the respective projected areas.

For a harmonically perturbed gas bearing, the perturbed film pressure is governed by the field equation [45]

$$\begin{aligned} \nabla \cdot \left[\frac{h_o^3}{12\mu} \nabla (p_o \delta p) - \frac{\vec{v}}{2} h_o \delta p \right] - jv h_o \delta p \\ = - \nabla \cdot \left[\left(\frac{h_o^2 p_o \nabla p_o}{4\mu} \right) \delta h - \frac{\vec{v}}{2} p_o \delta h \right] + jv p_o \delta h \end{aligned} \quad (50)$$

where h_o is the film thickness at the static equilibrium condition and p_o is the corresponding static equilibrium film pressure. The perturbed film thickness is

$$\delta h = -\delta x' \cos \theta - \delta y' \sin \theta \quad (51)$$

for the journal bearing. δp is thus seen to be linearly dependent on $(\delta x', \delta y')$. The two groups on the right hand side of Equation (50) are associated with the real and imaginary parts of various elements of [Z]. The terms associated with the explicit factor jv on the right hands of Equations (49) and (50) are recognized as squeeze-film effects and are regarded as "damping" terms as suggested by their proportionality to jv .

The appearance of the factor jv on the lefthand side of Equation (50) is due to the dynamic mass storage effect. Its presence is a peculiar feature in the dynamic perturbation analysis of gas lubricated bearings and is responsible for the dependence of $(k_{xx}, b_{xx}; \text{etc.})$ on v . In the extreme case of very high frequency motions, Equation (50) shows the asymptotic behavior

$$\lim_{v \rightarrow \infty} \delta p = - \left(\frac{p_o}{h_o} \right) \delta h \quad (52)$$

which suggests that the high frequency gas film behaves like a distributed spring. For this reason, the gas bearing is generally regarded to have limited damping capacity for high frequency motions.

4.4 Characteristic Stiffness and Damping of a Journal Bearing

Although the real and imaginary parts of the impedance matrix are commonly recognized as stiffness and damping matrices, their physical roles in the dynamics of the rotor are better revealed by the characteristic stiffness

and damping coefficients which are defined by the homogeneous equation

$$[Z] \{\delta w_\alpha\} \equiv (k_\alpha + j\nu b_\alpha) \{\delta w_\alpha\} \quad (53)$$

The subscript " α " associates (k_α, b_α) with the corresponding characteristic orbit $\{\delta w_\alpha\}$. For Equation (53) to be valid for any non-trivial $\{\delta w_\alpha\}$, its homogeneous character requires that the characteristic determinant vanishes:

$$|[Z] - (k_\alpha + j\nu b_\alpha)[I]| = 0$$

yielding two solutions

$$k_\alpha + j\nu b_\alpha = \frac{1}{2} (Z_{xx} + Z_{yy}) \mp \frac{1}{2} \sqrt{(Z_{xx} - Z_{yy})^2 + 4Z_{xy}Z_{yx}} \quad (54)$$

So that α may take on (1 or 2). Note that the imaginary side of Equation (54) may not vanish with ν . Thus it is the temporal phase shift factor j instead of the proportionality to ν that governs the damping aspect of the perturbation reaction of the journal bearing.

With $(k_\alpha + j\nu b_\alpha)$ given by Equation (54), the characteristic orbit is determined by either line of Equation (52); i.e.,

$$\left[\frac{1}{2} (Z_{xx} - Z_{yy}) \pm \frac{1}{2} \sqrt{(Z_{xx} - Z_{yy})^2 + 4Z_{xy}Z_{yx}} \right] \delta x_\alpha + Z_{xy} \delta y_\alpha = 0 \quad (55a)$$

$$Z_{yx} \delta x_\alpha + \left[\frac{1}{2} (Z_{yy} - Z_{xx}) \pm \frac{1}{2} \sqrt{(Z_{xx} - Z_{yy})^2 + 4Z_{xy}Z_{yx}} \right] \delta y_\alpha = 0 \quad (55b)$$

These two equations are mutually redundant except for the degenerate condition $Z_{xy}Z_{yx} = 0$; then both are needed to describe the two distinct characteristic orbits. Since these modal equations are homogeneous, the size and temporal reference of the characteristic orbits are indeterminate. The characteristic orbits are thus known only in terms of its geometric shape parameters $(\delta r_2/\delta r_1, \beta_1)_\alpha$.

A negative value of b_{α} indicates the existence of potential instability. A sufficient condition for instability for a single mass-bearing system is that the negativity of b_{α} is realized at $\nu = \sqrt{k_{\alpha}/m}$ where m is the rotor mass. For a multi-bearing system, the sufficient condition for instability requires attention to the dynamic impedance of the entire rotor-bearing system [82].

To illustrate the concepts associated with the problem of whirl instability, consider the perturbation of a plain, gas-lubricated, journal bearing from its concentric position. The static equilibrium condition is satisfied by

$$h_o = C; \quad p_o = p_a \quad (56)$$

which corresponds to an unloaded condition. Elements of the perturbation impedance matrix are

$$\begin{aligned} Z_{xx} &= Z_{yy} \\ &= \left(\frac{p_a LD}{C}\right) \left(\frac{1}{2}\right) \left\{ \frac{-j\Lambda_{(-)}}{1-j\Lambda_{(-)}} \left[1 - \frac{\tanh \sqrt{1-j\Lambda_{(-)}} L/D}{\sqrt{1-j\Lambda_{(-)}} L/D}\right] \right. \\ &\quad \left. + \frac{j\Lambda_{(+)}}{1+j\Lambda_{(+)}} \left[1 - \frac{\tanh \sqrt{1+j\Lambda_{(+)}} L/D}{\sqrt{1+j\Lambda_{(+)}} L/D}\right] \right\} \quad (57a) \end{aligned}$$

$$\begin{aligned} Z_{xy} &= -Z_{yx} \\ &= \left(\frac{p_a LD}{C}\right) \left(\frac{1}{2}\right) \left\{ \frac{\Lambda_{(-)}}{1-j\Lambda_{(-)}} \left[1 - \frac{\tanh \sqrt{1-j\Lambda_{(-)}} L/D}{\sqrt{1-j\Lambda_{(-)}} L/D}\right] \right. \\ &\quad \left. + \frac{j\Lambda_{(+)}}{1+j\Lambda_{(+)}} \left[1 - \frac{\tanh \sqrt{1+j\Lambda_{(+)}} L/D}{\sqrt{1+j\Lambda_{(+)}} L/D}\right] \right\} \quad (57b) \end{aligned}$$

where, $\Lambda_{(\pm)} = \frac{6\mu(\omega \pm 2\nu)R^2}{p_a C^2}$. Accordingly, the impedances for the two

characteristic modes are

$$k_1 + j\omega b_1 = \left(\frac{p_a LD}{C}\right) \left\{ \frac{-j\Lambda_{(-)}}{1-j\Lambda_{(-)}} \right\} \left\{ 1 - \frac{\tanh \sqrt{1-j\Lambda_{(-)}} L/D}{\sqrt{1-j\Lambda_{(-)}} L/D} \right\} \quad (58a)$$

$$k_2 + j\omega b_2 = \left(\frac{p_a LD}{C}\right) \left\{ \frac{j\Lambda_{(+)}}{1+j\Lambda_{(+)}} \right\} \left\{ 1 - \frac{\tanh \sqrt{1+j\Lambda_{(+)}} L/D}{\sqrt{1+j\Lambda_{(+)}} L/D} \right\} \quad (58b)$$

and the corresponding orbit equations are

$$j\delta x_1 + \delta y_1 = 0 \quad (59a)$$

$$-j\delta x_2 + \delta y_2 = 0 \quad (59b)$$

These are seen to be respectively forward and backward circular whirls. It turns out

$$b_1 < 0 \quad \text{for} \quad 0 < \nu < \omega/2 \quad (60)$$

Furthermore,

$$\lim_{\nu \rightarrow \omega/2} k_1 = \left(\frac{p_a LD}{C}\right) \left\{ 1 - \frac{\tanh(L/D)}{L/D} \right\} \left[\frac{6\mu(\omega-2\nu)R^2}{p_a C^2} \right]^2 \quad (61)$$

This means, for any rotor with a finite mass, the homogeneous state would be satisfied at some frequency $0 < \nu/\omega < 0.5$, at which the forward circular motion is dynamically unstable according to Equation (60). This is the notorious "half frequency whirl" of an unloaded, plain journal bearing.

External pressurization can be used to stabilize a high speed journal bearing [57,58]. A pressurized supply of gas or air forces a continuous flow through

the journal bearing gap. The flow enters the bearing gap through a series of feed holes which are spaced uniformly around the circumference of one or two feed planes. The feed holes are of small diameter so that the minimum flow area is at the feedhole periphery. The "hydrostatic" bearing stiffness (without journal rotation) is maximized through proper sizing of the feed holes. The presence of the pressurized flow through the restricted feed holes increases the characteristic stiffness values k_1 and k_2 roughly by an amount equal to the "hydrostatic" stiffness. Although the general behavior of the characteristic damping due to self acting effects are not significantly altered, in particular, b_1 becomes negative in the range $0 < v/\omega < 0.5$, stable operation of the externally pressurized journal bearing can be maintained up to a relatively high stability threshold. The threshold speed of instability represents the lowest speed at which the homogeneous state occurs with $v/\omega \leq 0.5$. Consequently it can be estimated as twice the natural frequency of the non-rotating system. This is known as the "rule of two". External pressurization is not suitable for aero-propulsion machinery because it unfavorably impacts the power to weight ratio of the system.

4.5 Stability Criteria from the Isotropic Impedance Matrix

The "half frequency whirl" can be suppressed by the application of a static load [12,55,56]. Since static loading introduces directional bias in the impedance matrix, it is a common heuristic rule to examine the isotropic part of the impedance matrix for clues related to the cause for whirl instability.

The isotropic components of the impedance matrix is defined as

$$[Z]_{iso} = \begin{bmatrix} Z_{//} & Z_{\perp} \\ -Z_{\perp} & Z_{//} \end{bmatrix} \quad (62)$$

where,

$$\begin{aligned} Z_{//} &= \frac{1}{2} (Z_{xx} + Z_{yy}) = k_{//} + jv b_{//} \\ Z_{\perp} &= \frac{1}{2} (Z_{xy} - Z_{yx}) = k_{\perp} + jv b_{\perp} \end{aligned} \quad (63)$$

Then Equation (54) becomes

$$k_{\alpha} + j\omega b_{\alpha} = (k_{\parallel} \pm \omega b_{\perp}) + j(\omega b_{\parallel} \mp k_{\perp}) \quad (64)$$

b_{\parallel} is usually positive. Therefore, the necessary condition for instability is usually recognized as $k_{\perp} > \omega b_{\parallel}$. By the same reasoning, reduction or elimination of the cross-coupling term (Z_{\perp}) of the journal bearing impedance is often the strategy of the bearing designer to secure safeguard against whirl instability.

4.6 Whirl Free Journal Bearing Configurations

Since whirl instability became recognized as a major issue in the high speed operation of gas lubricated journal bearings, the search for whirl-free journal bearing designs has received much attention [59]. Some of the more popular approaches with potential application to aero propulsion machinery are described below.

Tilting-Pad Journal Bearings

Use of the tilting-pad arrangement to design gas lubricated journal bearings to achieve high speed rotor stability is a logical technological extension of the favorable experience in the use of such bearings with oil lubrication for the support of industrial rotating machines. The tilting-pad journal bearing also offers the advantage of an inherent self-aligning capability. Each load carrying bearing pad is located at a pivot point which is attached to the bearing housing either rigidly or through a spring mounted arrangement. Since an ideal pivot cannot support a moment, the bearing force vector necessarily passes through the pivot point and the journal center, provided the pivot point is truly frictionless and that the inertia of the bearing pad is negligible. A bearing assembly of several tilting-pads can be designed so that its perturbed reaction always directly opposes the displacement vector of the journal. Consequently, the cause for whirl instability as indicated by Equation (63) would be totally removed. A conceptual design of a three pad, tilting-pad journal bearing for an advanced gas turbine [60] is illustrated in Figure 13.

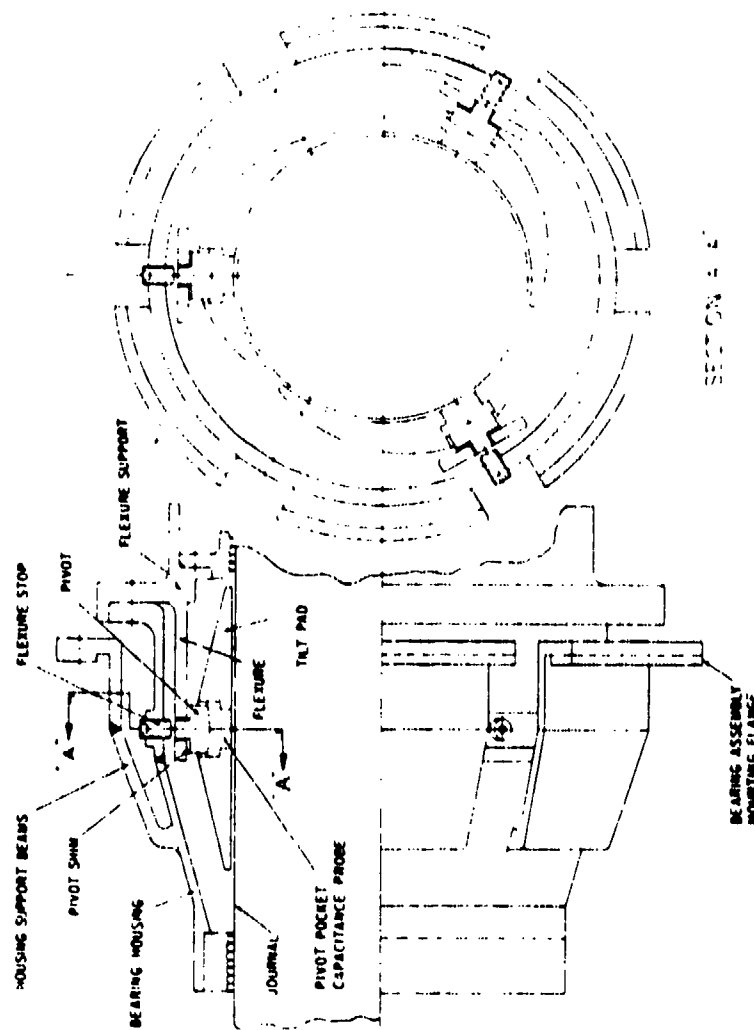
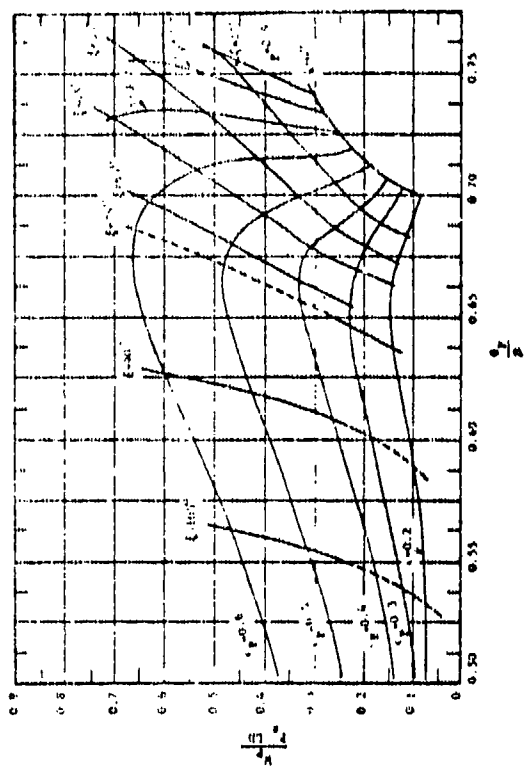
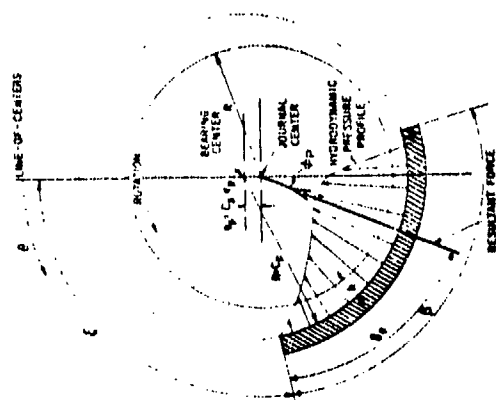
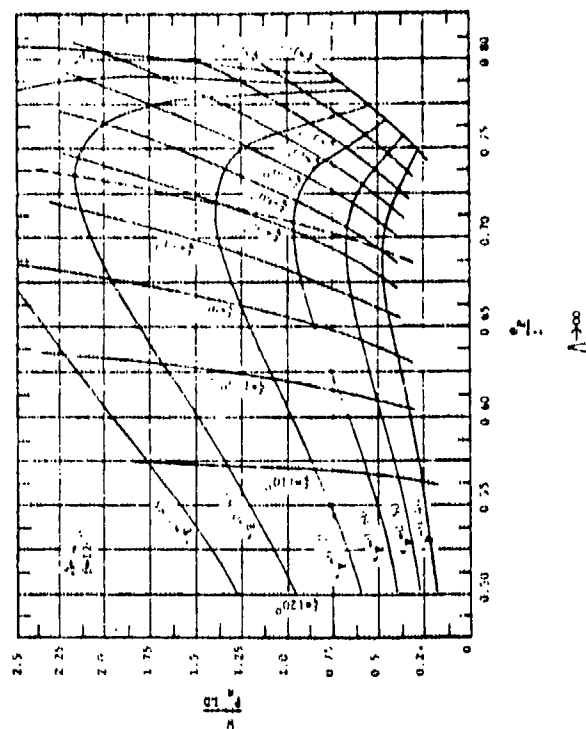


Figure 13 Conceptual Design of a Pivoted Pad Journal Air Bearing
for a 3.5 lb/sec Flow Rate Gas Turbine

The angular mobility about the pivot point allows each bearing pad to have the ability to pitch, roll, and yaw. For the proper function of the gas bearing, these three degrees of freedom of each bearing pad relative to the journal surface must also be stabilized. The primary design parameters for the control of pad stability is the preload factor which is determined by the radial pivot location. The general rule for the proper pivot location is that each pad should maintain a convergent-divergent gap configuration at all operating conditions. Pad inertias, consequently, the number of pads in each bearing assembly, and the L/D ratio also contribute to the dynamics of pad-journal motions. Usually a light pad is desirable.

Complete dynamical analysis of the tilting-pad journal bearing is an involved undertaking [61,62]. Fortunately, experience has indicated that a design approach based on static considerations is usually quite adequate [63,64, 65,66]. Representative design charts for a 120° pad are shown in Figure 14. Lubricant compressibility influences the tilting pad journal bearing mainly in the optimum circumferential location of the pivot point and the existence of the compressibility load limit. The pivot location on the gas lubricated tilting pad should be somewhat more rearward than that on a liquid lubricated tilting pad in order to realize the maximum load capacity. The optimized pivot location would be a function of the operating compressibility number and, to a lesser extent, the desired minimum film thickness. For a bearing operating in a pressurized environment with a moderately low journal speed, the compressibility number could be quite small, the optimum pivot should be located at about 55% of the pad arc from the leading edge. With a normal or reduced ambient condition and a relatively high speed, a moderately large compressibility may prevail, then the desired pivot location may be at 65% of the pad arc. The presence of a compressibility load limit is evident for $\Lambda > 3$. Thus there may be some advantage to control the pressure level in the bearing cavity.

A variation of the tilting pad journal bearing is the elastomer mounted partial arc journal bearing [67,68] as illustrated in Figure 15. Replacement of the pivot by the compliant mount (45 durometer silicone rubber was


$$\hat{r}_i = 10$$


Schematic

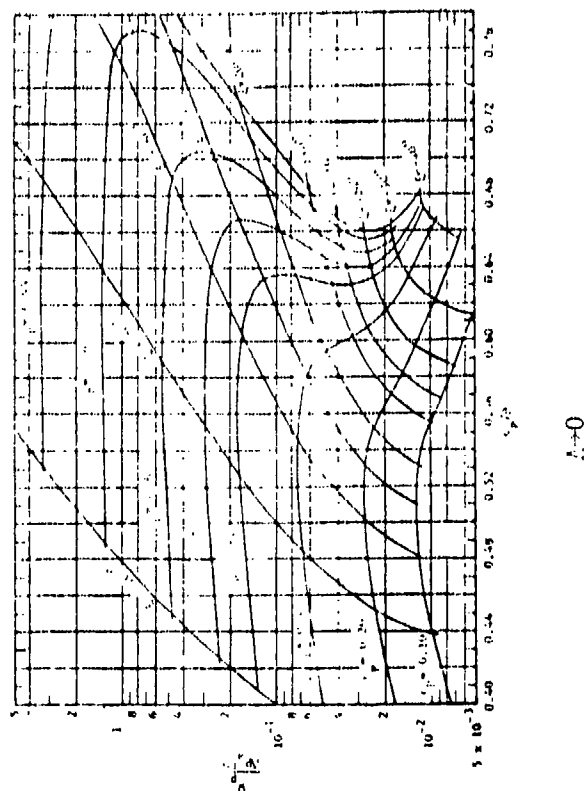


Figure 14 Load Chart, 120° Partial Arc
L/D = 1 [63]

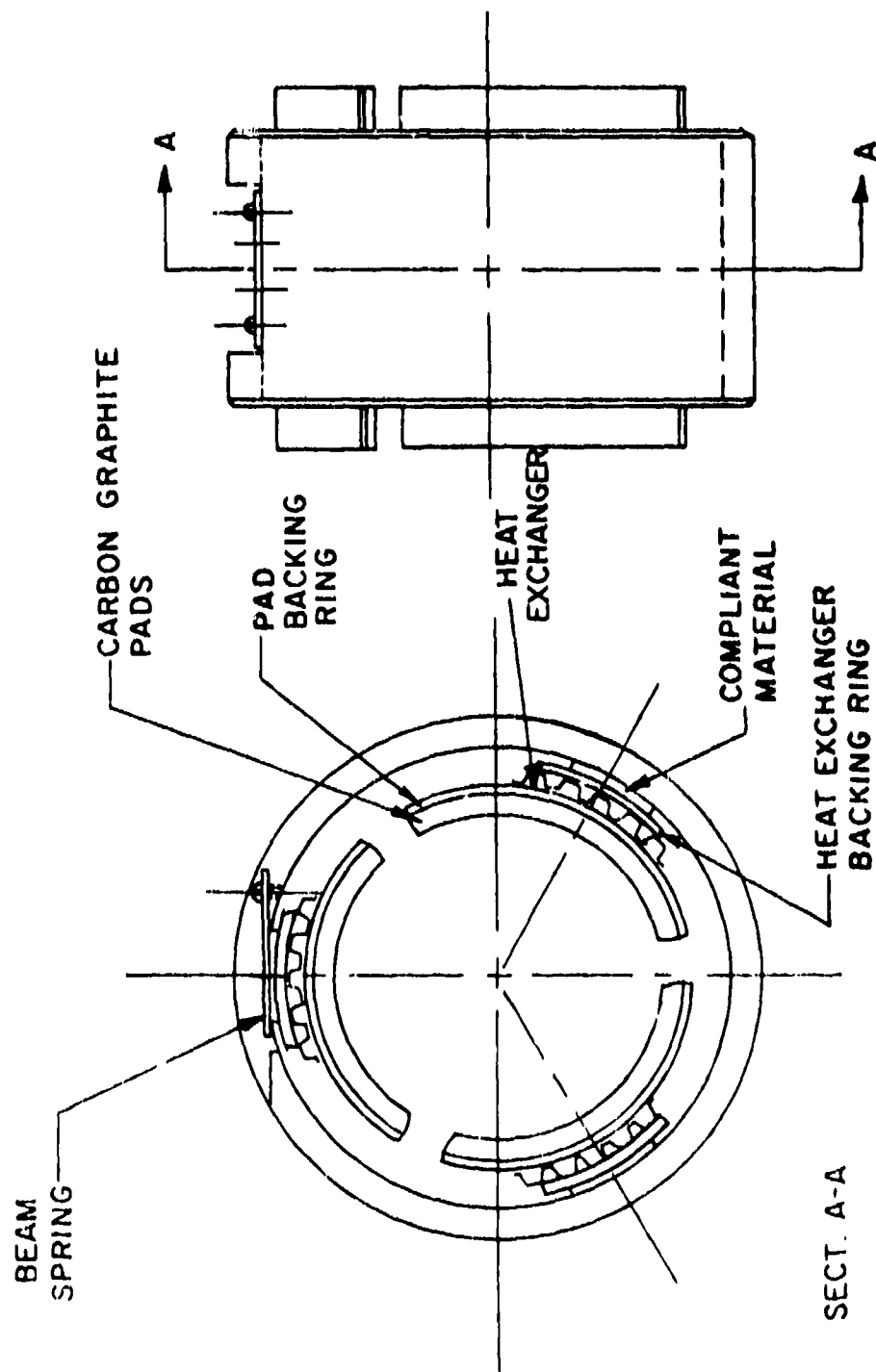


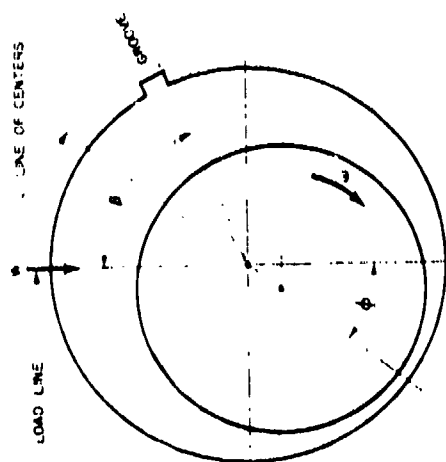
Figure 15 Spring-Mounted Compliant-Pivot Journal Bearing [68]

actually used) gains some simplification in its construction. The elastomer mount also provides some damping to suppress the fluttering tendency of the unloaded pad. The elastomer material presents some limitation on the usable temperature level. Separation of the load carrying pad from the compliant mount by the heat exchanger is an obvious attempt to isolate the elastomer from the heat source. There is also the problem of excessive differential expansion since the coefficient of thermal expansion of a typical elastomer is about 10 times that of steel. Use of a spring mounted top pad can alleviate this difficulty only if the load direction is fixed relative to the bearing housing.

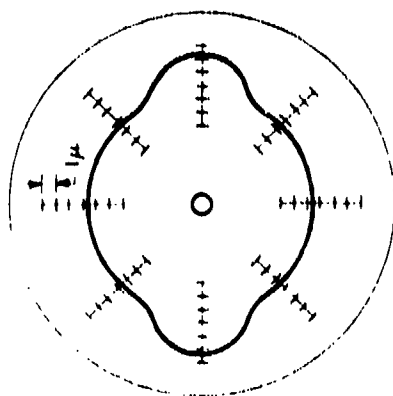
Stabilizing Surface Features

An alternate way to enhance high speed stability of a self-acting journal bearing without resorting to movable bearing parts is to control the hydrodynamic action with surface features. A number of possibilities exists, as illustrated in Figure 16. They are briefly enumerated with heuristic supportive arguments for its consideration in each case.

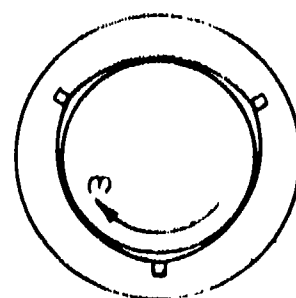
- Partial arc or axial groove journals. Since whirl instability may be associated with the possibility to annihilate the wedge action for pressure generation by a suitable steady whirl speed, interruption of the continuous gap geometry would prevent the continuous buildup of the disruptive influence of the whirl motion. The fixed axial grooves in the bearing bore assures the presence of space fixed squeeze-film dampers.
- Lobed bearing bore. Lobing of the bearing bore goes another step beyond the partial arc concept in that the load carrying surface is allowed to depart from that of a continuous circular cylinder. One type of lobing is used to avoid whirl instability of the spin bearing of a gyroscope [15,69]. The cross-section of a typical lobed bore as indicated by a roundness trace is shown in Figure 16(b). A different type of lobing illustrated by Figure 16(c) was studied theoretically and found to be capable of stable operation without radial load [61]. The calculated



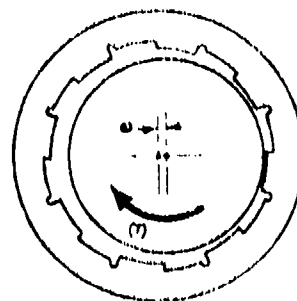
(a) Axial Groove



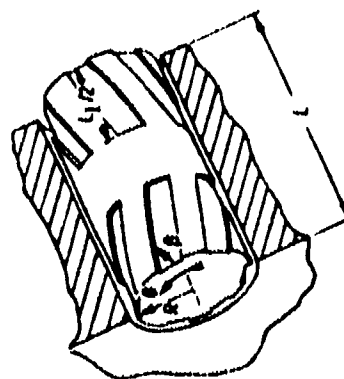
(b) Roundness Trace of Lobed Bore



(c) Preloaded Arc
3 Lobes



(d) Rayleigh Step

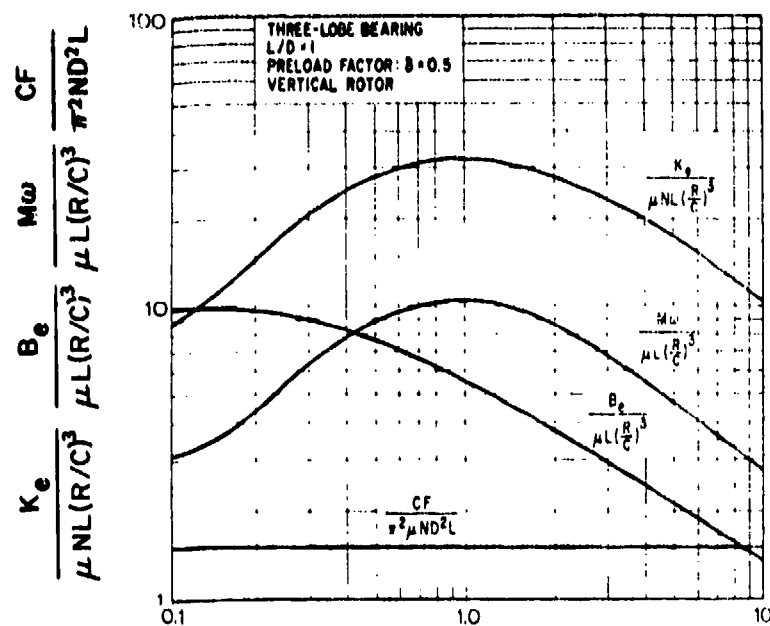


(e) Herringbone

Figure 16 Stabilizing Surface Features of Journal Bearing

stability map is reproduced as Figure 17.

- Rayleigh step journal bearing. The configuration, shown as Figure 16(d), is an adaptation of the celebrated optimum (incompressible) slider [51]. Its static load capacity is quite impressive [70]. An early attempt to analyze the dynamic characteristics of such a bearing gave some qualitative argument of its advantages [16].
- Spiral Grooving. This type of surface feature is also known as helical grooves, herringbone, or chevron pattern. First appearing in the form of a self-acting thrust bearing [71], it is now widely used as spin bearings to carry both radial and thrust loads in a variety of configurations, including conical, spherical, opposed hemispheres, in addition to the cylindrical journal bearing [27,72]. The spiral grooved surface essentially functions as a viscous pump (compressor). It can be thus regarded as a self-pressurizing bearing and stabilization is realized in a similar manner as the externally pressurized journal bearing. Since the self-pressurizing process increases with rotational speed, this type of journal bearing gains stability with little sacrifice of load capacity. Laboratory experiments on bearing sizes suitable for machinery application showed possibility of stable operation upwards of 60,000 rpm [73,74]. The theoretical basis for the determination of its static and dynamic characteristics has been well established [23,75,76]. Availability of a multitude of controllable configuration parameters allows this type of bearing to be optimized either for load capacity or stability margin [77,78]. Application of this bearing type for computer magnetic storage drums is under consideration [34]. Feasibility of extending its use to aero propulsion systems depends mainly on whether misalignment and distortion problems can be circumvented.



$$\Lambda = \frac{6\mu\omega}{P_a} \left(\frac{R}{C}\right)^2$$

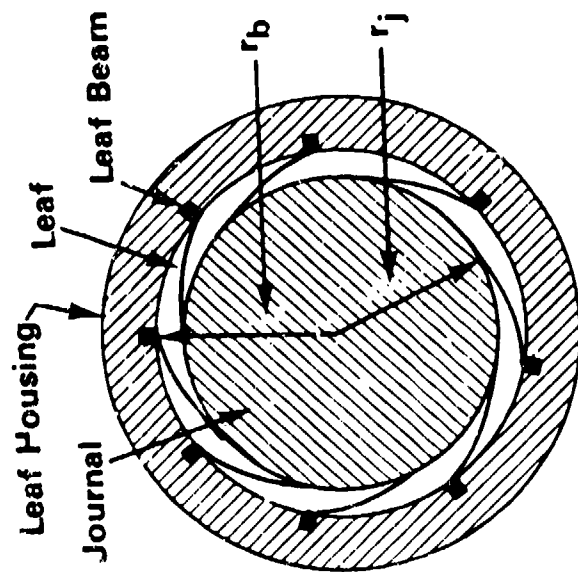
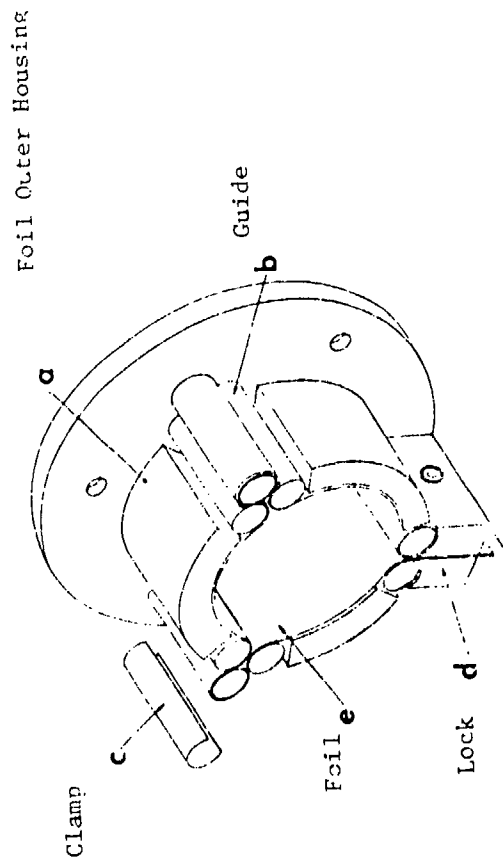
- B_e Effective Damping Coefficient
- K_e Effective Stiffness Coefficient
- F Friction Force
- M Critical Mass for Instability

Figure 17 Characteristics of 3 Lobe, Preloaded Journal Bearing [61]

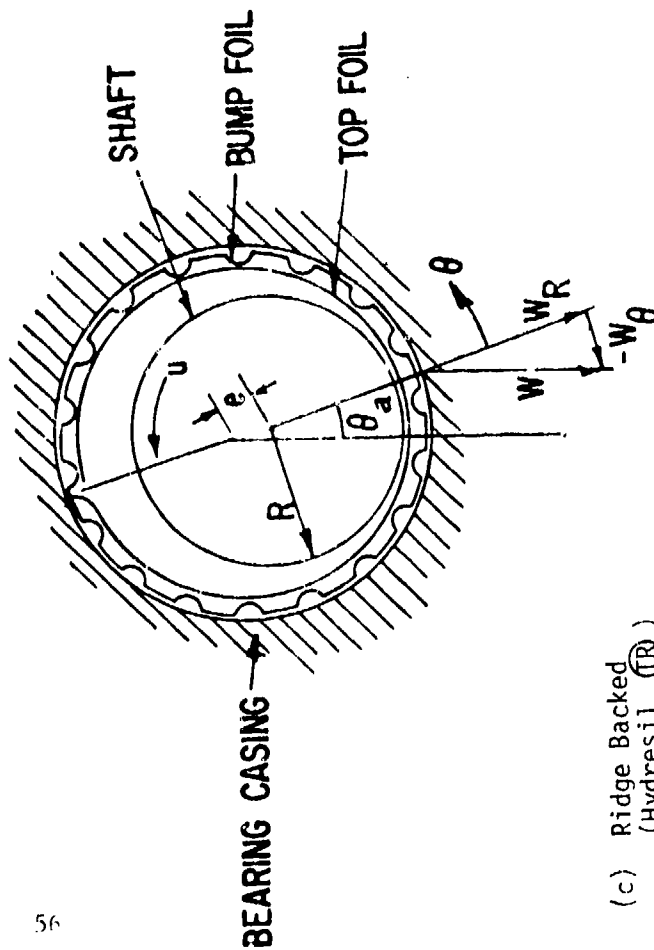
Foil Type Journal Bearings

Structural features of the foil type journal bearings tend to enforce codirectionality between journal displacement and bearing reaction and thus avoid whirl instability. A variety of foil type journal bearings have been considered. Figure 18 shows the most commonly known ones. In each case, the load carrying air film more or less surrounds the high speed journal surface. Flexibility of the foil structure allows "natural" conformity to the journal geometry. Relative tolerance to misalignment and other effects of housing distortion is regarded as an additional inherent advantage. Foil journal bearings first received attention as a potential means to support high speed dynamic power conversion equipment in space programs [18,36,37, 38,79]. More recently, its favorable field experience in aircraft environment conditioning equipment [39] spurred interest in the use of the foil type bearing in various small gas turbine power plants [19,40,41,42,80]. Foil type journal and thrust bearings are now regarded as leading candidates in the large scale use of gas bearings for aero propulsion machines. A separate section of the report will review the technology status of gas lubricated foil bearings more thoroughly.

(a) Tension Dominated



(b) Multi-Leaf



(c) Ridge Backed
(Hydresil (TR))

Figure 18 Foil Type Journal Bearings

SECTION V

GAS LUBRICATED THRUST BEARINGS

For an aero propulsion engine application, the thrust bearing deserves special attention. The thrust load of the engine depends a great deal on the gas path design and also on power output and flight attitude [60]. The thrust load of a conventional axial flow type turbine is, for all practical purposes, beyond the load capacity which can be expected of a gas lubricated thrust bearing. By employing the radial flow turbine, shrouding the impellers, and appropriate location of seals, the thrust load can theoretically be fully balanced to null at a design condition; so that the thrust bearing is required to support mainly effects of vehicle maneuver and off-design operation. The potential penalties in cost, weight, and efficiency of such design approaches appear to be rather modest. Therefore, consideration of the use of an air lubricated thrust bearing must be treated in sufficient depth in the selection of a design configuration.

5.1 External Pressurization

Air bleed from the compressor can be used to feed an externally pressurized thrust bearing. A typical externally pressurized thrust bearing would have a continuous annular plan form. Pressurization is realized by supplying the high pressure bleed to an array of feed holes which are equally spaced at a circumference somewhere between the inner and outer radii, as illustrated in Figure 19. The upstream sides of the feed holes are connected to a manifold. The feed hole should be sharp-edged and perpendicular to the bearing surface. In contrast to the incompressible hydrostatic bearing, upstream restriction and feed pocket should be avoided to prevent a type of instability known as pneumatic hammer, which is associated with transient mass storage anywhere between the supply manifold and the bearing film [82]. The radius of the feed hole circle should be the geometrical mean of inner and outer radii in order to minimize flow requirements.

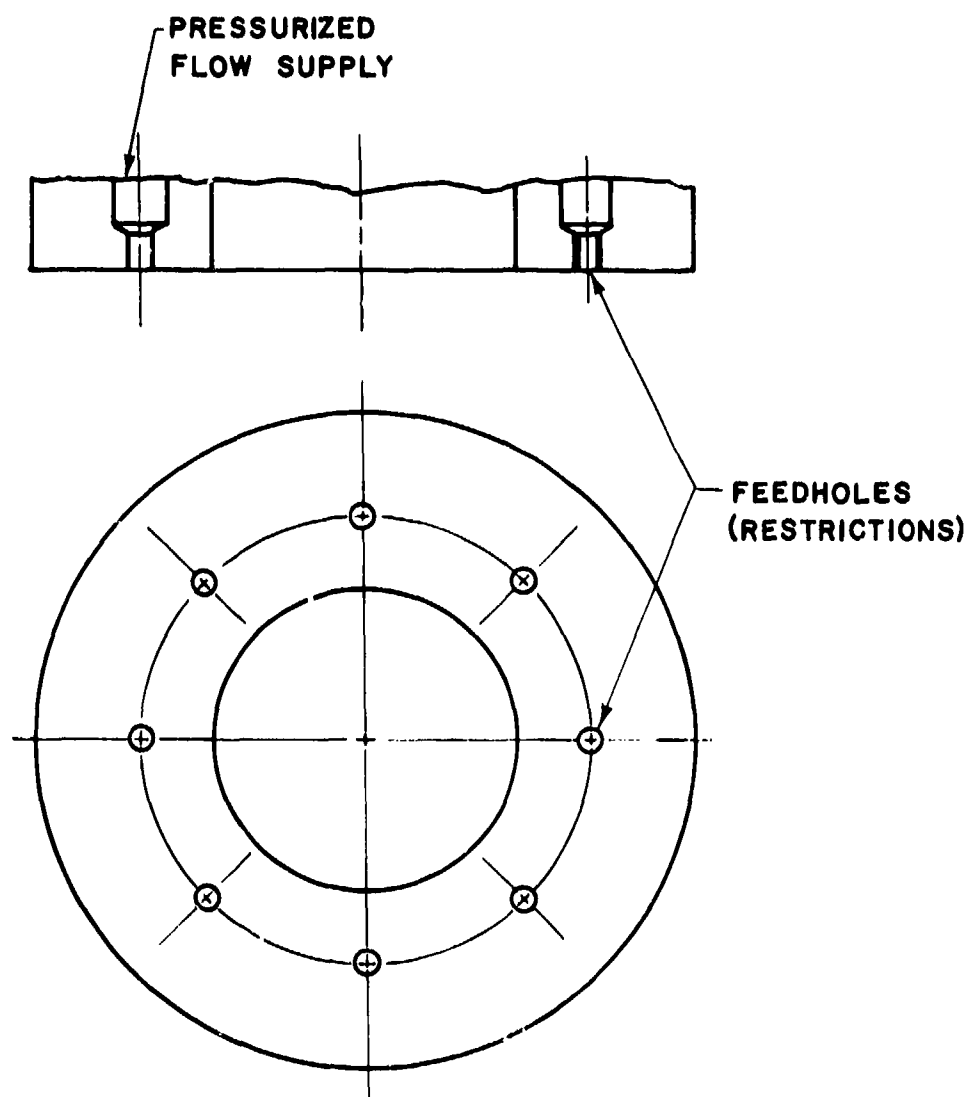


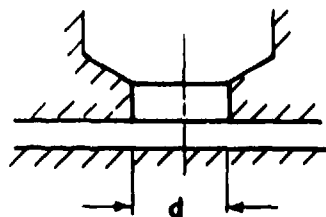
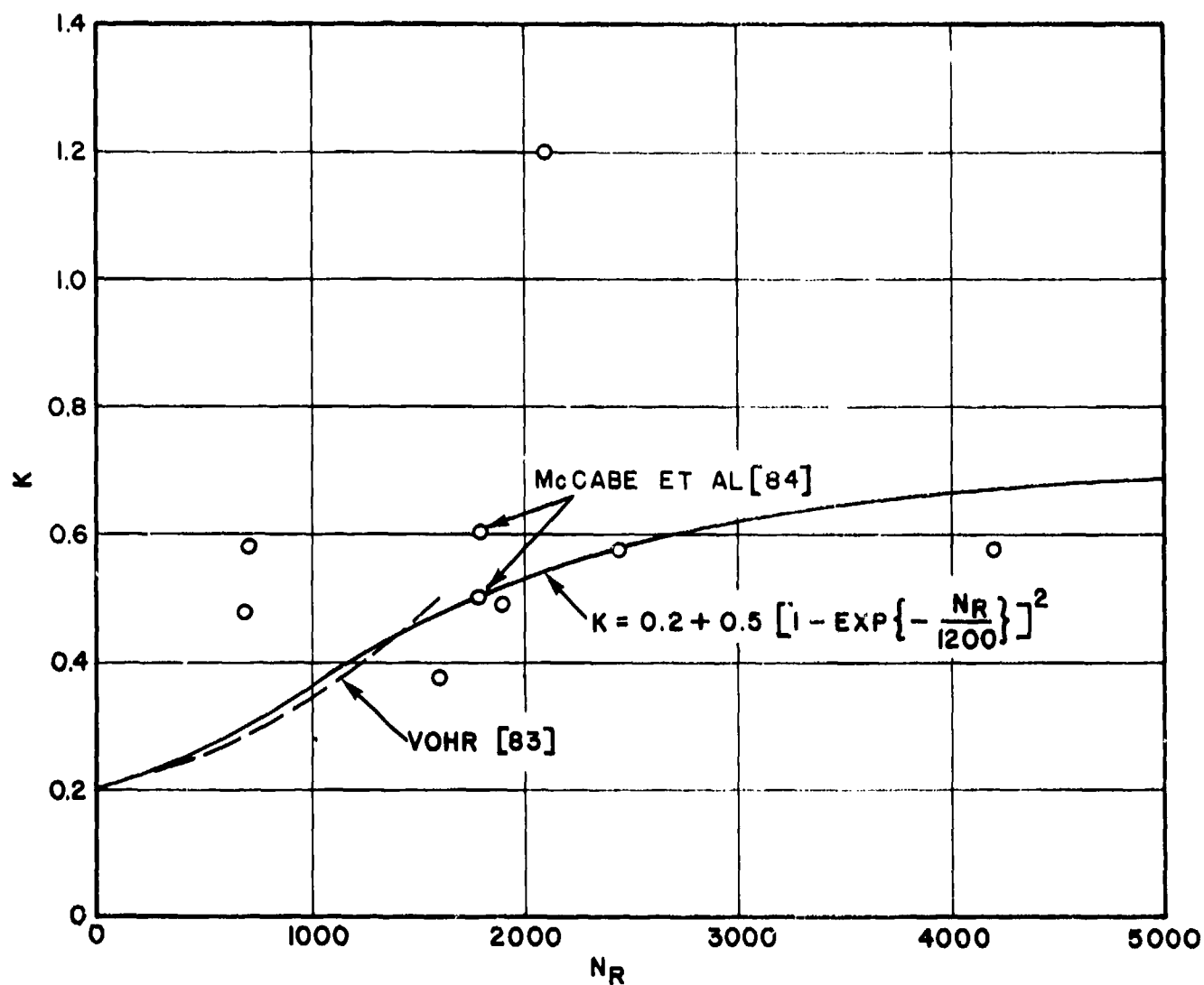
Figure 19 Schematic of Externally Pressurized Annular Thrust Bearing

The feed holes serve as restrictors such that the film pressure would resist a gap change to render an axial bearing stiffness. The pressure loss through each feed hole is a function of the "throat" Reynolds number [83,84] as illustrated in Figure 20. If a maximum stiffness is desired, the number and diameter of feed holes should be selected to match the desired operating film thickness so that perturbation of the film inlet pressure with respect to gap change is maximal [45] as illustrated in Figure 21. The feed holes should be sufficiently closely spaced to "fill in" the film pressure between adjacent holes. A general rule to follow is to make the hole spacing not larger than the distance between the feed circle and the nearest ambient edge. If the supply/ambient pressure is more than 2.0, the maximum stiffness design point is usually associated with a sonic feed condition. Operation at a larger gap will result in a supersonic expansion process immediately downstream of the feed hole [85]. A sonic condition can also develop at a discharge edge. This is likely to happen if the supply/ambient pressure ratio is very large, say in excess of 10 to 1, and the film pressure would develop a convex distribution with a vertical slope at the ambient edge. Consequently, with respect to a gap variation, the film force perturbation may have a non restoring effect. Discharge choking is more likely to take place at the inner radius than at the outer radius for an annular thrust bearing.

Because there are thrust bearing designs of the self-acting type which appear to possess the desired level of load capacity for aero propulsion equipment, the penalty in efficiency due to compressor bleed off in the use of external pressurization appears to be unwarranted. However, the possibility of augmenting thrust load by pressurization in a hybrid arrangement should not be overlooked [21].

5.2 Surface Features for Self Acting Thrust Bearings

The basic topography of a thrust bearing surface, i.e., a flat disc which is perpendicular to the axis of rotation, is not conducive to the generation of a load carrying capacity by the "hydrodynamic wedge". Although there are liquid lubricated devices, notably the face seal, which appear to contradict the above statement, the actual load capacity is of a very small magnitude,



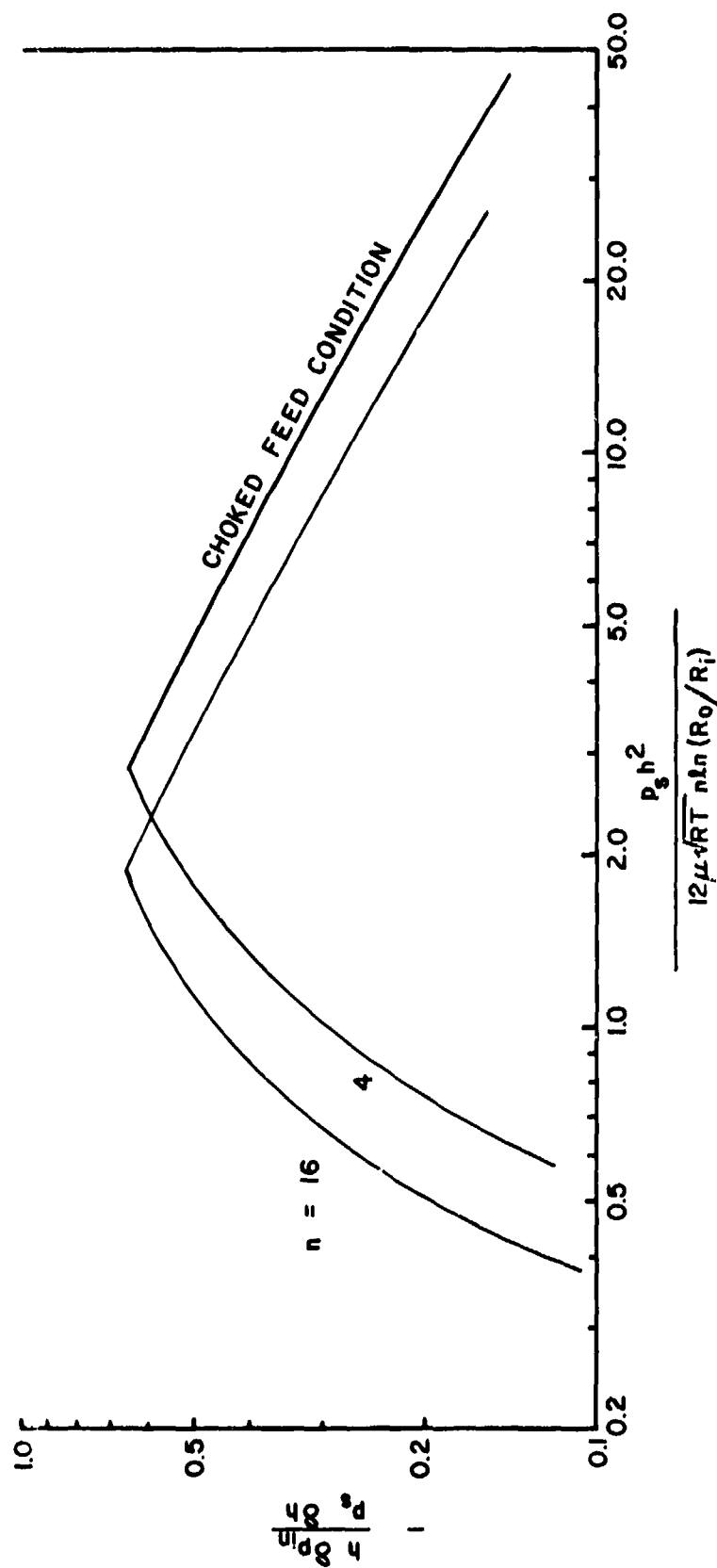
$$K = \frac{\text{TOTAL PRESSURE LOSS}}{\text{SUPPLY - TOTAL PRESSURE DROP}}$$

$$N_R = \frac{2 \dot{m}}{\pi d \mu}$$

\dot{m} = MASS FLOW RATE d = THROAT DIAMETER

μ = VISCOSITY

Figure 20 Pressure Loss Characteristics of Inherently Compensated Restrictor



FEED CIRCLE DIAMETER: 1.25"
 O.D.: 2.061"
 I.D.: 0.758"
 SUPPLY PRESSURE: 147.0 PSIA
 AMBIENT PRESSURE: 14.7 PSIA
 AIR AT 540 °R

NUMBER OF FEED HOLES (n) 4 16
 FEEDHOLE DIAMETER (d) 0.061" 0.015"

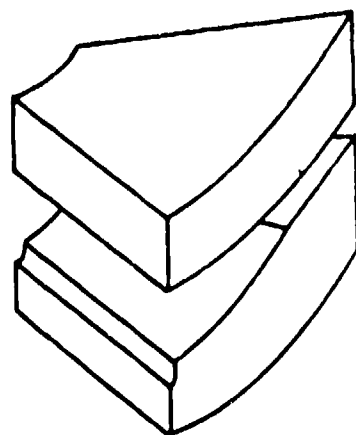
Figure 21 Film Inlet Pressure Perturbation Coefficient of Externally Pressurized Annular Thrust Bearing

and the mechanism is believed to be secondary effects, such as a wobbling runner and thermally induced waviness, which in turn create the necessary hydrodynamic wedges. For the application of gas lubrication to aero propulsion equipment, the required load capacity is relatively high; therefore it is necessary to alter the topography of the perpendicular flat disc by engineering.

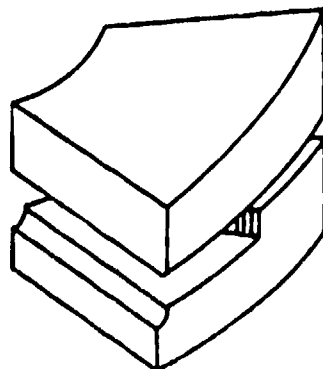
The Michell-Kingsbury type tilting-sector thrust bearing is again a logical adaptation of the experience in liquid lubricated thrust bearings. Pad crowning and offset of pivot location are necessary features to realize a large load capacity. Each pivoted sector seeks its own alignment with the runner; however, load equilization must still depend on precision control of the overall bearing geometry or additional kinematic contrivances. Radial crowning, as may be induced by thermal effects, can aggravate side leakage and thus reduce the load capacity and roll-yaw stability. The tilting-sector thrust bearing shares the same drawback with the tilting-pad journal bearing in its mechanical complexity.

There are various ways to bring about the hydrodynamic wedge on a fixed flat disc as illustrated in Figure 22. The first three are obvious adaptations of the slider concept. A major contribution to the design art of these bearing types was the result of a collaborative effort [86], in which analytical prediction methods were checked by a series of experimental studies in the formulation of a recommended design practice.

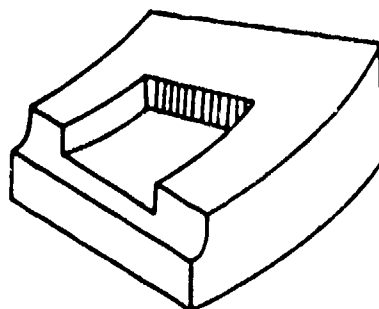
The spiral-groove thrust bearing is often known as the Whipple bearing in recognition of the pioneering contribution of the first major effort to evaluate this concept [71]. In Whipple's original treatment, both the single-sided and herringbone grooving patterns are considered. However, variation of sliding speed and the area constriction with radius were neglected. Subsequent studies [23,87,88] revealed that the inward pumping design is invariably the best grooving pattern. Its relative superiority over alternative configurations is associated with annular geometries with a relatively small inner/outer radius ratio (<0.6) and a relatively large compressibility number. The optimized load capacity as a function of these two parameters is shown



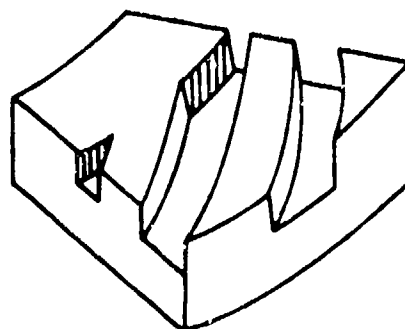
TAPER-LAND



STEP



POCKET



SPIRAL-GROOVE

Figure 22 Surface Features of Self-Acting Thrust Bearings

in Figure 23.

The grooving parameters including

- α width fraction
- Δ groove-depth/gap ratio
- γ radial fraction
- β helix angle measured from circumference

have been optimized for maximum load at each combination of the effective compressibility number $6\mu\omega(R_o^2 - R_i^2)/(p_a h^2)$ and the radius ratio R_i/R_o as listed below.

$\frac{6\mu\omega(R_o^2 - R_i^2)}{p_a h^2}$	$\frac{R_i}{R_o}$	α	Δ	γ	$\beta(\text{deg})$
4.0	0.4	0.600	3.00	0.725	17.5
	0.5	0.614	3.04	0.724	17.5
	0.6	0.625	3.04	0.725	17.7
	0.7	0.641	3.04	0.733	18.1
	1.0	0.659	3.05	0.735	18.8
50.0	0.4	0.605	2.96	0.701	17.1
	0.5	0.613	2.98	0.695	17.3
	0.6	0.627	3.05	0.689	17.9
	0.7	0.637	3.08	0.692	18.4
	1.0	0.659	3.05	0.735	18.8
100.0	0.4	0.610	2.99	0.673	17.4
	0.5	0.617	3.03	0.669	17.7
	0.6	0.625	3.02	0.664	17.9
	0.7	0.635	3.05	0.667	18.3
	1.0	0.659	3.05	0.735	18.8
200.0	0.4	0.608	2.96	0.638	17.2
	0.5	0.627	3.02	0.638	17.9
	0.6	0.635	3.05	0.632	18.4
	0.7	0.640	3.05	0.632	18.5
	1.0	0.659	3.05	0.735	18.8

For comparison, shown in the same graph are the expected load capacity of the recommended stepped-sector bearing [86] and the optimized slider in a six-sector arrangement.

The recommended step pad-sector bearing has a fixed groove depth which is

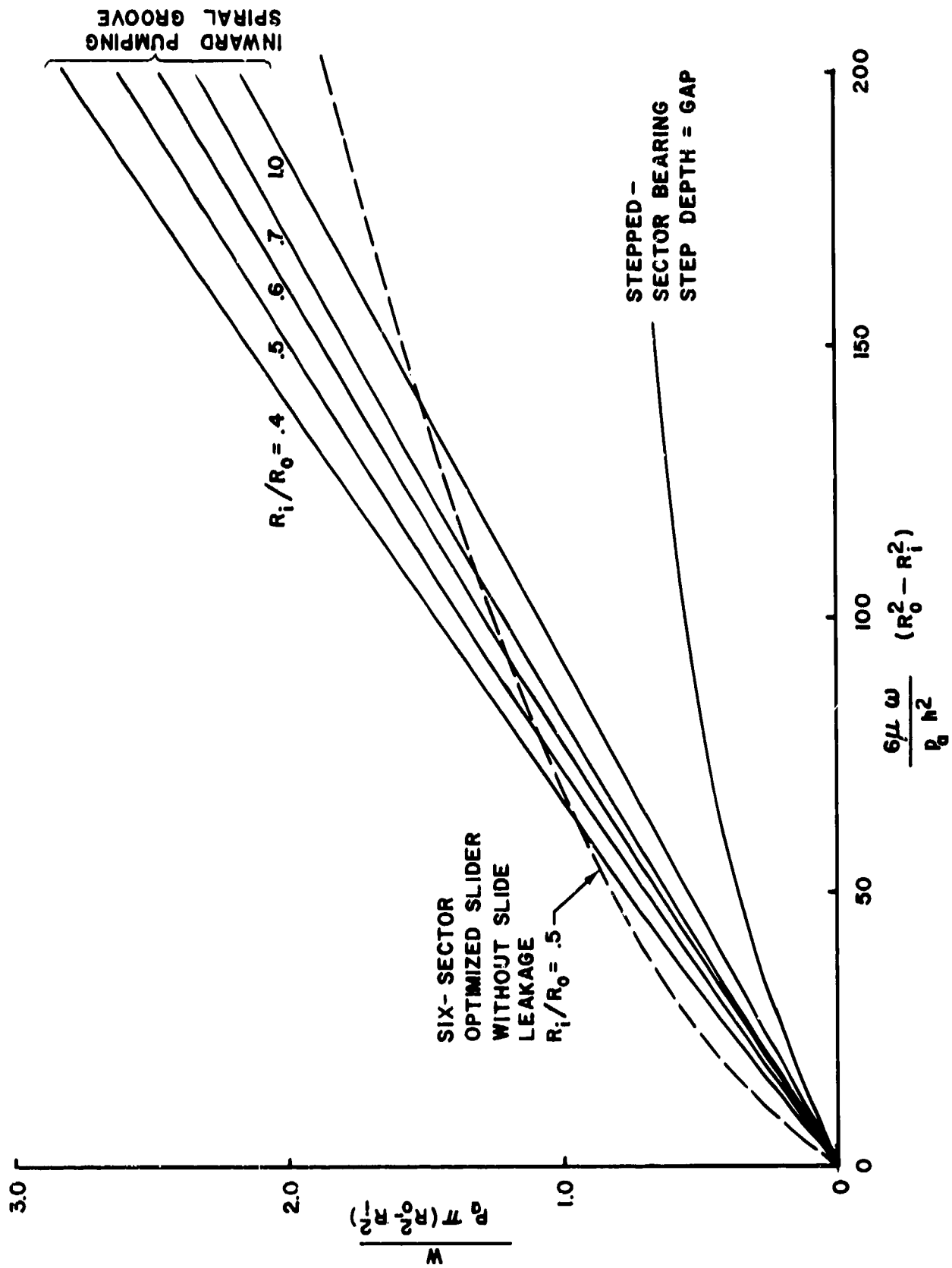


Figure 23 Optimized Load Capacity of Fixed Thrust Bearings

equal to the design gap. This is very close to the Rayleigh step of 0.866 times the gap. The optimum step width is dependent on the effective compressibility number. The optimum number of sectors is dependent on both the effective compressibility number and the radius ratio.

The curve for the optimized slider is plotted on the basis of the mean sliding speed and the mean circumference. The plan form of six sectors is chosen to agree with that of the optimized stepped-sector for a radius ratio of 0.5 and an effective compressibility number in excess of 50. End leakage is, of course, neglected.

The general trends of the optimized slider and the stepped sector are very similar. Throughout the whole range of the compressibility number, the ratio between the two curves is about 2.5. Since the gap geometries are very similar at a low effective compressibility number, the discrepancy can most likely be attributed to end leakages. At high effective compressibility number, end leakages should be relatively subdued. Therefore, the larger load capacity of the optimized slider should be approachable, at least partially, by using the optimized gap profile of a tapered step as indicated in Figure 8. Thus, a case may be made for the potential relative advantage of the optimized slider over the spiral groove thrust bearing in some moderate range of the effective compressibility number.

The superior load capacity of the spiral groove thrust bearing is particularly impressive at large compressibility numbers. The observation has been made, if there are a sufficient number of grooves, the blocked flow spiral groove thrust bearing is theoretically without compressibility effects, hence, there is a constant proportional relationship between the load capacity and the compressibility number [87]. With radial through flow, the film pressure distribution actually varies with the compressibility number. In the grooved region, the viscous pumping capacity, i.e., the radial pressure gradient for the blocked-flow condition, is directly proportional to the sliding speed, which is in turn proportional to the radius. Radial through flow detracts from the pressure gradient by an amount which is inversely proportional to the product (pr). In the absence of curvature, i.e., if the radius ratio is

near unity, then the reduction of pressure gradient by radial through flow is inversely proportional to p , so that the pressure profile in the grooved region would become more concave. At the same time, the pressure profile in the smooth region would become more convex. The integral of the pressure profile, while still dependent on the compressibility number, is not bounded by an asymptotic constant, but gradually assumes a $1/2$ power relationship as the compressibility number becomes incessantly larger [88]. This fact alone makes the spiral groove bearing very attractive at very high speeds. For the inward pumping design, the relative effect of radial through flow to that of viscous pumping is $1/(pr^2)$, r^2 relieves the effect due to p alone at least in part. Consequently, any dependence on the compressibility number is even more subdued.

Since the narrow groove analysis, as first used by Whipple, implies that the local variation of fluid density is negligible, the question has been raised as to whether or not the favorable characteristics as predicted by the narrow groove analysis may be fortuitous. An approximate analysis of this issue was performed by assuming the bearing topography to be a skewed sinusoidal wave and only effects up to the second order of the wave amplitude need to be considered [89]. This study revealed that the narrow groove approximation is adequate so long as a local compressibility number is sufficiently small. Otherwise the viscous pumping effect would not be realized. The requirement of a small local compressibility number is readily achievable for bearing sizes typical of those to be used in aero propulsion machines.

The theoretical load capacity of the inward pumping spiral groove thrust bearing is sufficiently large so that the use of self-acting thrust bearings in aero propulsion machines appears very promising.

5.3 Dimensional Control

Alignment of bearing parts, or the lack of it, is an everpresent problem in the engineering of turbomachines. Reliable operation of the bearing components requires that parallelism between mating surfaces be maintained and that unavoidable differential growths between various parts of the machine

do not significantly alter the operating gaps of the fluid film bearings. Transient fluctuations in the thermal environment as well as thermal gradients in aero propulsion equipment can be substantial. Associated dimensional changes in the housing, in the rotor, and of the bearing parts may all cause deviations of the bearing gaps from their ideal conditions. It is essential that such dimensional changes do not cause and sustain inadvertent high speed sliding contact of gas lubricated bearing surfaces.

For applications in aero propulsion equipment, the operating gap of a gas lubricated journal bearing at maximum load is expected to be in the order of $2-3 \times 10^{-4}$ per unit radius, and that of a gas lubricated thrust bearing is similar per unit outer radius.

The respective alignment tolerances, assuming 1/5 of the gap at maximum load is affordable, are about $0.05(D/L)$ milliradians for the journal bearing and about 0.05 milliradians for the thrust bearing. If rigid geometry bearings are to be used, these alignment requirements are totally controlled by the relevant dimensional integrities of the bearing housings. With a thermal coefficient of expansion typically in the order of $15 \times 10^{-6}/^{\circ}\text{C}$ of structural materials and bearing environment temperature up to 1200°C , it is quite obvious that bearings with self-alignment capability are desirable in this application.

In the case of the thrust bearing, since the rotor axis is located by the centers of the journal bearings, precise control of the perpendicularity of the runner relative to the rotor axis is absolutely crucial. In addition, irrespective of the possibility of using self-aligning bearing sectors, overall parallelism of the entire stator surface to that of the runner can be realized only by the employment of a self aligning mechanism such as a double-ring gimbal or a flexure mount as illustrated in Figure 24.

Alignment problems discussed above are associated with global structural distortions. The issues of local thermoelastic distortions are more subtle but equally important. It is well known that the journal bearing bushing would become out of round if natural circulation is allowed to be a non-negligible

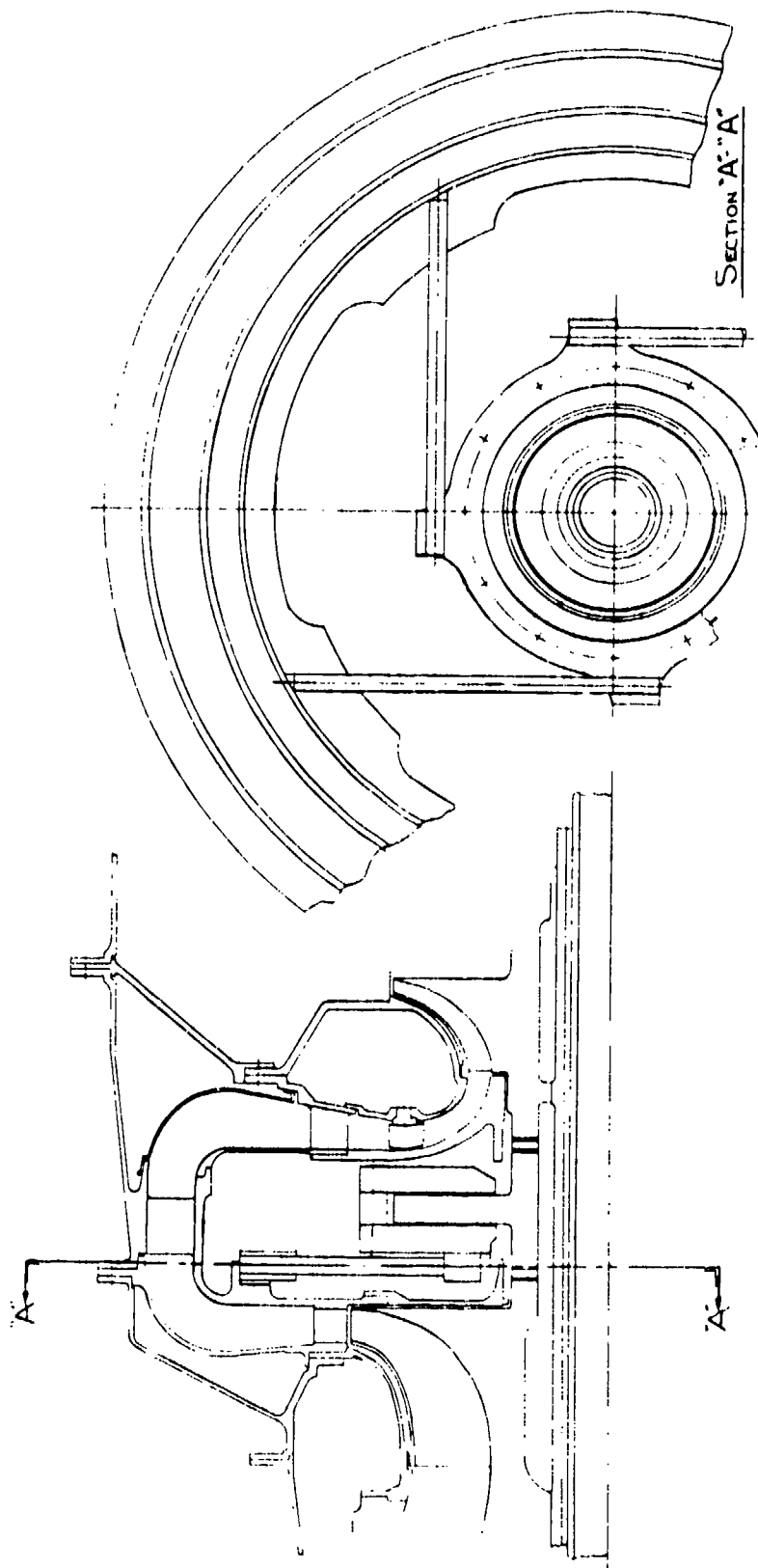


Figure 24 Thrust Bearing Support Flexure [21]

cooling mode of a horizontal rotor. For similar reasons, it is a good practice to maintain structural isotropy.

The thrust bearing, regardless of the particular design of the gap profile, is always vulnerable to radial non-uniformity of the film thickness. The simplest, but also representative example, is the thermal crowning which is always present to some degree because the heat generated by bearing friction power necessarily has to pass through the bearing parts [22]. If the thrust plate is not restrained axially in some distributed manner, an axial temperature gradient which is associated with the conduction heat flux, would induce radial crowning to an extent which is proportional to the product of the heat flux and the coefficient of thermal expansion, and is inversely proportional to the thermal conductivity of the thrust plate. For illustration, this model analysis was applied to a statically optimized spiral groove thrust bearing which has an outer diameter of 5.35 in. to carry 92 lbs load at 24,000 rpm at a gap of 0.00080 in. The degree of thermal crowning varies significantly with the bearing material. With a molybdenum alloy, overall crowning would be 0.00007 in. and the minimum gap at the design condition would be reduced slightly to 0.00075 in. If a nitriding steel is used instead, the crowning would equal the design gap and the minimum gap would be reduced to 0.00030 in. Aside from material choice, engineering control of this type of thermal distortion may be achieved by redirecting the conduction heat flux radially, preferably inward [90].

Experimental verification of thrust bearing gap non uniformity was performed on an experimental gas bearing gyroscope at the running condition by making synchronized interferometric studies through a silica thrust plate [91]. In this case, bending of the thrust plate by film pressure as well as mechanical distortion from assemblage clamping were found to be equally important. An elaborate analytical study making use of finite-element thermo-elastic calculations was attempted. Unfortunately, the credibility of the analysis was obscured by uncertainties related to modeling the attachment constraints between assembled bearing parts [92].

5.4 Stability of Thrust Bearings

The possibility of a self-acting gas-lubricated, thrust bearing to experience a self-excited instability was realized in a theoretical study which was concerned with the operation of the spiral-groove thrust bearing at a large compressibility number [23]. It was found that the quasi-dynamic damping coefficient of a spiral groove thrust bearing, which is optimized for maximum load capacity, can become negative with respect to a translational axial perturbation if the effective compressibility number exceeds a value between 12.0 and 16.0 depending on the radius ratio. This is a necessary condition for instability and is reasoned to be analogous to the pneumatic hammer phenomenon [82]. In the spiral groove bearing, the grooves, while functioning as viscous compressors, also act as restricted mass storage sites. It was found possible to ensure non-negativity of the quasi-dynamic damping coefficient by reducing the radial extent of the grooves with a moderate compromise in the load capacity.

The bearing design with the reduced groove length has been referred to as possessing absolute stability which is an exaggerated claim since only the instability of the translational mode can be so eliminated. The self-acting thrust bearing can also develop instability in the angular (wobbly) mode. Because the rotor motion is primarily controlled by the journal bearings, the angular mode of instability was experienced only with thrust plates which are either gimbal-mounted or compliantly mounted through flexures [24,21], involving both stepped-sector and spiral groove designs. The basic mechanism here, from the fluid film point of view, is related to the journal bearing whirl phenomenon; however, the mechanical arrangement dictates that the thrust plate instead of the rotor to provide the unstable motion. A thorough analytical study of the phenomenon was performed for the spiral groove design with the objective of identifying controlling parameters [25]. The most effective and yet easy means to stabilize the thrust plate is to apply a damping restraint; the Coulomb type damper has been found to be adequate. The required level of damping can be readily determined analytically. In decreasing order of effectiveness, alternative means to stabilize the thrust plate are fluid film design adjustment and introduction of inertia asymmetry.

Since self aligning type thrust bearing installation appears to be necessary, this issue should not be ignored.

SECTION VI

STATUS OF AIR BEARING MATERIALS TECHNOLOGY APPLICABLE TO AERO PROPULSION SYSTEMS

The main advantage in the use of gas lubrication to support the gas turbine rotor in an aero propulsion system is the prospect of allowing the bearing components to be exposed to a high temperature level. Presently, an operating temperature of bearing parts at 650°C is regarded to be a reasonable goal. No other lubrication concept offers this potential capability. Along with the high temperature capability, the gas bearing allows the shaft rotational speed to increase substantially. For a small engine, a rotor speed of 60,000 rpm with a turbine inlet temperature of 1400°C is believed to be feasible by using gas bearings to support the gas generator rotor.

In the gas bearing applications, technological burden of high temperature is shifted from the lubricant to bearing materials. Given the temperature and chemical environments, the generic functional requirements can be divided into two main areas. Firstly, overall dimensional accuracy and structural strength must be maintained. Secondly, topographical integrity of the bearing surface must be preserved despite contact sliding prior to lift-off and, hopefully, will also survive upon occasional contact incidents at full speed. The prevailing approach in the development of gas bearing materials is to separate these two generic functions by surface coating. The substrate provides the structural function. Endurance of contact sliding is realized by the use of a hard coating and/or a solid lubricant. Because the degree of trauma from the sliding friction is intimately related to the design features of the bearing, the material development effort cannot be treated as an isolated materials science problem. The chemical aspect of the environment is an important factor in the sliding behavior of bearing materials. Thin oxide films of low shear strength can reduce sliding friction and thereby improve endurance. The same material may behave quite differently in an inert environment [10].

For rigid bearings, materials suitable for use in the environment of aero propulsion machines have been successfully tested [21,93]. Chrome oxide appears to be the leading coating material. For temperatures above 425°C, modification with NiCr is necessary to gain improved endurance of thermal cycling. There is considerable experience in applying this type of coating by plasma spraying and by the detonation gun process. The thickness of the coating is typically 100-200 μm . More recently, experience on thinner coatings of about 20 μm applied by sputtering has been reported [94]. Success for this type of coating as a gas bearing material is generally attributed to its extreme hardness. Inadvertent entry into the bearing gap of particulate matter, which is too large to pass through the minimum gap, would result in the pulverization of the intruder without altering the topography of the bearing surfaces. It is clear that substrate hardness would become a relevant parameter if tolerance of particulate ingestion should be required of the bearing. Wear debris formed of the coating material tends to be a fine powder with no tendency for conglomeration in a normally dry environment.

Foil type gas bearings introduce new material problems partly because the surface would experience cyclic strains of large magnitude and partly because the lift-off speed of a foil bearing is relatively high. Overall consideration of structural properties led to the selection of Inconel X-750 as the foil material. Since this material tends to gall, desired sliding behavior must rely entirely on the coating. MoS_2 and teflon type coating for the foil are satisfactory at low temperatures, up to about 350°C [94,95], in sliding against hard coated surfaces of the journal bearing or the runner. The issue is yet not resolved at higher temperatures. A proprietary coating of Cr_2O_3 base looked very promising when tested in the partial arc journal bearing configuration but did not live up to expectation when tested in the full complement configuration [94]. A large amount of wear debris was found entrapped in the bearing gap.

SECTION VII

PROSPECTS OF COMPLIANT GAS BEARINGS

7.1 The Evolution

Study of fluid film lubrication, with the film thickness significantly affected by the deformation of the bearing surface, has for a long time been known as elastohydrodynamic lubrication and has for the most part been associated with concentrated contact devices such as rolling element bearings, gears, and traction drives [96]. In these cases, although the film pressure remains a small fraction of the elastic modulus of the material, the cumulative strain in the substrate results in a distribution of normal displacements which is much larger than the thickness of the lubricating film. Scaling down proportionally both the elastic modulus and the film pressure, one finds that the lubrication of elastomeric dynamic seals obeys the same fundamental mechanism. Occasionally, engineers turn to seek wisdom from nature and learned that the most efficient bearing, which is capable of carrying varied static and dynamic loads "painlessly" without friction, does not require precision control of its bearing surface. The synovial joint is now regarded as a model of the ultimate in lubrication technology. A highly compliant layer of cartilage at each end of the mating bones distributes the transmitted load uniformly to a "comfortable" level and at the same time traps a fluid film which facilitates free swiveling of the joint [97].

In a foil bearing, compliance of the bearing surface is realized because of structural flexibility, even though the elastic modulus of the foil material is among the highest of metals. Interest in its use for rotor support was originally related to dynamic energy conversion equipment on a space platform. At that time, the possibility of a stable high speed operation in a zero-G environment was a primary motivation. While other means for stable, high speed rotation soon became known,

(see Section IV), compliant bearings have been recognized for relative tolerance to dimensional uncertainties. By that time, the stringent dimensional control required in the use of rigid gas bearings for aero propulsion applications had been well established [98]. Exploration thus continued in earnest to consider use of air lubricated foil bearings in small high speed, gas turbine power plants [18,19,40,41,42]. In the meantime, favorable experience in the large scale use of foil bearings for the support of high speed rotating machines in relatively benign environments [39,42] has kindled the expectation of the successful development of foil bearings in aero propulsion applications.

7.2 Panoramic View of Foil Bearing Technology

Most of the technology related to the tension dominated, air-lubricated, foil-journal bearing was mainly the outcome of space-application studies. The state of development was sufficiently advanced to warrant a comprehensive documentation of the design procedure [99]. Some notable events in the development experience of the tension dominated foil bearings are recounted below.

- Non-synchronous whirls of both harmonic and ultra harmonic orders were occasionally observed. They were always of harmless amplitude [36, 37,38].
- Largest rotor motions were recorded at low speeds during startup and were attributed to friction excitation [38]. Generally the amplitude of such motions reduced with lessened preload tension.
- Severe thermal gradient could be tolerated with no unusual behaviors of the rotor observed [37].
- High speed seizure induced by artificial transient chilling was demonstrated. The bearing relieved itself unassisted and permitted rotation to resume without repair [37].
- No attempt was made to avoid entry of dirt and dust into the bearings. No ill effects attributable to lack of cleanliness were experienced [38].

Development studies related to space-power applications cited above did not attempt to establish the ultimate load capacity of the tension dominated

foil bearing. Some knowledge on this question was gained on a similar bearing consisting of three preassembled pads as shown in Figure 25 [100]. Load-deflection testing of a single pad version of such a configuration at 36000 rpm passed a load level of 36 lbs. The journal diameter was 1.5 in and the foil width was 1.0 in. Failure occurred at 46 lbs, representing a unit load of 30.7 psi. However, spurious contact was suspected at loads above 30 lbs. The mode of failure was in the form of tension rupture along the edge of the small radius of the support pad.

In an independent study [101], tension dominated foil bearing of the two construction types, Figure 18(a) and Figure 25 respectively, were tried as the support system of a high speed wire spool. The preassembled pad version, Figure 25, failed during an attempt to pass a violent critical speed at approximately 15,000 rpm. The "threaded" version, Figure 18(a), did permit the spool to go through the critical speed to reach its operating speed of 105,000 rpm.

The multi-leaf type foil bearing is a patented design of AiResearch, Garrett Corporation. Its claim to fame is due to its successful application in the air cycle turbo machines presently used in commercial, passenger, aircraft [39]. It is also being considered for various gas-turbine type applications including the diesel supercharger. AiResearch is presently under contract with U.S. Air Force to evaluate the feasibility of its use in an advanced Auxiliary Power Unit (APU). A typical journal bearing of this type was shown in Figure 18(b). A thrust bearing version of the multi-leaf foil bearing is illustrated in Figure 26. Unit load levels in excess of 20 psi have been reported for both journal and thrust bearings of this variety. Failure of the journal bearing appeared to be preceded by structural bottoming of the loaded leaf, which event is generally followed by the appearance of unstable whirl motion. Analytical design tools for the multi-leaf foil bearings have been released to the public through the sponsorship of U.S. Air Force [102, 103]. Independent analytical techniques for the multi-leaf journal bearing have been developed by workers of General Motors Research Laboratories [104, 105].

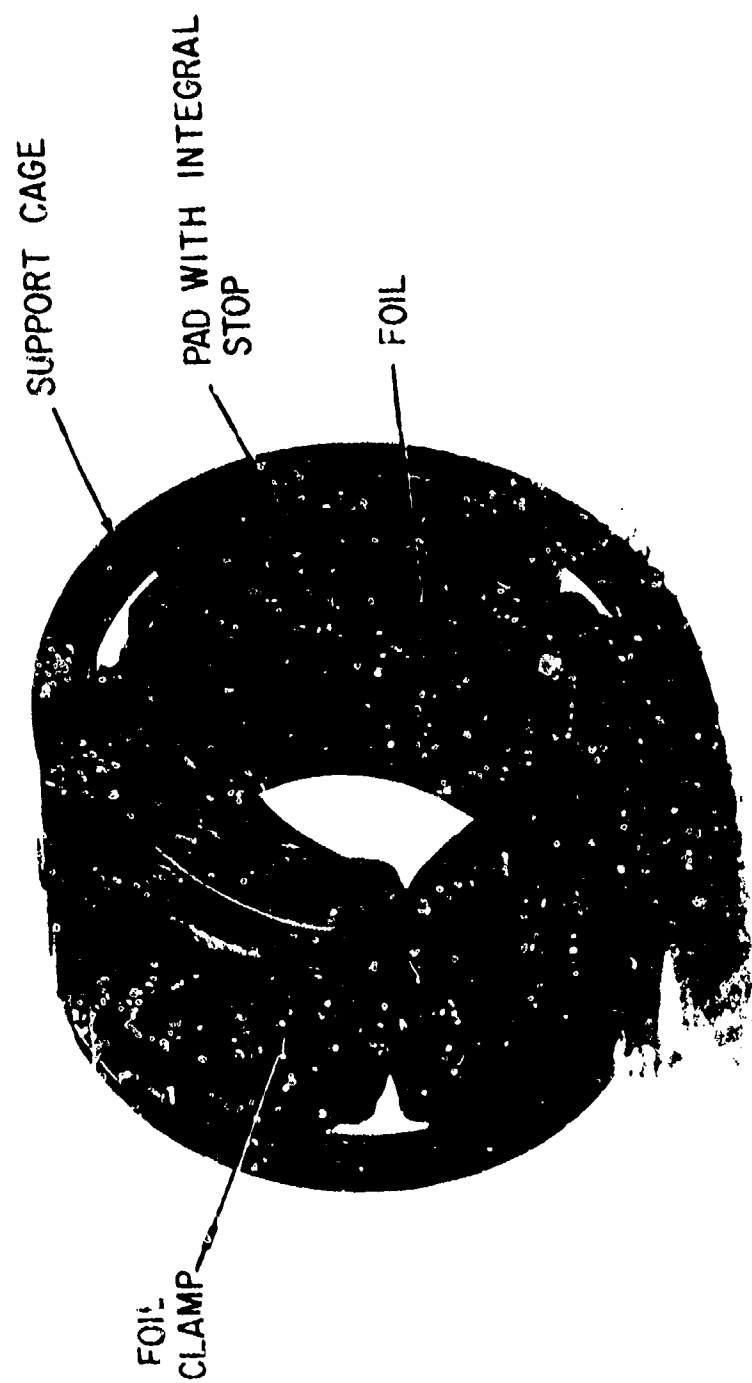


Figure 24 Tension Intershaft Foil Bearing Assembly

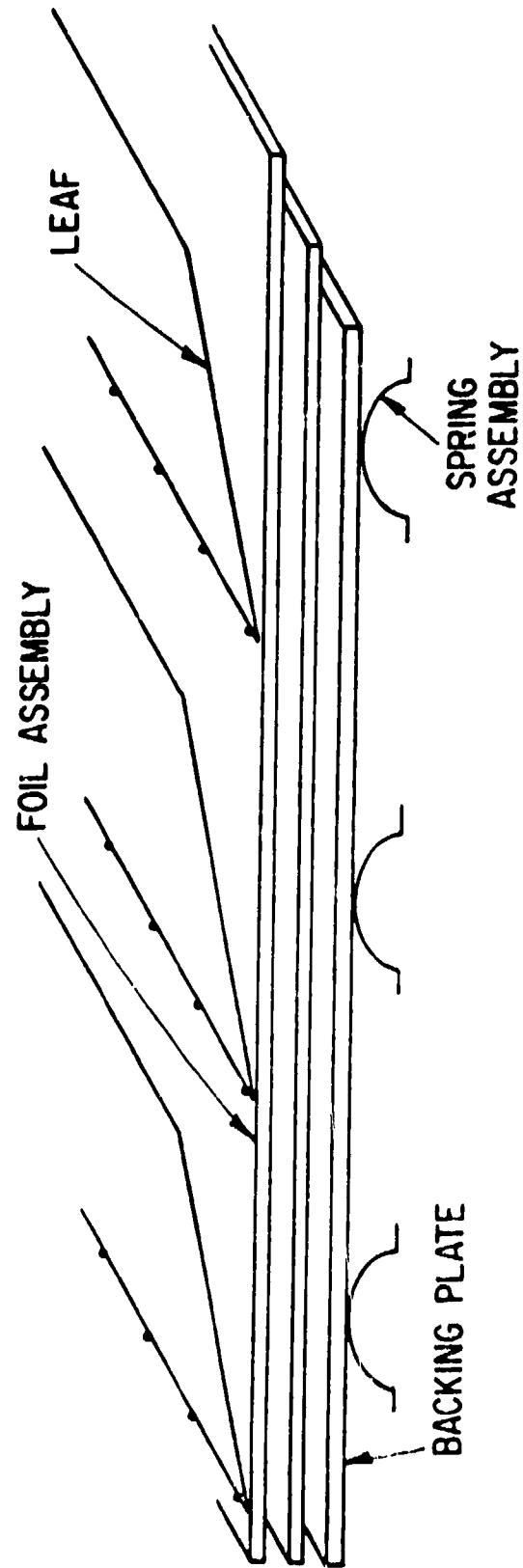


Figure 26 Schematic of One-Dimensional Leaf Thrust Bearing

Another category of foil bearing, as shown in Figure 18(c) in the journal version, is commonly known as the Hydresil, which is the trademarked acronym of Mechanical Technology Incorporated and is derived from the description "HYDrodynamic RESILient" bearing. It is, in essence, the overlay of a smooth foil over a more-or-less compliant substructure which is typically a corrugation (often called the bump foil or ridged foil). The same features are also applicable to a thrust bearing configuration. An alternate version of the compliant substructure is the pleated foil. The folded edge of the pleat turned out to be vulnerable to fatigue failure [102] and therefore, the pleated substructure is no longer in use. The Hydresil bearings have been successfully installed and field tested in a prototype blower for household vacuum cleaners, and are also used to support the turbine end of the gas generator of an experimental automotive gas-turbine [42]. Technology information on the Hydresil design has been made available to the public through the sponsorship of government agencies [102, 94, 106]. Unit load levels in the order of 20 psi have been reported. Pre-failure data of the journal bearing usually contained symptoms of unstable whirl, suggesting "friction-frozen" contacts between the top foil and the compliant substructure when the latter became fully seated under heavy load. Friction excited vibrations were believed to be present during start up [94].

The latest entries of air lubricated compliant journal and thrust bearings are illustrated in Figures 27 and 28 respectively. Both are patented designs of the same inventor. Operating characteristics of these novel bearings were previously released in a contract report [107]. Two companion papers [108, 109] will present this information to the public in the forthcoming ASME-ASLE Joint International Lubrication Conference August 18-24, 1980, at San Francisco. The journal bearing shown in Figure 27 is the first conscious attempt to combine a highly compliant integral substructure with a multi-layered foil to provide for Coulomb damping. Quiescent operation of an overhung rotor, weighing 19.08N, up to 50,000 rpm was demonstrated despite the deliberate addition of 43 $\mu\text{m.N}$ in pitching unbalance. Maximum synchronous response was noted at about 25,000 rpm. Non-synchronous motions were negligible. All dynamic data reported were taken during coast-down, no information was given regarding startup behavior of the rotor. Figure 28 shows two

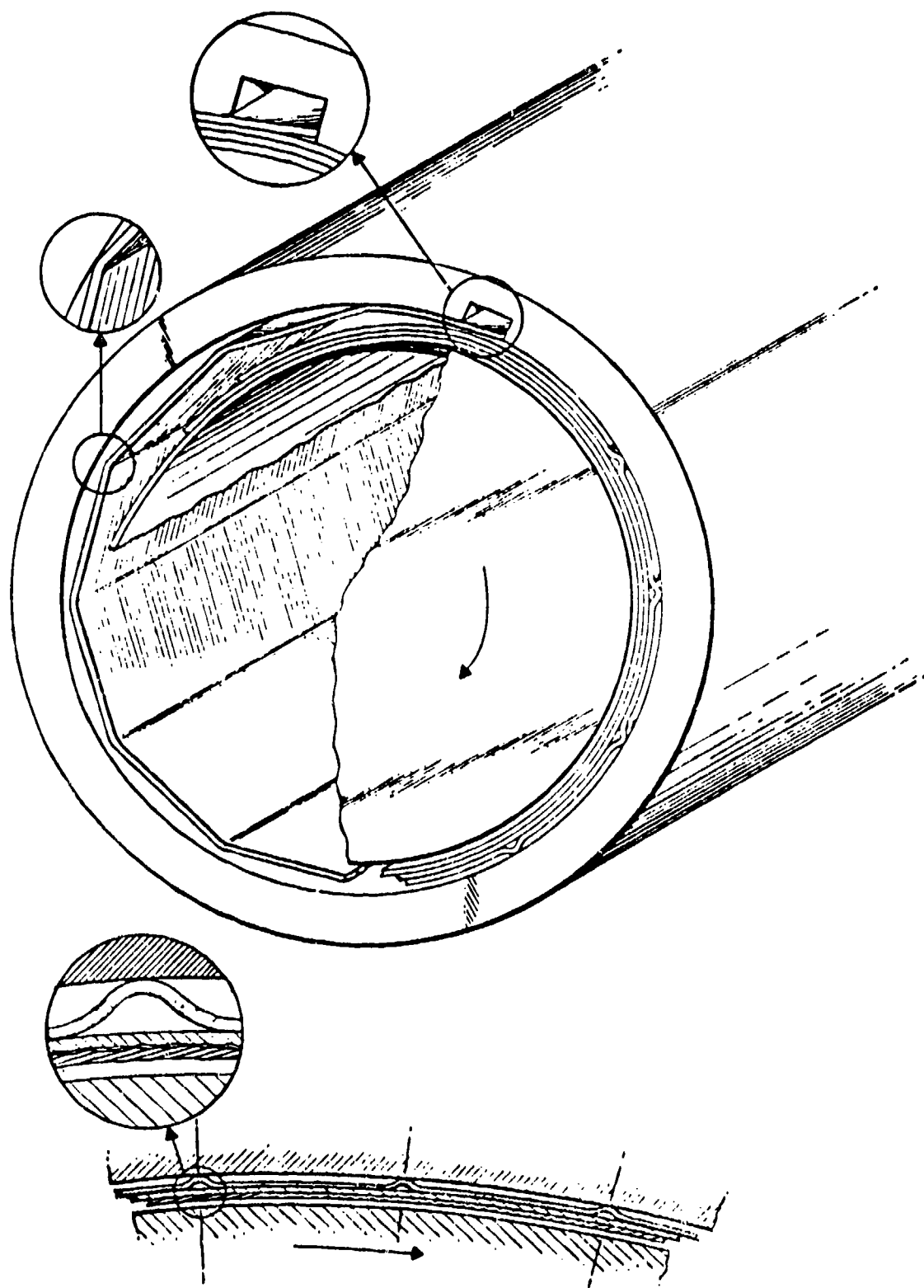


Figure 27 Schematic Drawing of Coil Type
Journal Foil-Bearing With Integral
Leaf Spring [107]

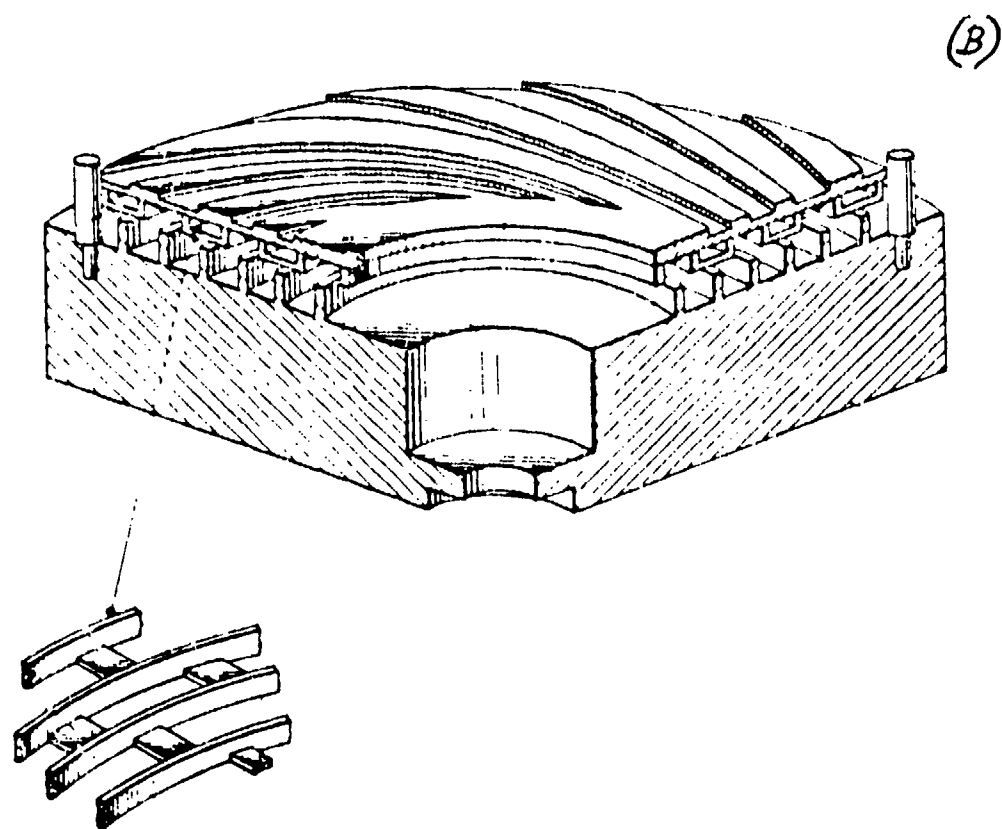
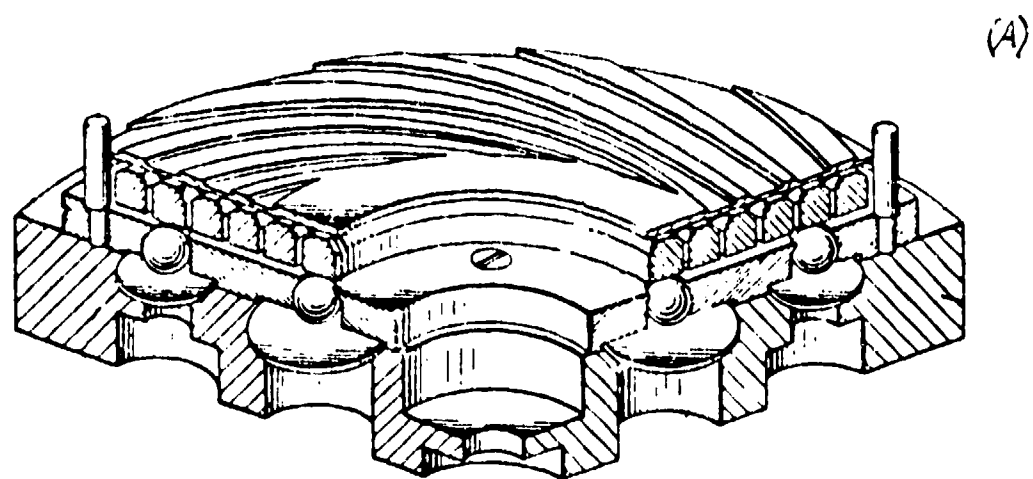


Figure 28. Campbell's Supported Spiral Groove
Burst Bearing (108)

alternate ways to design for parallel film operation of the spiral groove bearing at the design point (presumably the maximum load condition). Global alignment for perpendicularity to the rotation axis is still necessary, however,

The three main types of foil journal bearings have been evaluated as a mid-span damper [100,110,111]. A common disappointment of these studies is the insensitivity of the rotor to the presence of the mid-span device in passing through the first critical speed (but not vice versa)* unless external pressurization is used [111]. Essentially the same response amplitude is experienced by the foil bearing upon its insertion in place. This suggests that Coulomb friction for damping in a foil bearing may not be activated unless it is directly addressed as a design feature. Since the journal bearings in support of a gas turbine rotor must not only be free from potential self-excited instabilities, but must also provide for damping to control whirl excitation from the impellers, the ability to "dial in" the required damping in the support system must somehow be done. The high (elastic) compliance of foil journal bearings makes this issue particularly critical. Without the necessary damping, violent aerodynamically excited whirl can be triggered at the imposition of a high journal bearing load (e.g., due to maneuver).

7.3 Challenges in Aero Propulsion Applications

In order that the full potential of air bearings be realized in applications related to aero propulsion equipment, feasibility must be established with respect to several requirements. Need of a suitable bearing material for the high temperature environment has already been indicated in Section VI. Other major requirements, some of which have already been identified [19], will be briefly discussed below.

Load Capacity - An advanced, high speed, aircraft gas turbine inherently has a large gyroscopic inertia. To accommodate typical maneuver environments, the maximum radial load to be carried by each journal bearing can well exceed 10 G's, and in some cases, approach 20 G's. The aerodynamic thrust load would be well above the level that can ever be realized by an air lubricated

* A large shaft vibration amplitude near the first critical speed is likely to cause failure of the mid-span device.

thrust bearing, unless the gas-path/impeller design can be selected for an optimum thrust balance. Even so, linear acceleration would amount to 10 G's in either direction. Therefore, the combined aerodynamic-acceleration thrust load would be 10-12 G's double-acting. Translated into representative unit loads, upwards to 40 psi level is desired of both journal and thrust bearings.

Total Compliance - Foil type bearings do not require stringent dimensional control mainly because of their relatively large compliances. The combination of a large compliance with a large radial load means a very large excursion of the rotor axis. Thus, in order to avoid rubbing of shaft seals and impellers, clearances at both places would have to be proportionally large. Consequently, efficiency of the engine would be penalized. This consideration should include dynamic compliance as may be related to running through one or more critical speeds. Therefore, provision of a suitable level of dynamic damping is one aspect of compliance control.

Stability - Although foil type journal bearings are known to be relatively free of the danger of whirl instabilities, conditions still exist for violent unstable motions to develop. Some of the known foil bearing designs can become structurally bottomed if the load is sufficiently high. When this happens, the bearing in essence has reverted to a rigid condition and thus can allow whirl instability to develop. Even if structural bottoming does not happen, the large rotor excursion may be accompanied by aerodynamic whirl excitation from either an impeller or from a shaft seal, unless the foil journal bearing possesses an adequate level of damping capacity. The latter type of instability is particularly dangerous for a high power density machine.

Tolerance of Particulate Matter - The intrusion of particulate matter into the air bearing compartment may not be totally avoided in a field situation. If oversized hard particles should become caught in the bearing gap at full speed, the resulting thermal trauma can be considerable.

Lift-Off Speed - Start-stop sliding is the main cause of wear of the air bearing. Given the same friction coefficient and wear resistance of the material, a reduction of the lift-off speed should be directly related to

lowering of the actual wear rate. Stick-slip vibration has been reported with foil bearings during start up in at least two instances [38,94]. Its occurrence may be a contributing factor to the present difficulties in materials development. Lowering of the lift-off speed should decrease the intensity of stick-slip vibrations and thus ease materials development.

These five problems, together with the high temperature material requirement, await solutions by the ingenuity of technologists engaged in the invention and upgrading of air lubricated, compliant bearings.

REFERENCES

1. Dowson, D., History of Tribology, Longman, London (1979).
2. Charron, M.E., "Rôle Lubrifiant de l'air Dans Le Frottement Des Solids. Frottement Dans le Vide", *Comptes Rendus*, 150, 960-8 (1910).
3. Ferranti, S.Z. de., "Improvements in, and Relating to Methods of and Apparatus for, Spinning, Doubling, and the Like", British Patent No. 115583 (1904).
4. Ferranti, F.J. de, "Air Bearing for High Speeds", U.S. Patent No. 930851 (1909).
5. Ferranti, G.R. de, "Improvements in and Relating to Spinning, Doubling, and Twisting Machinery", British Patents Nos. 416717, 416718, and 416719 (1934).
6. Sawtelle, W.H., "Some Points Regarding the Transverse Spindle Grinders", *Am. Mach.* 32, Pt. 2, pp. 248-249, Aug. 5, 1909.
7. Hardy, W.B. and Doubleday, I., "Boundary Lubrication - The Temperature Coefficient", *Proc. R. Soc.*, A101, 487-492 (1922).
8. Hardy, W.B. and Doubleday, I., "Boundary Lubrication - The Paraffin Series", *ibid.*, 550-574.
9. Hardy, W.B. and Doubleday, I., "Boundary Lubrication - The Latent Period and Mixtures of Two Lubricants", *Proc. R. Soc.*, A104, 25-39 (1923).
10. Murray, S.F., "Material Combinations for Hydrodynamic Inert Gas-Lubricated Bearings", *Journal of Lubrication Technology*, *Trans. ASME*, Series F, Vol. 90, No. 4, Oct. 1968, pp. 49-55.
11. Marsh, H., "The Stability of Aerodynamic Gas Bearings", *Mechanical Engineering Science Monograph No. 2*, Institute of Mechanical Engineers, London, 1965.
12. Castelli, V. and Elrod, H.G., "Solution of the Stability Problem for 360 Deg Self-Acting, Gas-Lubricated Bearings", *Journal of Basic Engineering*, Series D, Vol. 87, No. 1, March 1965, pp. 199-212.
13. Pan, C.H.T., "Spectral Analysis of Gas Bearing Systems for Stability Studies", Developments in Mechanics, Vol. 3, Proceedings of the 9th Midwestern Mechanics Conference, Pt. 2, Dynamics and Fluid Mechanics, Wiley, N.Y. 1965, pp. 431-447.

14. Mech, Christian, "Some Practical Performance Aspects of the Design of Gas-Bearing Blowers and Some Performances of Industrial Machines", Paper No. 16, Gas Bearing Symposium, University of Southampton, April 25-28, 1967.
15. Lavender, M., "Some Practical Results on the Stability of Non-Circular Aerodynamic Journal Bearings", Paper No. 15, *ibid.*
16. Foster, D.J., "Analytical Description of Means for Stabilizing a Hydrodynamic Gas Bearing", ASME Paper No. 64-LUB-23.
17. Malanoski, S.B., "Experiments on an Ultrastable, Gas Journal Bearing", *Journal of Lubrication Technology*, Trans. ASME, Series F., Vol. 89, No. 4, Oct. 1967, pp. 433-438.
18. Barnett, M.A., and Silver, A., "Application of Air Bearings to High-Speed Turbomachinery", SAE Paper No. 700720, Combined National Farm, Construction and Industrial Machinery and Powerplant Meeting, Wisconsin, Sept. 1970.
19. Heuer, D.F., and Collins, R.A., "Dynamic and Environmental Evaluation of Compliant Foil Gas Lubricated Bearings", Technical Report AFAPL-TR-73-56, Air Force Aero Propulsion Laboratory, Wright-Patterson Air Force Base, Ohio, June 1973.
20. Licht, L., Branger, M. and Anderson, W.J., "Gas-Lubricated Foil Bearings for High-Speed Turbo-Alternator - Construction and Performance", *Journal of Lubrication Technology*, Trans. ASME, Series F, Vol. 96, No. 2, April 1974, pp. 215-223.
21. Waldron, W.D., Young, W.E., and Curwen, P.W., "An Investigation of Air Bearings for Gas Turbine Engines", Mechanical Technology Incorporated Technical Report 71TR23, Prepared for U.S. Army Air Mobility Research and Development Laboratory Contract No. DAAJ02-69-C-0062.
22. Pan, C.H.T. and Sternlicht, B., "Thermal Distortion of a Spiral-Groove Gas-Lubricated Thrust Bearing Due to Self-Heating", *Journal of Lubrication Technology*, Trans. ASME, Series F, Vol. 89, No. 2, April 1967, pp. 197-202.
23. Malanoski, S.B. and Pan, C.H.T., "The Static and Dynamic Characteristics of Spiral-Groove Thrust Bearings", *Journal of Basic Engineering*, Trans. ASME, Series D, Vol. 87, No. 3, Sept. 1965, pp. 547-558.
24. Colsher, R. and Shapiro, J., "Implementation of Time-Transient and Step-Jump Dynamic Analyses of Gas-Lubricated Bearings", *Journal of Lubrication Technology*, Trans. ASME, Series F, Vol. 92, No. 3, July 1970, pp. 518-529.

25. Gu, A., Pan, C.H.T. and Badgley, "Dynamic Stability of Gimbaled Spiral-Grooved Thrust Bearing", Journal of Lubrication Technology, Trans. ASME, Series F, Vol. 95, No. 2, April 1973, pp. 222-235.
26. Wooley, R.W., "Some Developments in the Application of Externally Pressurized Air Bearings to Industry", Paper No. 9, Gas Bearing Symposium, University of Southampton, April 25-28, 1967.
27. Denhard, W.G. and Pan, C.H.T., "Application of Gas-Lubricated Bearings to Instruments", Journal of Lubrication Technology, Trans. ASME, Series F, Vol. 90, No. 4, Oct. 1968, pp. 731-740.
28. Powell, J.W., "A Review of the Experience Gained in Producing Over 20,000 Air Bearing Dental Turbines", Paper No. 10, Gas Bearing Symposium, University of Southampton, April 25-28, 1967.
29. Kilmister, G., Minutes of ONR Gas Bearing Research Coordination Meeting, Columbia University, 1977.
30. Baumeister, H.K. and Nejezchleb, V., "Hydrodynamically Air Lubricated Magnetic Tape Head", U.S. Patent 3,170,045, 1965.
31. Gross, W.A., "Application of Gas Bearings to Digital Computers", Paper No. 14, Gas Bearing Symposium, University of Southampton, March 31 - April 2, 1965.
32. Kaneko, R., Matsuda, R. and Hara, S., "The Designing and Application of Floating Head Mechanics for Magnetic Recording", Paper No. E3, Gas Bearing Symposium, University of Southampton, March 27-29, 1974.
33. Sereny, A. and Castelli, V., "Experimental Investigation of Slider Gas Bearings With Ultra-Thin Films", Journal of Lubrication Technology, Trans. ASME, Vol. 101, No. 4, October 1979, pp. 510-515.
34. Kaneko, R., Mitsuya, Y. and Oguchi, S., "High-Speed Magnetic Storage Drums with Grooved Hydrodynamic Gas Bearings", Paper No. C2, Gas Bearing Symposium, University of Southampton, March 27-29, 1974.
35. Stahler, A.F., "Analyzation, Design, Fabrication, and Testing of a Foil Bearing Rotor Support System", Ampex Research Report, RR 66-8, 1966.
36. Licht, L., "The Dynamic Characteristics of a Turborotor Simulator Supported on Gas-Lubricated Foil Bearings - Part I: Response to Rotating Imbalance and Unidirectional Excitation", Journal of Lubrication Technology, Trans. ASME, Series F, Vol. 92, No. 4, Oct. 1970, pp. 630-649.
37. Licht, L., "The Dynamic Characteristics of a Turborotor Simulator Supported on Gas-Lubricated Foil Bearings - Part II: Operation with Heating and Thermal Gradients", *ibid*, pp. 650-660.

38. Licht, L., "The Dynamic Characteristics of a Turborotor Simulator Supported on Gas-Lubricated Foil Bearings - Part III: Rotation in Foil Bearings of Reduced Length, with Starting and Stopping Unaided by External Pressurization", *Journal of Lubrication Technology*, Trans. ASME, Series F, Vol. 94, No. 3, July 1972, pp. 211-222.
39. Bangs, S., "Foil Bearings Help Air Passengers Keep Their Cool", *Power Transmission Design* (An Industrial Publishing Magazine), February 1973, pp. 27-31.
40. Swenson, K.R., Hughes, N.M. and Heuer, D.F., "Evaluation of Gas Lubricated Hydrodynamic Bearings in a Gas Turbine Environment", Technical Report AFAPL-TR-72-41, Air Force Aero Propulsion Laboratory, Wright-Patterson Air Force Base, Ohio, June 1972.
41. Gray, S., Sparks, N. and McCormick, J., "The Application of Gas-and-Oil-Lubricated Foil Bearings for the ERDA/Chrysler Automotive Gas Turbine Engine", ASME Paper No. 76-GT-115, March 21-25, 1976.
42. Decker, O., "Where, How and Why Gas Bearings Compete with Rolling Contact Bearings", Paper No. F1, Gas Bearing Symposium, University of Southampton, March 27-29, 1974.
43. Gross, W.A., Gas Film Lubrication, John Wiley and Sons, New York, 1962.
44. Constantinescu, V.N., Gas Lubrication, English Translation Published by ASME, 1969.
45. Pan, C.H.T., "Gas Bearings", Chapter 4 in Tribology, edited by A.Z. Szeri, McGraw-Hill Book Company, 1979, pp. 103-228.
46. Castelli, V., "Gas Bearing Analysis", Chapter 8, Engineering Applications of Digital Computers, Academic Press Inc., 1968, pp. 213-234.
47. Castelli, V. and Pirvics, J., "Review of Numerical Methods in Gas Bearing Film Analysis", *Journal of Lubrication Technology*, Trans. ASME, Series F, Vol. 90, No. 4, Oct. 1968, pp. 777-792.
48. Harrison, W.J., "The Hydrodynamical Theory of Lubrication with Special Reference to Air as a Lubricant," Trans. Camb. Phil. Soc., xxii, 1913, pp. 37-54.
49. Maday, C.J., "The One-Dimensional Optimum Hydrodynamic Gas Slider Bearing", *Journal of Lubrication Technology*, Vol. 90, 1968, pp. 281-284.
50. McAllister, G.T., Rohde, S.M., and McAllister, M.N., "A Note on the Optimum Design of Slider Bearings", *Journal of Lubrication Technology*, Vol. 102, Jan. 1980, pp. 117-119.

51. Lord Rayleigh, "Notes on the Theory of Lubrication", Phil. Mag. Vol. 35, 1918, pp. 1-12.
52. Elrod, H.G., Jr. and McCabe, J.T., "Theory for Finite-Width High-Speed Self-Acting Gas-Lubricated Slider (and Partial-Arc) Bearings", Journal of Lubrication Technology, Vol. 91, No. 1, January 1969, pp. 17-24.
53. Elrod, H.G., Jr., Private Communications.
54. Poritsky, H., "Contribution to the Theory of Oil Whip", Trans. ASME, Vol. 75, 1953, pp. 1153-1161.
55. Cheng, H.S. and Trumpler, P.R., "Stability of the High Speed Journal Bearing under Steady Load", Journal of Engineering for Industry, Trans. ASME, Series B, Vol. 85, 1963, pp. 274-286.
56. Cheng, H.S. and Pan, C.H.T., "Stability of Gas-Lubricated, Self-Acting, Plain, Cylindrical, Journal Bearings of Finite Length, Using Galerkin's Method", Journal of Basic Engineering, Trans. ASME, Series D, Vol. 87, No. 1, March 1965, pp. 185-192.
57. Lund, J.W., "The Hydrostatic Gas Journal Bearing With Journal Rotation and Vibration", Journal of Basic Engineering, Trans. ASME, Series D, Vol. 86, No. 2, June 1964, pp. 328-336.
58. Lund, J.W., "A Theoretical Analysis of Whirl Instability and Pneumatic Hammer for a Rigid Rotor in Pressurized Gas Journal Bearings", Journal of Lubrication Technology, Trans. ASME, Series F, Vol. 89, No. 2, April 1967, pp. 154-166.
59. Fuller, D.D., "A Review of the State-of-the-Art for the Design of Self-Acting Gas-Lubricated Bearings", Journal of Lubrication Technology, Trans. of ASME, Series F, Vol. 91, No. 1, January 1969, pp. 1-16.
60. Waldron, W.D., Young, W.E., and Curwen, P.W., "An Investigation of Air Bearings for Gas Turbine Engines", Mechanical Technology Incorporated USAAMRDL Technical Report 71-59, Contract No. DAAJ02-69-C-0062, Task 1G162203D14413, December 1971.
61. Lund, J.W., "Calculation of Stiffness and Damping Properties of Gas Bearings", Journal of Lubrication Technology, Trans. ASME, Series F, Vol. 90, No. 4, October 1968, pp. 793-803.
62. Colsher, R., and Shapiro, W., "Implementation of Time-Transient and Step-Jump Dynamic Analyses of Gas-Lubricated Bearings", Journal of Lubrication Technology, Trans. ASME, Series F, Vol. 92, No. 3, July 1970, pp. 518-529.

63. Gunter, E.J., Jr., Hinkle, J.G., and Fuller, D.D., "Design Guide for Gas-Lubricated Tilting-Pad Journal and Thrust Bearings with Special Reference to High Speed Rotors", Report NYO-2512-1, U.S. Atomic Energy Commission, November 1964.
64. Gunter, E.J., Jr., Hinkle, J.G., and Fuller, D.D., "The Effects of Speed, Load, and Film Thickness on the Performance of Gas-Lubricated Tilting-Pad Journal Bearings", ASLE Trans., Vol. 7, 1964, pp. 353-365.
65. Arwas, E.B., "Tilting Pad Journal Bearings", Design of Gas Bearings, Volume I, Section 6.2, Mechanical Technology Incorporated, 1967.
66. Pitts, G., "Improved Presentation of Design Curves for the 120° Tilting Pad Bearing", Paper 10, Gas Bearing Symposium, University of Southampton, April 22-25, 1969.
67. Shapiro, W., and Colsher, R., "Development of Compliant-Mounted Gas Bearings for a Small, High-Speed, 10 KW Turboalternator", Franklin Institute Research Laboratories Report, prepared for U.S. Army Mobility Equipment Research and Development Command, Fort Belvoir, Va., under Contract DAAK02-72-6-0571, September 1976.
68. Shapiro, W., and Colsher, R., "Development of Compliant-Mounted Gas-Lubricated Journal Bearings with High-Speed, High-Load Capability", Franklin Institute Research Laboratories Report I-C4965, April 1978.
69. Marsh, H., "The Stability of Aerodynamic Gas Bearings, Part 2, Non-Circular Bearings", Research Report for Ministry of Aviation, June 1964.
70. Archibald, F.R., and Hamrock, B.J., "The Rayleigh Step Bearing Applied to a Gas-Lubricated Journal of Finite Length," Journal of Lubrication Technology, Trans. ASME, Series F, Vol. 89, No. 1, January 1967, pp. 38-46.
71. Whipple, R.T.P., "Theory of the Spiral Grooved Thrust Bearing With Liquid or Gas Lubricant", Atomic Energy Research Establishment T/R 622, 1951.
72. Keating, W.H., and Pan, C.H.T., "Design Studies of an Opposed-Hemisphere Gyro Spin-Axis Gas Bearing", Journal of Lubrication Technology, Trans. ASME, Series F, Vol. 90, No. 4, October 1968, pp. 753-760.
73. Malanoski, S.B., "Experiments on an Ultrastable Gas Journal Bearing", Journal of Lubrication Technology, Trans. ASME, Series F, Vol. 89, No. 4, October 1967, pp. 433-438.
74. Cunningham, R.E., Fleming, D.P., and Anderson, W., "Experimental Stability Studies of the Herringbone-Grooved Gas-Lubricated Journal Bearing", Journal of Lubrication Technology, Trans. ASME, Series F, Vol. 91, No. 1, January 1969, pp. 52-59.
75. Vohr, J.H., and Chow, C.Y., "Characteristics of Herringbone-Grooved, Gas Lubricated Journal Bearings", Journal of Basic Engineering, Trans. ASME, Series D, Vol. 87, No. 3, September 1965, pp. 568-578.

76. Vohr, J.H., and Pan, C.H.T., "Design Data of Gas-Lubricated Spin Axis Bearings for Gyroscopes", Mechanical Technology Incorporated Technical Report MTI-63TR29, Prepared for Office of Naval Research under Contract N00014-67-C-0530, June 1968.
77. Hamrock, B.J., and Fleming, D.P., "Optimization of Self-Acting Herringbone Grooved Journal Bearings for Maximum Radial Load Capacity", Paper No. 13, Gas Bearing Symposium, University of Southampton, March 23-26, 1971.
78. Fleming, D.P., and Hamrock, B.J., "Optimization of Self-Acting Herringbone Journal Bearings for Maximum Stability", Paper No. C1, Gas Bearing Symposium, University of Southampton, Fluid Engineering, March 27-29, 1974.
79. Licht, L., and Branger, M., "Design, Fabrication and Performance of Foil Journal Bearings for the Brayton Rotating Unit (BRU)", NASA Report No. CR-2243, Contract No. NAS3-15341, NASA Lewis Research Center, Cleveland, Ohio, July 1973.
80. Ruscitto, D., McCormick, J., and Gray, S., "Development of a Hydrodynamic Air Lubricated Compliant Surface Bearing for an Automotive Gas Turbine Engine. Part 1 - Journal Bearing Performance", Report on NASA Contract NAS3-19427, NASA Report CR-135368, April 1978.
81. Pan, C.H.T., Krauter, A.I., and Wu, E.R., "Rotor Bearing Dynamics Technology Design Guide, Part I, Flexible Rotor Dynamics", AFAPL-TR-78-6, November 1979, Air Force Aero Propulsion Laboratory, Wright Patterson Air Force Base, Ohio.
82. Licht, L., and Elrod, H.G., Jr., "A Study of the Stability of Externally Pressurized Gas Bearings", Journal of Applied Mechanics, Vol. 27, Trans. ASME, Series E, Vol. 82, No. 2, June 1960, pp. 250-258.
83. Vohr, J.H., "A Study of Inherent Restrictor Characteristics for Hydrostatic Gas Bearings", Paper No. 30, Gas Bearing Symposium, University of Southampton, April 22-25, 1969.
84. McCabe, J.T., Elrod, H.G., Jr., Carfagno, S., and Colsher, R., "Summary of Investigations of Entrance Effects of Circular Thrust Bearings", Paper No. 17, *ibid*.
85. Mori, H., "A Theoretical Investigation of Pressure Depression in Externally Pressurized, Gas-Lubricated Circular Thrust Bearings", Journal of Basic Engineering, Trans. ASME, Series D, Vol. 83, pp. 201-208, 1961.
86. Wildmann, M., Glaser, J., Gross, W.A., Moors, D.E., Rood, L., and Cooper, S., "Gas-Lubricated Stepped Thrust Bearing -- A Comprehensive Study", Journal of Basic Engineering, Trans. ASME, Series D, Vol. 2, March 1965, pp. 213-229.

87. Muyderman, E.A., Spiral Groove Bearing, Phillips Technical Library, Cleaver-Hume Press Ltd. (Macmillan and Co., Ltd), 1966.
88. Whitley, S., "The Design of the Spiral Groove Thrust Bearing", Paper No. 13, Gas Bearing Symposium, Southampton University, April 25-28, 1967.
89. Wildmann, M., "On the Behavior of Grooved-Plate Thrust Bearings With Compressible Lubricant", Journal of Lubrication Technology, Trans. ASME, Series F, Vol. 90, No. 1, Jan. 1968, pp. 226-232.
90. Wachmann, C., Malanoski, S.B., and Vohr, J.H., "Thermal Distortion of Spiral Grooved Gas-Lubricated Thrust Bearings", Journal of Lubrication Technology, Trans. ASME, Series F, Vol. 93, No. 1, Jan. 1971, pp. 102-111.
91. Huxley, A.S., "An Optical Method for Measuring the Running Clearance of a Spiral Grooved Thrust Bearing", Paper E2-15, Gas Bearing Symposium, University of Southampton, March 27-29, 1974.
92. Jones, D.A., et.al., "Thermal and Mechanical Distortions of Self-Acting Gas Bearing Systems - Part 1: Theoretical, and Part 2: Experimental," 7th International Gas Bearing Symposium, Paper Nos. G4 and G5, BHRA Fluid Engineering, Cranfield, Bedford, Great Britain, 1976.
93. Waldron, W.D., and Young, W.E., "High Performance Bearing Study", WPAFB Report No. AFAPL-TR-72-63, July 1972.
94. Bhushan, Bharat, Ruscitto, David, and Gray, Stanley, "Hydrodynamic Air Lubricated Compliant Surface Bearing for an Automotive Gas Turbine Engine II - Materials and Coatings", Mechanical Technology Incorporated, NASA Report CR-135402, Prepared under Contract NAS3-19427, July 1978.
95. W. F. Koepsel, "Gas Lubricated Foil Bearing Development for Advanced Turbomachines", AFAPL-TR-76-114, March 1977.
96. Dowson, D. and Higginson, G.R., Elastohydrodynamic Lubrication - The Fundamentals of Roller and Gear Lubrication, Pergamon Press, Oxford, 1966.
97. Dowson, D., "Modes of Lubrication in Human Joints", Lubrication and Wear in Living and Artificial Human Joints, Proc. Instn. Mech. Engrs., 181, Pt. 3J, London, pp. 45-54.
98. Wilson, D., and Murray, S.F., "Gas Lubrication Research for 1900°F, Non-Isothermal Operation; Bearing Distortion Effects on Performance and High Temperature Material Investigations", Mechanical Technology Incorporated, AFAPL-TR-67-57, Part I, May 1957.
99. Eshel, A., and Licht, L., "Foil Bearing Design Manual", Ampex Report No. RR71-18, 1971.
100. Waldron, Warren D., and Van Huysen, Robert S., "Pneumomechanical Critical Speed Control of Gas Turbine Engine Shafts", Technical Report AFAPL-TR-75-86, Air Force Aero Propulsion Laboratory, Wright-Patterson Air Force Base, Ohio, September 1975.

101. Woolley, R., "Difficulties Encountered with a Small Tension Dominated Foil Bearing", Paper No. 14, Gas Bearing Symposium, University of Southampton, April 18-19, 1978.
102. Walowit, J., Murray, S.F., McCabe, J., Arwas, E.B., and Moyer, T., "Gas Lubricated Foil Bearing Technology Development for Propulsion and Power Systems", AFAPL-TR-73-92, Air Force Aero Propulsion Laboratory, Wright-Patterson Air Force Base, Ohio, December, 1973.
103. Zorzi, Edward S., "Gas Lubricated Foil Bearing Development for Advanced Turbomachines", Technical Report AFAPL-TR-76-114, Volume II - Analytical Tools, Air Force Aero Propulsion Laboratory, Wright-Patterson Air Force Base, Ohio, April 1977.
104. Oh, K.P., and Rohde, S.M., "A Theoretical Investigation of the Multi-leaf Journal Bearing", Journal of Applied Mechanics, Trans. ASME, Vol. 47, Series E, No. 2, June 1976, pp. 237-242.
105. Trippet, R.J., Oh, K.P., and Rohde, S.M., "Theoretical and Experimental Load-Deflection Studies of a Multileaf Journal Bearing", ASME Publication 100118, 1978.
106. Ruscitto, D., McCormick, J., and Gray, S., "Development of a Hydrodynamic Air Lubricated Compliant Surface Bearing for an Automotive Gas Turbine Engine. Part I - Journal Bearing Performance," NASA Technical Report CR-135368, issued under NASA Contract NAS3-19427, April 1978.
107. Licht, L., "Foil Bearings for Axial and Radial Support of High Speed Rotors - Design, Development and Determination of Operating Characteristics", NASA Contractor Report 2940, ONR Contract N00014-76-0191, NASA Purchase Request C-75012-C, January 1978.
108. Licht, L., Anderson, W.A., and Doroff, S., "Dynamic Characteristics of a High-Speed Rotor with Radial and Axial Foil-Bearing Supports", Paper to be presented at the 1980 ASME-ASLE Joint Lubrication Conference, August 18-24, 1980, San Francisco.
109. Licht, L., Anderson, W.A., and Doroff, S., "Design and Performance of Compliant Thrust Bearings with Spiral-Groove Membranes on Resilient Supports", *ibid.*
110. Cundiff, R.A., Badgley, R.H., and Reddecliff, J., "Pneumomechanical Critical Speed Control for Gas Turbine Engine Shafts", Technical Report AFAPL-TR-73-101, Air Force Aero Propulsion Laboratory, Wright-Patterson Air Force Base, Ohio, November 1973.
111. Collins, R.A., Heuer, D.F., "Pneumomechanical Critical Speed Control for Gas Turbine Engine Shafts", Technical Report AFAPL-TR-73-102, Air Force Aero Propulsion Laboratory, Wright-Patterson Air Force Base, Ohio, October 1973.